

**STUDIES ON SOME
NEW SCHIFF BASE COMPLEXES OF
RUTHENIUM AND NEODYMIUM**

THESIS SUBMITTED TO THE
COCHIN UNIVERSITY OF SCIENCE AND TECHNOLOGY
IN PARTIAL FULFILMENT OF THE REQUIREMENTS FOR THE DEGREE OF

DOCTOR OF PHILOSOPHY
IN
CHEMISTRY
IN THE FACULTY OF SCIENCE

BY
PEARLY SEBASTIAN CHITILAPPILLY

DEPARTMENT OF APPLIED CHEMISTRY
COCHIN UNIVERSITY OF SCIENCE AND TECHNOLOGY
KOCHI-682 022, KERALA

MARCH 2007

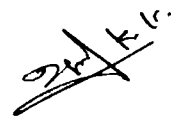
Dedicated to my beloved parents

CERTIFICATE

This is to certify that the thesis entitled "*Studies on some new Schiff base complexes of ruthenium and neodymium*" submitted by Ms. Pearly Sebastian Chittilappilly is an authentic and bonafide record of the original research work carried out by the author under my supervision, in partial fulfilment of the requirements for the degree of Doctor of Philosophy of Cochin University of Science and Technology and further, the results embodied in this thesis, in full or in part have not been presented before for the award of any other degree.

Kochi-22

23-03-2007



Prof. K.K.Mohammed Yusuff
Department of Applied Chemistry
Cochin University of Science
and Technology, Kochi-22

DECLARATION

I hereby declare that the work presented in this thesis entitled "*Studies on some new Schiff base complexes of ruthenium and neodymium*" submitted for the award of Ph.D degree is entirely original and was carried out by me independently under the supervision of Prof. K.K.Mohammed Yusuff, Department of Applied Chemistry, Cochin University of Science and Technology, Kochi-682 022 and further that no part thereof has been presented before for the award of any degree.

Kochi-22
23-03-2007


Pearly Sebastian Chittilappilly

ACKNOWLEDGEMENTS

With immense pleasure, I would like to record my sincere thanks to Prof. K.K.Mohammed Yusuf, for always being available with invaluable suggestions and infinite patience throughout the course of the investigations. The stimulating discussions with him were always a source of inspiration for my work, I appreciate and acknowledge his dedicated and selfless service.

I sincerely thank Prof. M.R.Prathapachandra Kurup, Head, Department of Applied Chemistry, Cochin University for his active support and motivation rendered to me.

I also wish to place on record my deep sense of gratitude to Dr. N.Sridevi for her generosity, timely assistance, encouragement and valuable suggestions throughout my work.

My sincere thanks are also due to Prof. S. Sugunan, former Head of the Department, Dr. S.Prathapan, Reader and all other members of the faculty, Department of Applied Chemistry, Cochin University, for their occasional suggestions and support.

I am grateful to Dr.Sr.Ranjana, Principal, Prof. Joseph Konikkara, Dr.Sr.Lilly Kachappilly, Daisy, Thressiama and other members of the faculty and staff, Department of Chemistry and Sr.Anjali, Senior Supdt., St. Joseph's college, Irinjalakuda for all the help rendered to me in the course of my work. A word of thanks to Ms.Jeena.K, Department of Bio-technology, St.Joseph's college, Irinjalakuda for helping me with biological studies.

I acknowledge in a special way the help and cooperation extended to me by my lab mates Arun, Manju, Leeju, Varsha, Annu and Robinson and other research scholars of the Department especially Raphael, Ambily and Kala. I also acknowledge the services rendered to me by the library and office staff of the Department of Applied Chemistry, Cochin University and St.Joseph's college, Irinjalakuda

I thank UGC for granting me fellowship under FIP and Govt.of Kerala for sanctioning my deputation.

I also acknowledge the services provided by the SAIF, Sophisticated Tests and Instrumentation Centre, Kochi, Central Drug Research Institute, Lucknow, IISc., Bangalore, IIT, Bombay and IIT, Roorkee.

I cannot leave out my husband, Mr. V.T. Davis and our children Nikil and Denil from the list of people whom I must thank, for providing me an atmosphere of love and support and for patiently bearing with me in the process of my research. I am particularly thankful to my nephews Biju Stephen and Nitin Chittilappilly who have contributed their share to my studies.

Above all I beseech before God Almighty for giving me His strength and grace to carry out this work to completion.

Pearly Sebastian Chittilappilly

PREFACE

Macrocyclic Schiff base ligands are currently under investigation as encapsulating ligands. They are very much like porphyrins, but can be more easily synthesized. Their multidentate nature results in very high binding constants for many d or f - block metals. They are able to stabilize many different metal ions in various oxidation states controlling the performance of metals in a variety of catalytic reactions. Many of the complexes find wide applications as heterogeneous catalysts. Immobilization of these complexes on to organic or inorganic supports has received wide attention as they offer advantageous features of heterogeneous catalysis to homogeneous systems.

In the present study an attempt has been made to synthesize some simple complexes of multidentate ligands. Analogous zeolite encapsulated complexes were also synthesized and characterized. Immobilization on to polymer supports through covalent attachment is expected to solve the problem of decomposition of many complexes during catalytic reaction. Hence the work is also extended to the synthesis and characterization of some polymer supported complexes of Schiff base ligands. All the three types of synthesized complexes, simple, zeolite encapsulated and polystyrene anchored, were subjected to catalytic activity study towards catechol-oxidation reaction. A selected group of complexes were also screened for their catalytic activity towards phenol-oxidation reaction. Biological screening of the synthesized ligands and neat complexes were done with a view to establish the effect of complexation on biological systems. Details of these studies are presented in this thesis.

The thesis is divided into nine chapters. Chapter I gives a brief account of the literature survey done on the subject. The materials and techniques employed in the study are given in Chapter II. Chapter III to VI deals with the synthesis and characterization of simple, zeolite encapsulated and polymer anchored complexes. Chapters VII and VIII deal with the catalytic studies of the synthesized complexes towards organic oxidation reactions. Chapter IX presents the *in Vitro* evaluation of the synthesized neat complexes towards microbes. The conclusions derived from the study are summarized at the end of the thesis.

CONTENTS

Page No

Chapter I

INTRODUCTION 1 - 25

1.1	Metal Complexes	1
1.1.1	Schiff bases	1
1.1.2	Quinoxaline complexes	4
1.1.3	Ruthenium complexes	4
1.1.4	Neodymium complexes	7
1.2	Catalysis	8
1.2.1	Zeolite encapsulated complexes	11
1.2.2	Polymer supported complexes	13
1.3	Scope of the present investigation	15
	References	17

Chapter II

MATERIALS AND METHODS 26 - 37

2.1	Reagents	26
2.2	Synthesis of ligands	26
2.2.1	N,N'-Bis(3-hydroxyquinoxaline-2-carboxalidene)- o-phenylene diamine (qpd)	27
2.2.2	3-Hydroxyquinoxaline-2-carboxalidene-o-aminophenol (qap)	28
2.2.3	3-Hydroxyquinoxaline-2-carboxalidene- 2-aminobenzimidazole (qab)	28
2.2.4	N,N'- Bis(salicylaldimine)-o-phenylenediamine (salpd)	28
2.2.5	Salicylaldimine- o-aminophenol (salap)	28
2.2.6	Salicylaldimine-2-aminobenzimidazole (salab)	29
2.3	Supports used	29
2.3.1	Zeolite-Y	29
2.3.2	Polystyrene beads	30

2.4	Preparation of polymer bound Schiff base	30
2.4.1	Preparation of polymer bound Schiff base with o-phenylenediamine (PS-opd)	30
2.4.2	Preparation of polymer bound Schiff base with o-aminophenol (PS-ap)	30
2.4.3	Preparation of polymer bound Schiff base with 2-aminobenzimidazole (PS-ab)	30
2.5	Analytical methods	31
2.5.1	CHN analysis	31
2.5.2	Chemical analysis	31
2.6	Physico-chemical methods	32
2.6.1	Surface area analysis	32
2.6.2	Magnetic susceptibility measurements	32
2.6.3	Thermogravimetry	33
2.6.4	Conductance measurements	33
2.6.5	SEM	33
2.6.6	X-ray diffraction spectroscopy	33
2.6.7	FAB mass spectra	34
2.6.8	Infrared spectra	34
2.6.9	Electronic spectra	34
2.6.10	EPR spectroscopy	35
2.7	Catalytic studies	35
2.7.1	Gas chromatography	35
2.7.2	UV/Visible spectroscopy	35
2.8	Biological activity	36
	References	37

Chapter III

	SYNTHESIS AND CHARACTERIZATION OF SCHIFF BASE COMPLEXES OF RUTHENIUM	38 - 69
3.1	Introduction	38
3.2	Synthesis of complexes	39
3.2.1	Ruthenium-qpd complex	39
3.2.2	Ruthenium-qap complex	39
3.2.3	Ruthenium-qab complex	39
3.2.4	Ruthenium-salpd complex	39
3.2.5	Ruthenium-salap complex	40

3.2.6	Ruthenium-salab complex	40
3.3	Results and discussion	40
3.3.1	Elemental analysis	40
3.3.2	Mass spectral analysis	41
3.3.3	Molar conductance	48
3.3.4	Thermogravimetric analysis	48
3.3.5	Infrared spectra	54
3.3.6	Magnetic susceptibility measurements	58
3.3.7	Electronic spectra	58
3.3.8	EPR spectra	61
	Conclusion	66
	References	67

Chapter IV

STUDIES ON ZEOLITE-Y ENCAPSULATED COMPLEXES OF RUTHENIUM 70 - 87

4.1	Introduction	70
4.2	Experimental	70
4.2.1	Synthesis of Ru(III) zeolite encapsulated complexes of qpd, qap, qab, salpd, salap and salab	71
4.3	Characterization techniques	71
4.4	Results and discussion	71
4.4.1	Elemental analysis	71
4.4.2	Surface area and pore volume	73
4.4.3	Thermogravimetric analysis	74
4.4.4	X-ray diffraction	79
4.4.5	SEM analysis	81
4.4.6	Infrared spectra	81
4.4.7	Electronic spectra	83
4.4.8	EPR spectra	84
	Conclusion	85
	References	86

Chapter V

SYNTHESIS & CHARACTERISATION OF NEAT AND ENCAPSULATED SCHIFF BASE COMPLEXES OF NEODYMIUM 88 – 110

5.1	Introduction	88
5.2	Simple complexes of neodymium	88
5.2.1	Synthesis	88
5.2.1.1	Neodymium-qpd complex	88
5.2.1.2	Neodymium-qap complex	89
5.2.1.3	Neodymium-qab complex	89
5.2.2	Results and discussion	89
5.2.2.1	Elemental analysis	89
5.2.2.2	Molar conductance	90
5.2.2.3	Thermogravimetric analysis	91
5.2.2.4	Infrared spectra	93
5.2.2.5	Magnetic susceptibility measurements	95
5.2.2.6	Electronic spectra	95
	Conclusion	99
5.3	Encapsulated complexes of neodymium	99
5.3.1	Synthesis	99
5.3.2	Results and discussion	100
5.3.2.1	Elemental analysis	100
5.3.2.2	Surface area	100
5.3.2.3	X-ray diffraction studies	101
5.3.2.4	SEM analysis	101
5.3.2.5	Thermogravimetric analysis	102
5.3.2.6	Infrared spectra	104
5.3.2.7	Electronic spectra	106
	Conclusion	108
	References	109

Chapter VI

POLYMER BOUND SCHIFF BASE COMPLEXES OF RUTHENIUM AND NEODYMIUM 111 – 132

6.1	Introduction	111
6.2	Synthesis of complexes	112
6.2.1	Ru(III) and Nd(III) complexes of PS-opd	112
6.2.2	Ru(III) and Nd(III) complexes of PS-ap	112
6.2.3	Ru(III) and Nd(III) complexes of PS-ab	113

6.3	Results and discussion	113
6.3.1	Elemental analysis	113
6.3.2	Magnetic susceptibility measurements	114
6.3.3	Surface area and pore volume	115
6.3.4	Thermogravimetric analysis	116
6.3.5	Infrared spectra	120
6.3.6	Electronic spectra	123
6.3.7	EPR spectra	126
	Conclusion	129
	References	130

Chapter VII

CATECHOL-H₂O₂ REACTION-A COMPARATIVE STUDY OF HOMOGENEOUS AND HETEROGENEOUS CATALYSIS BETWEEN RUTHENIUM AND NEODYMIUM 133 - 148

7.1	Introduction	133
7.2	Experimental	134
7.2.1	Reagents	134
7.2.2	Preparation of substrate solution	135
7.2.3	Preparation of stock solution of hydrogen peroxide	135
7.2.4	Preparation of solution of simple complexes	135
7.2.5	Screening studies	135
7.2.6	Kinetic procedure	135
7.3	Results and discussion	136
7.3.1	Comparison of catalytic activity of neat and encapsulated complexes of ruthenium	136
7.3.2	Comparison of catalytic activity of neat and encapsulated complexes of neodymium	139
7.3.3	Catalytic activity study of polymer supported complexes of ruthenium	140
7.3.4	Catalytic activity study of polymer supported complexes of neodymium	144
	Conclusion	146
	References	147

Chapter VIII

CATALYTIC HYDROXYLATION OF PHENOL 149 - 162

8.1	Introduction	149
8.2	Materials	150
8.3	Procedure	150
8.3.1	Analysis of products	150
8.4	Results and discussion	151
8.4.1	Comparison of the catalytic activity of the complexes under study at regular intervals	156
	Conclusion	160
	References	162

Chapter IX

***IN VITRO* EVALUATION OF ANTIBACTERIAL AND ANTIFUNGAL ACTIVITY OF CMPLXES OF RUTHENIUM AND NEODYMIUM 163 - 172**

9.1	Introduction	163
9.2	Experimental	164
9.2.1	Antibacterial screening test	164
9.2.2	Antifungal screening test	165
9.3	Results and discussion	165
9.3.1	Antibacterial screening	165
9.3.2	Antifungal screening	168
	Conclusion	170
	References	171

SUMMARY AND CONCLUSION 173 - 177

CHAPTER I

INTRODUCTION

Synthesis and characterization of new coordination compounds have always been a challenge to the inorganic chemists since they were identified in the nineteenth century. They play an active role in nature as exemplified by the function of macromolecules such as haemoglobin, chlorophyll etc. The functions of metalloproteins and metalloenzymes in natural biological systems are related to catalytic activity in reactions such as hydrogen exchange, hydrolysis of esters, formation of Schiff bases and carboxylation or decarboxylation.¹⁻⁴

1.1 Metal complexes

Metal complexes in which a single central metal atom or ion is surrounded by a set of ligands, play an important role in inorganic chemistry, especially for elements of the d-block. Interaction of metal ions with N, O and S containing organic moieties has attracted much attention in recent years.^{5,6} Such ligands and their complexes are important due to their biological activity⁷⁻⁹ and also because they provide a better understanding of metal protein binding.¹⁰ Schiff bases containing these groups could act as versatile model of metallic biosites.¹¹ Catalytic oxidation of many organic compounds is also of fundamental and industrial significance. Several transition metal Schiff base complexes are reported to be effective homogeneous catalysts for such oxidation reactions.^{12,13}

1.1.1 Schiff bases

Schiff bases are an important class of ligands in coordination chemistry and their coordinating ability containing different donor atoms is widely reported.¹⁴ They have wide applications in many biological aspects.^{15,16} The Schiff base complexes exhibit important properties such as anti-inflammatory activity,¹⁷ antibiotic activity,¹⁸ antimicrobial activity¹⁹ and antitumour activity.²⁰ Hodnet and Dunn²¹ have reported that

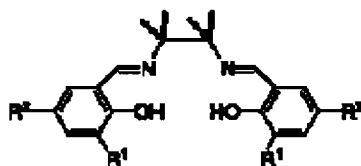
the Schiff bases in complexes play the key role in antitumour activity. Some of the Schiff base complexes are used as model molecules for biological oxygen carrier systems.²² Metal complexes are known to play a vital role in metabolic and toxicological functions in biological systems.¹⁷ These complexes have also applications in clinical field.^{23,24} These wide applications of Schiff bases have generated a great deal of interest in the synthesis of new metal complexes. The biological activity of the Schiff bases has been attributed to their coordination ability with suitable metal ions. Studies on metal complexes of biologically active ligands are important since they can sometimes be considered as models of the more complex biological systems. Several metal complexes of biologically important ligands have been synthesized and studied.²⁵

Only after 1950s concrete and rapid advances in the field of Schiff base metal complexes became evident. In the early days the main efforts were directed toward synthesis and characterization of rather fundamental complexes. The research field dealing with Schiff base metal complexes has now been far extended to the field of organometallic and bioinorganic chemistry.²⁶ Schiff base transition metal complexes are one of the most adaptable and thoroughly studied systems.^{27, 28} Interest in transition metal complexes of these Schiff bases continues not only due to the interesting structural and bonding modes they possess, but also because of their varied industrial applications.²⁹ Tetradentate Schiff base complexes are well known to form stable complexes, where the coordination takes place through the N_2O_2 donor set.³⁰⁻³²

The Schiff base ligands exert profound influence on the activity of the metal centre. The complexing ability of Schiff base is due to the presence of azomethine linkage. The azomethine group have a tendency to donate the lone pair of electrons present on the nitrogen atom of the azomethine moiety (C=N-). The presence of an acidic group like a phenolic OH or another donor group close to the azomethine group increases the coordinating effect of the lone pair of electrons, thereby increasing the stability of the metal complexes. The stability of Schiff base complex depends upon the strength of C=N

bond, the basicity of amino group and steric factors. The presence of an electron withdrawing ring system in the ligand decreases the availability of the lone pair of electrons.

The chemistry of metal complexes containing *salen*- type Schiff base ligands derived from condensation of salicylaldehyde and amines is of enduring significance, since they have common features with metalloporphyrins with respect to their electronic structures and catalytic activities that mimic enzymatic hydrocarbon oxidation.³³ The term “salen” was used originally to describe the tetradentate Schiff base derived from salicylaldehyde and ethylenediamine. Now this term is used in literature to describe the class of [O, N, N, O] tetradentate Schiff base ligands. Chiral salen type ligands upon coordination with metal ions can induce high stereoselectivity for organic transformations. The design and synthesis of these ligands play an important role in modern coordination chemistry. In this context, a lot of attention has been directed to chiral salens.^{13, 34-36}



Salens

The synthesis and structures of several metal complexes of these chiral ligands and the catalytic properties of such metal complexes toward various organic transformations are known. Chiral binaphthyl Schiff base ligands catalyze the stereo selective organic reactions like hydroxylation of styrene, aldol reactions and alkene epoxidation reactions.³⁷

As a major part of our present investigation is based on the synthesis and characterization of ruthenium and neodymium complexes of Schiff bases derived from quinoxaline, a brief discussion on these complexes is presented below.

1.1.2 Quinoxaline complexes

Diazines are a group of compounds derived from benzene by the replacement of the two ring C atoms by nitrogen. The benzo derivative of 1,4-diazine is known as quinoxaline. Diazines with two nitrogen atoms in the ring are aromatic. Quinoxaline^{38, 39} is commonly called 1,4-diazanaphthalene or benzopyrazine. Quinoxaline and its derivatives are mostly of synthetic origin. They are also used as reactive dyes and pigments, azo dyes, fluorescein dyes and it forms a part of certain antibiotics.⁴⁰ Quinoxaline has frequently been employed as a bridging ligand in both homobimetallic and heterobimetallic complexes.⁴¹ The X-ray structures of polymeric copper⁴² and silver⁴³ complexes containing bridging quinoxalines have been reported. A lot of work has been done on transition metal complexes of Schiff bases formed with quinoxaline-2-carboxaldehyde. Schiff bases with an electron withdrawing ring system derived from 3-hydroxyquinoxaline-2-carboxaldehyde would be weaker. However the increase in coordination sites increases the stability of the complexes by the chelate effect. Schiff bases derived from 3-hydroxyquinoxaline-2-carboxaldehyde with diamines forms quadridentate ligands. They bond through the carboxylic oxygen and azomethine nitrogen atoms. Transition metal complexes with N,N' bis(3-hydroxyquinoxaline-2-carboxaldehyde)-o-phenylenediamine and 3-hydroxyquinoxaline-2-carboxaldehyde-hydrazone gives valuable information on the structure and geometry .

Some quinoxaline derivatives are known to possess antibacterial activities. The quinoxaline antibiotics are found to possess activity against gram positive bacteria and certain tumours. They also inhibit RNA synthesis.²¹

1.1.3 Ruthenium complexes

Ru(III) complexes are generally low spin with one unpaired electron and possess octahedral geometry. Apart from compounds such as $[\text{RuCl}_2(\text{PPh}_3)_3]$ which is square pyramidal as the sixth coordinating position is blocked stereochemically, Ru(II)

compounds are octahedral and diamagnetic. Geometry of the complexes are reported to be tetrahedral, squarepyramidal and octahedral for coordination numbers 4,5,6 respectively.⁴⁴ Ruthenium also provides examples of binuclear compounds in which the metal is present in a mixture of oxidation states. Due to their increasing potential as versatile catalysts for organic synthesis and polymer chemistry, ruthenium complexes witnessed a spectacular development during the last decade. Several families of ruthenium compounds have been prepared and extensively used in a variety of chemical transformations such as hydrogenation,⁴⁵ hydration,⁴⁶ oxidation,⁴⁷ epoxidation,⁴⁸ isomerization,⁴⁹ decarbonylation,⁵⁰ cyclopropanation,⁵¹ olefin metathesis,⁵² Diels–Alder reaction,⁵³ enol-ester synthesis,⁵⁴ atom transfer radical polymerization.⁵⁵

Some of the novel ruthenium complexes are chiral⁵⁶ or immobilized on solid supports.⁵⁷ As result of their particular structure, these ruthenium complexes display an enhanced activity and selectivity in a multitude of organic transformations.⁵⁸ Significantly, some of the Schiff base ligands impart to the catalyst a good tolerance towards organic functionalities, air and moisture, in this way widening the area of their application.⁵⁹⁻⁶¹

Complexes with dibasic tridentate ligands are proved to be biological model compounds.⁶² The synthesis and characterization of some hexacoordinate octahedral complexes of Schiff bases derived from salicylaldehyde or o-vanillin with o-aminophenol and aminothiophenol are reported. These complexes are found to be toxic against bacterial species.⁶³ Ruthenium compounds are also known for their varied industrial applications.²⁹ The ruthenium(II) complexes are generally better catalysts for the homogeneous hydrogenation of alkenes^{64,65} and aldehydes.⁶⁶

For several reasons, Schiff bases have been found to be among the most convenient and attractive ligands for ruthenium complexes. The chemistry of organoruthenium compounds is of current interest in the synthesis,⁶⁷⁻⁶⁹ reactivity⁷⁰⁻⁷⁴ and

photophysical properties.^{75,76} Panda synthesized novel quinolin-8-olato chelated ruthenium organometallic complexes which are potentially luminescent in the visible region.⁷⁷ Firstly, steric and electronic effects around the ruthenium core can be finely tuned by an appropriate selection of bulky and/or electron withdrawing or donating substituents incorporated into the Schiff bases. Variation in coordination environment around ruthenium plays a key role in modulating the redox properties of its complexes. Secondly, the two donor atoms, N and O, of the chelated Schiff base exert two opposite electronic effects: the phenolate oxygen is a hard donor known to stabilize the higher oxidation state of the ruthenium atom whereas the imine nitrogen is a softer donor and accordingly, will stabilize the lower oxidation state of the ruthenium. Presence of nitrogen and oxygen donor atoms in the complexes are effective and stereospecific catalysts for oxidation,⁷⁸ reduction,⁷⁹ hydrolysis⁸⁰ and attributed to the carcinostatic, antitumour, antiviral and antibacterial activity.⁸¹ Thirdly, Schiff bases are currently prepared in high yield through one-step procedures via condensation of common aldehydes with amines, in practically quantitative yields.⁸² These are some of the reasons for the wide applicability of bidentate, tridentate and tetradentate Schiff base-ligated ruthenium complexes, as catalysts in numerous organic reactions.

Tetradentate Ru–salen⁸³ and Ru–porphyrin⁸⁴⁻⁸⁶ complexes, exhibit excellent activity and remarkably high enantioselectivity in catalyzing a variety of organic processes. Studies with ruthenium complexes containing salen-type ligands in the catalysis of organic hydroxylation reactions have been reported in the literature.^{87, 88} Reports show that hexacoordinated octahedral Ru(III) complexes of the type $[\text{RuX}_2(\text{PPh}_3)(\text{L})]$, where L is a monobasic tridentate ligand derived by the condensation of o-phenylenediamine or ethylenediamine with salicylaldehyde or o-hydroxyacetophenone act as effective catalysts for the oxidation of benzyl alcohol and cyclohexanol.⁸⁹ The so-called “dangling-ligands”, particularly those of salicylaldiminato-type, have been recently introduced in arene, alkylidene, indenylidene, vinylidene and diene ruthenium complexes.^{90, 91} In association with other commonly used ligands like chloride,

phosphane, imidazol-2-ylidene, cyclodienes, a novel class of ruthenium catalysts of versatile application and utility in organic synthesis and polymer chemistry have been prepared. This approach opens access to rather robust and quite stable catalysts at room temperature and highly active systems at slightly elevated temperatures that ideally promote several organic transformations such as olefin radical reactions for example, atom transfer radical addition (ATRA or Kharash addition) and atom transfer radical polymerization (ATRP) as well as alkyne dimerization and enol-ester syntheses

1.1.4 Neodymium complexes

Coordination chemistry of lanthanides is of special significance to a wide variety of chemical, biological and applied problems. The applications of macrocyclic Schiff base complexes of f-block metals in magnetic resonance imaging^{92,93} and encapsulated complexes in pharmaceuticals⁹⁴ have been reported. Schiff base derivatives of the TREN moiety $[N(CH_2CH_2NH_2)_3]$ with salicylaldehyde have proved to be very effective.⁹⁵ Williams and co-workers^{96, 97} demonstrated that lanthanide cations are excellent NMR probes of their immediate environment in enzymes. Lanthanide Schiff base complexes find varied applications in agriculture and medicine.⁹⁸⁻¹⁰⁰

Increased coordination numbers are seen in the case of the complexes of lanthanides. Coordinated complexes with even up to twelve coordination numbers have been reported in rare cases.¹⁰¹ In fact it is a challenge to prepare lanthanide complexes with low coordination numbers. Several lanthanide Schiff base complexes have been reported in the literature. The synthesis and spectral studies of lanthanide perchlorates with Schiff base derived from salicylaldehyde were reported. The metal ion in these complexes are seven coordinated.¹⁰² Complexes of neodymium(III) ions with macrocyclic ligands containing pyridine were prepared in which neodymium(III) ions act as templates for the cyclic condensation of organic carbonyl compounds with primary diamines.¹⁰³ Maurya *et al.* synthesized seven coordinate $[NdL_2(NO_3)_3]$ with ligands formed by the condensation of 4-antipyrenecarboxaldehyde and aromatic amines.¹⁰⁴ Lanthanide complexes are known to be the best non enzymatic agent which selectively

hydrolyze DNA and RNA with high specificity.¹⁰⁵⁻¹¹² The *in vivo* behavior of the lanthanide complex is very much dependent on the structure, the coordination number, the presence of coordinated water and the formation of poly nuclear species. Complexes derived from Schiff bases are important in biological field to understand chemistry of the biological systems particularly of enzymes. The studies on biological activity of $[\text{Nd}(\text{Phen})_2\text{Fu}-(\text{NO}_3)](\text{NO}_3)_2$ where Fu = 5-fluorouracil *in vitro* indicated that the complex posses good anticancer activity.¹¹³ These type of complexes were considered as models for study of the more complicated lanthanide-nucleic acid interactions.

The stability of the lanthanide complexes can be increased by means of chelate effect.¹¹⁴ Neodymium complex formed from hydrated Nd(III) nitrate with N,N'-disalicylideneethylenediamine in DMSO¹¹⁵ crystallizes in monoclinic system. Geometry of the crystallized complex is reported to be monocapped square antiprism, coordination number being nine.

1.2 Catalysis

Catalysis is now a relatively mature field with diverse reactions being explored along with informative studies of mechanism and theory. Applications to important areas such as heterogenous catalysis, organometallic chemistry and biocatalysis have been firmly established. Many Schiff base metal chelates catalyse reactions like hydrolysis, carboxylation, decarboxylation, elimination, aldol condensation, redox reactions.^{116, 117}

Molecular design techniques, in which organic and inorganic surfaces are chemically modified, revolutionized scientific world increasing their usefulness in catalytic field. The modified materials have considerable potential as alternatives to conventional homogeneous and heterogeneous catalysts. Scientists are in a way to explore new techniques and compounds which could give promising results in various biological and industrial field. Properties of the compounds are tuned by altering the positions and nature of atoms or radicals to satisfy our needs. This outlook has resulted in

the production of several compounds with wide range of applications in various fields. Literature survey supports this fact.

The purpose of the present work is to highlight the synthesis, characterization and some of the applications of Schiff base complexes as catalysts. The subject matter of this will consist of the comparative study of the neat, polymer supported as well as zeolite encapsulated complexes of ruthenium and neodymium to act as catalyst. Transition metal atoms have one s three p and five d orbitals those possess geometrical and energetic features suitable for bonding with ligands. In certain cases these nine orbitals permit the formation of the bonds with nine ligands. Complexes in which metals having high oxidation state can bind with the ligands in both covalent as well as coordinate fashion. This kind of versatility is the basis for the catalytic activity of transition metal complexes to a great extent. Upon coordination to a metal ion changes take place in the electronic distribution in a ligand, which result in the modification of the reactivity of the ligand molecules.

A compound is said to be coordinately saturated if the nine potentially bonding orbitals of a metal are completely filled. Such a compound would be stable toward nucleophilic attack on the metal because the added electrons will have to occupy orbitals at high energy. Therefore ligand substitution reactions in such cases proceed by S_N^1 type mechanism, that is one ligand dissociates from the complex resulting in a coordinately unsaturated species, a species having 16 electrons in the valence orbitals of the metal. The coordinately unsaturated complex would then bind with other potential ligands rather readily. This switching of electron count between 16 and 18 drives the catalytic cycle.¹¹⁸

There has been an upsurge of research in the area of catalysis by transition metal complexes since 1940s. The demand for cheaper and more efficient processes in the industry necessitated a major explosion of research in the area of synthetic chemistry to develop new systems that can act as catalysts. This also resulted in a rapid development

of newer process technologies relevant to industrial scale reactions for the production of organic compounds using transition metal complexes as catalysts. The notable contributions of Ziegler and coworkers in this area of chemistry fetched them the Nobel prizes in 1963 and 1973 respectively. Their pioneering work is the stepping stone for the development of homogeneous catalysis. A great number of soluble metal complexes are now being employed in industry as catalysts for the generation of a variety of useful compounds. More are being developed in order to find processes that would yield products in greater selectivity and purity in high yields with the advent of a variety of highly sophisticated and accurate spectroscopic techniques, the study of mechanisms of catalytic reactions has been made possible compared to earlier days. These techniques have in fact enhanced our understanding of the difficult chemistry involved in the catalytic processes.¹¹⁹ The metal ions that are catalytically active have two stable oxidation states created by one electron transfer reactions. For catalysis to occur there must be a chemical interaction between catalyst and reactant- product system, but this reaction must not change the chemical nature of the catalyst except at the surface. Transition metals which are resistant to oxidation act as good oxidation catalysts.

Homogeneous catalysts immobilized on an organic or inorganic support possess both experimental advantages of typical heterogeneous catalysts and the reactivity and selectivity of their homogeneous analogs. Immobilization of transition metal complexes provide a reliable route to a type of heterogeneous catalyst whose nature and mechanism may be more readily understood and offers ways to manipulate metal particle and crystallite size to achieve new types of catalytic reactions. By 1920, several significant contributions had been made to the study of heterogeneous catalysis. Heterogeneous catalysts have played a key role in the development of industrial processes for chemical industry. There are three general methods to heterogenize homogeneous catalysts: (i) by polymerization of homogeneous catalyst itself¹²⁰⁻¹²⁴ and thus making them insoluble in solvents (ii) by immobilization of homogeneous catalyst through covalent bonding with polymeric materials^{36, 125-127} (iii) by encapsulating them in the nanocavity of zeolites.¹²⁸⁻

¹³² Latter two methods provide additional characteristic properties such as activity, selectivity, thermal stability and reusability of the catalysts.

1.2.1 Zeolite encapsulated complexes

Zeolite encapsulated complexes are receiving wider attention in the field of catalysis. The zeolite pores act as reaction centers for binding and catalysis of molecules.^{133,134} The ligand molecules coordinated to the metal tunes the selectivity of the catalyzed reaction. Schiff base complexes are of particular importance in this area. Several zeolite encapsulated salen complexes of transition metals were synthesized and characterized.¹³⁵⁻¹³⁹ These complexes are known to be catalytically active in oxidation reaction.^{140,141} Copper(salen) complexes show enhanced catalytic activity¹⁴² towards the oxidation of cyclohexanol to cyclohexanone using H₂O₂ as oxidant. The replacement of aromatic hydrogen of the salen ligand with electron withdrawing groups like Cl, Br and NO₂ in copper(salen) complexes result in enhancement in retention and concentration of the complex in the zeolite cavities.¹⁴³

The NaY encapsulated Mn(III) Schiff base complexes show high activity and selectivity for the substrate and products in the aerobic epoxidation of 1-octene.¹⁴⁴ Mn(III) complexes of salen are reported to be effective homogeneous catalysts for the oxidation of olefins.^{12,13} The major drawback of O₂ catalysed oxidation using Mn salens in homogeneous solution is the formation of oxodimers and other polymeric Mn species which lead to irreversible catalyst deactivation. This problem may be avoided by isolating the Mn salen complexes from each other by encapsulation in the cavities of a molecular sieve. The greater stability of the encapsulated catalyst is attributed to the suppression of dimeric and other polymeric oxo complexes of Mn due to geometric constraints on their formation, on encapsulation in zeolites. Bowers and Dutta¹³⁶ studied the oxidation of cyclohexene, styrene and trans- and cis- stilbene over zeolite encapsulated Mn(III) salen complex. The rate of reaction is found to be lower compared to the homogeneous counterpart. This might be due to the diffusional constraints imposed by the zeolite pores

to prevent the substrate molecules from reaching the active sites located inside the supercage of zeolites. The chloro, bromo substituted salen complexes of Mn(III) catalyses the aerobic oxidation of styrene.¹⁴¹ Zeolite encapsulated Schiff base cobalt(II) complexes of salophen was found to be active in the ruthenium catalysed selective oxidation of benzyl alcohol to benzaldehyde with 99% selectivity.¹⁴⁵ Encapsulated copper(II) and dioxovanadium(V) complexes of Schiff bases derived from salicylaldehyde and 2-aminomethylbenzimidazole in the super cages of zeolite Y are effective catalysts for the oxidation of phenol and styrene using H₂O₂ as oxidant.¹⁴⁶

Liquid phase hydroxylation of phenol by molecular oxygen and H₂O₂ is an industrially important reaction. Several heterogeneous catalytic methods have been employed for the oxidation of phenol. In these cases high product selectivity is noted¹⁴⁷⁻¹⁵¹ Encapsulated metal complexes as catalysts play vital role in this regard.¹⁵²⁻¹⁵⁴ Maurya *et al.* reported oxidation of phenol using salen based transition metal complexes and found that selectivity towards the formation of catechol was *ca* 90% with [VO(salen)] encapsulated in zeolite Y.¹⁵⁵

Zeolite encapsulated Schiff base complexes can also act as catalysts for hydrogenation reactions.^{139,156-159} Although Pd(II)(salen) complex catalyses the hydrogenation of alkene, substrate selectivity is less.¹⁶⁰ But encapsulated Pd(II)(salen) complex¹³⁹ show selectivity towards the hydrogenation of linear alkene. Zeolite Y encapsulated Ni(salen) complexes were reported to have similar selectivity for the hydrogenation of hexene-1 in the presence of cyclohexene.¹⁵⁶

Several encapsulated complexes have been found to function as efficient catalysts^{139, 161-164} for several other reactions like watergas shift reaction, carbonylation of methanol and aromatic compounds, hydroformylation of alkenes. Zeolite Y encapsulated Co(II) Schiff base complex derived from 3,5-di-*tert*-butylsalicylaldehyde and 1,2-diaminobenzene was reported to be an efficient oxygen-activating catalyst in the

palladium-catalysed aerobic 1,4-diacetoxylation of 1,3-dienes.¹⁶⁵ The selectivity of the organic transformation was controlled by the homogeneous part while the heterogeneous part plays the role of oxygen activation.

1.2.2 Polymer supported complexes

Recent reviews reveal that modification of organic surfaces or organic polymers have been employed for developing new catalysts.¹⁶⁶⁻¹⁷⁰ The chemically modified polymers contain a ligand suitable for immobilization or “heterogenization” of a catalyst derived from a transition metal complex or metal cluster.^{166, 167} Of the various types of chemically modified organic polymers for use as catalysts divinylbenzene (DVB) crosslinked polystyrene has been the most widely used polymer. Crosslinked polystyrene is a valuable catalyst support since it is easily functionalized and available with a wide range of physical properties. Polymers offer several advantages as catalyst supports. The primary advantage of immobilization of these catalysts is their facile recovery and the ease with which the reaction products can be separated from the catalysts. In suitable cases, a polymer bound catalyst can be used in continuous processes in which the polymeric catalyst is used as a part of a fixed bed into which reactants enter and products exit. Other advantages of immobilized homogeneous catalyst over their analogs in solution include the possibility of not requiring solvent and the potential of increased catalyst stability. Another potential advantage would be the possibility of altering catalytic activity and selectivity.

Organic polymers can also be designed with certain other properties to improve the utility of the homogeneous catalyst after immobilization. For example, the flexibility of a crosslinked polymer and, in turn, the extent of interaction between reactive sites on which a polymer can be controlled either by varying the extent of cross linking in the polymer backbone or by changing the loading of the catalyst species on the polymer. Diffusion of reactants into a DVB-cross linked polystyrene bead containing a catalyst is dependent on the polymer’s pore size which depends partly on the extent of cross linking

and the nature of solvent swelling of the polymer. The result, in one example involving a polystyrene bound rhodium(1) complex catalyzed alkene hydrogenation, was a physical discrimination between different sized substrates by the polymer analogous to the shape selectivity seen with zeolite catalyst.¹⁷¹ In addition to the advantages associated with immobilizing homogeneous transition metal complexes on polymers for catalytic reactions, there are certain disadvantages. This include their lack of stability at high temperatures and their fragility- many polymers cannot be used in stirred reactors without being pulverized. It is difficult to determine the actual structures present on the heterogeneous material and the distribution of the reactive species in the solid polymer or on the surface.

Catalysts immobilized in an organic polymer network differ from their homogeneous counterparts because of the altered microenvironment within a polymer network relative to bulk solution. In cases where preexisting polymers are chemically modified to facilitate attachment of catalysts, the success of the reaction used to modify the polymer and the success of the reaction step in which the catalyst is bound to the polymer can also be problematic. Specific problems, which are not uncommon, include the presence of undesirable but unavoidable impurities as a result of side reactions, incomplete reactions or the formation of insoluble by-products. Further potential experimental problems, which often have to be considered, include the mechanical fragility of some organic polymer systems and the low thermal stability associated with organic polymers relative to inorganic refractory materials such as silica or alumina. This later property of organic polymers can pose serious experimental problems in exothermic reactions in which heat transfers from an organic polymer is not very efficient.

Modification of the surface of inorganic materials such as silica or alumina in order to transform such surfaces into catalyst is an alternative to modify organic polymer surfaces.^{166,167} Inorganic materials also offer certain advantages over organic materials in

some cases as a result of the properties of inorganic polymers. For example, inorganic materials are typically very thermally stable, these materials often possess highly ordered structures, and these materials can be obtained with both good mechanical stability and high surface areas.

The modification of surfaces in order to develop new types of catalysts has great promise. Although many problems remain unresolved, the potential of this area of chemistry has continued to attract attention from both industrial and academic laboratories. It is expected that future developments in this area will continue and that the combination of organic, inorganic and surface chemistry will produce new types of catalysts whose capabilities differ from those of conventional catalysts.

1.3 Scope of the present investigation

A review on literature reveals the influence of heterocyclic ligands in complexes especially in biological and catalytical field. Presence of heterocyclic ring as an integral part of the ligand system can influence the nature and electronic properties of the metal ion in the complex. Heterogenization of complexes improves the properties such as selectivity, ease of catalyst separation, recyclability, thermal stability etc. in catalysis. Immobilization of the complexes on polymer supports and encapsulation in zeolite cages has received much attention in industrial field recently. This has prompted us to direct our studies to this area of interest.

The main objectives of the present investigation are

- 1) Synthesis and characterization of some simple complexes of biologically important ligands.
- 2) Synthesis and characterization of analogous complexes encapsulated in zeolite cages.

- 3) Synthesis of some polymer supported complexes and study of their structural properties.
- 4) The application of the synthesized complexes as homogeneous/heterogeneous catalysts in certain organic reactions.
- 5) Screening of the synthesized simple complexes for antibacterial activity.

The study also aims at a comparison of catalytic and biological activities of ruthenium and neodymium in their complexes.

References

- [1] Williams R.J.P., *Polyhedron* **6**, 61 (1987).
- [2] Spiro T.G.,(Ed.), *Zinc Enzymes*, Wiley, New York (1983).
- [3] Williams R.J.P., *Nature* **338**, 709 (1989).
- [4] Hay R.W., in Williams D.R. (ed.), *An Introduction to Bioinorganic Chemistry*, Thomas, Springfield, U.S.A. (1976).
- [5] Tandon J.P.; Kiron; Singh, *Synth. React. Inorg. Met.-Org. Chem.* **16**, 1341 (1986).
- [6] Kandil S.S., *Trans. Met. Chem.* **23**, 461 (1998).
- [7] Dave L.D.; Thampy S.K.; Shelat, *J. Inst. Chem. (India)* **53**, 169, 237 (1981).
- [8] Singh H.; Yadav L.D.S.; Mishra S.B.S., *J.Inorg. Nucl. Chem.* **43**, 1701 (1981).
- [9] Albanus L.; Bjorklund B.; Gustafsson B.; Johnson M., *Acta Pharm. Toxic Suppl.* **26**, 93 (1975).
- [10] Bermejo M.R.; Sousa A.; Garcia-Deibe A.; Maneiro M.; Sanmartin J.; Fondo F., *Polyhedron* **18**, 511 (1998).
- [11] Casella L.; Gullotti M.; Vigano P.; *Inorg. Chim. Acta* **121**, 124 (1986).
- [12] Jacobsen E.N.; Deng L.; Furukawa Y.; Martinez L.E., *Tetrahedron* **50**, 4323 (1994).
- [13] Katasuki T., *Coord. Chem. Rev.*, **140**, 189 (1995).
- [14] Vinod K Sharma.; Shipra Srivastava, *Indian J. Chem.* **45A** (2006).
- [15] Witkop B.; Ramachandran L.K., *Metabolism* **13**, 1016 (1964).
- [16] Tovrog B.S.; Kitko D.J.; Drago R.S., *J. Am. Chem. Soc.* **98**, 5144 (1976).
- [17] Rips R.;Lachaize M.; Albert O.; Dupont M., *Chim.Ther.* **6**, 126 (1971); *Chem. Abstr.* **75**, 63675 (1971).
- [18] Rotmistrov M.M.; Kulik G.V.; Vasilevska I.O.; Stavska S.S.; Lisenko L.M.; Gorvonos T.V.; Skrinik E.M.; Shkovska D.F., *Mikrobiol. Nor. Gospad. Med. Mater. Zizdu. Ukr. Mikrobiol. Tov.* **1**, 189 (1965).; *Chem. Abstr.* **70**, 45132 (1969).
- [19] Lipkin A. E.; Chichkanova I. S.; Degtyarern T. A., *Khim. Fram. Zh.* **4**, 18 (1970); *Chem. Abstr.* **74**, 12725 (1971).

-
- [20] Sabnis S. S. ; Kulkarni K. D., *Indian J. chem.* **1**, 447 (1963).
- [21] Hodnett E.M.; Dunn W.J., *J.Med.Chem.* **13**, 768 (1970).
- [22] Hester R.E.; Nour E.M., *J. Raman Spectrosc.* **11**, 49 (1981).
- [23] Mahindra A.M.; Fisher J.M.; Rabinovitz, *Nature (London)* **303**, 64 (1983).
- [24] Palet P.R.; Thaker B.T.; Zele S., *Indian J. Chem.* **38 A**, 563 (1999).
- [25] Herron N., *Chemtec.* **542** (1995).
- [26] Toscano P.J.; Marzilli L.G., *Prog. Inorg. Chem.* **31**,105 (1984).
- [27] Fakhr I.M.I.; Hamdy N.A.; Radwan M.A.; Ahmed Y.M., *Egypt. J. Chem.* **201** (2004).
- [28] Dixit P.S.; Srinivasan K., *Inorg. Chem.* **27**, 4507 (1988).
- [29] Coucouvanis, *Prog. Inorg. Chem.***26**, 301 (1979).
- [30] Nour E.M.; Taha A.A.; Alnaimi I.S.; *Inorg. Chim. Acta* **141**, 139 (1988).
- [31] Nour E.M.; Al-Kority A.M.; Sadeek S.A.; Teleb S.M., *Synth. React. Inorg. Met.-Org. Chem.* **23**, 39 (1993).
- [32] Wang W.; Zeng F. L.; Wang X.; Tan M. Y, *Polyhedron* **15**, 1699 (1996).
- [33] Groves J.T.; In: P. Ortiz de Montellano (Ed.), *Cytochrome P-450: Structure, Mechanism and Biochemistry* Plenum Press, New York, **7**, 1 (1986).
- [34] Jacobsen E.N., in: E.W. Abel, F.G.A. Stone, G. Wilkinson (Eds.), *Comprehensive Organometallic Chemistry II*, vol. 12, Pergamon,Oxford, 1097 (1995).
- [35] Bedioui F., *Coord. Chem. Rev.* **144**, 39 (1995).
- [36] Canali L.; Sherrington D.C., *Chem. Soc. Rev.* **28**, 85 (1999).
- [37] Chi-Ming Che.; Jie-Sheng Huang, *coord. Chem. Rev.* **242**, 97 (2003).
- [38] Cheesman G.W.H.; Cookson R. F, in "The chemistry of Heterocyclic Compounds", ed., Weissberger A. and Taylor E.C., vol.35, John Wiley, New York (1979).
- [39] Simpson J.C.E, "Condensed Pyradazine and Pyrazine rings", Interscience, New York (1953).
- [40] Raj K Bansal, "Heterocyclic Chemistry, Synthesis, Reactions & Mechanisms", Wiley Eastern Limited (1990).
-

-
- [41] Kaim W.; *Angew. Chem. Int. Ed. Eng.* **22**, 171 (1983).
- [42] Lumme P.; Lindroos S.; Lindell F, *Acta Crystallogra. C* **43**, 2053 (1987)
- [43] Tsuda T.; Ohba S.; Takahashi M.; Ito M, *Acta Crystallogra C* **45**, 887 (1989).
- [44] Greenwood N.N.; Earnshaw A., *The Chemistry of elements*, Maxwell Macmillan International Editions (1989).
- [45] Clapham S.E.; Hadzovic A.; Morris R.H.; *Coord. Chem. Rev.* **248**, 2201 (2004).
- [46] Tokunaga M.; Suzuki T.; Koga N.; Fukushima T.; Horiuchi A.; Wakatsuki Y., *J. Am. Chem. Soc.* **123**, 11917 (2001).
- [47] Ramesh R., *Inorg. Chem. Commun.* **7**, 274 (2004).
- [48] Shrikanth A.; Nagendrappa G.; Chandrasekaran S., *Tetrahedron* **59**, 7761 (2003).
- [49] Antonya R.; Tembea G.L.; Ravindranathana M.; Ramb R.N.; *Polymer* **39**, 4327 (1998).
- [50] De Vries J.G.; Roelfes G.; Green R., *Tetrahedron Lett.* **39**, 8329 (1998).
- [51] Lebel H.; Marcoux J.F.; Molinaro C.; Charette A.B., *Chem.Rev.* **103**, 977 (2003).
- [52] Furstner A. (Ed.), *Alkene Metathesis in Organic Synthesis*, Springer, Berlin, 1998.
- [53] Odenkirk W.; Reingold A.L.; Bosnich B., *J. Am. Chem. Soc.* **114**, 6392 (1992).
- [54] De Clercq B.; Verpoort F., *Adv. Synth. Catal.* **344**, 639 (2002).
- [55] Kamigaito M.; Ando T.; Sawamoto M., *Chem. Rev.* **101**, 3689 (2001).
- [56] Perry M.C.; Burgess K., *Tetrahedron: Asymm.* **14**, 951 (2003).
- [57] Beerens H.I.; Verpoort F.; Verdonck L., *J. Mol. Catal. A: Chem.* **151**, 279 (2000).
- [58] Doyle M.P.; McKervey M.P.; Ye T., *Modern Catalytic Methods for Organic Synthesis with Diazo Compounds*, Wiley, New York, 1998.
- [59] Schwab P.; Grubbs R.H., Ziller J.W, *J. Am. Chem. Soc.* **118**, 100 (1996).
- [60] Nguyen S.T.; Johnson L.K.; Grubbs R.H.; Ziller J.W., *J. Am. Chem. Soc.* **114**, 3974 (1992).
- [61] Fu J.C.; Nguyen S.T.; Grubbs R.H., *J. Am. Chem. Soc.* **115**, 9856 (1993).
- [62] Banbe W.; Fliegner J.; Sawusch S.; Schilde U.; Uhlemann E., *Inorg.Chim.Acta* **269**, 350 (1998).
-

-
- [63] Jayabalakrishnan C.; Natarajan K.; *Trans. Met. Chem.* **27**, 75 (2002).
- [64] Huh S.; Cho Y.; Jun M.J.; Whang D.; Kim K., *Polyhedron* **13**, 1887 (1994).
- [65] Huh S.; Sung K.M.; Cho Y.; Jun M.J.; Whang D.; Kim K., *Polyhedron* **15**, 1473 (1996).
- [66] Na K.I.; Huh S.; Sung K.M.; Cho Y.; Jun M.J., *Polyhedron* **15**, 1841 (1996).
- [67] Cabeza J.A.; Rio I.D.; Granda S.G.; Riera V.; Suarez M., *Organometallics* **21**, 2540 (2002).
- [68] Poyatos M.; Mata J.A.; Falomir E.; Crabtree R.H.; Peris E., *Organometallics* **22**, 1110 (2003).
- [69] Perez J.; Riera V.; Rodriguez A.; Miguel D., *Organometallics* **21**, 5437 (2002).
- [70] Ghosh K.; Pattanayak S.; Chakravorty A., *Organometallics* **17**, 1956 (1998).
- [71] Ghosh K.; Chattopadhyay S.; Pattanayak S.; Chakravorty A., *Organometallics* **20**, 1419 (2001).
- [72] Ferstl W.; Sakodinskaya I.K.; Sutter N.B.; Borgne G.L.; Pfeiffer M.; Raybovad., *Organometallics* **16**, 411 (1997).
- [73] Panda B.K.; Chattopadhyay S.; Ghosh K.; Chakravorty A., *Organometallics* **21**, 2773 (2002).
- [74] Ritleng V.; Pfeiffer M.; Sirlin C., *Organometallics* **22**, 347 (2003).
- [75] Yam V.W.W.; Chu B.W.K.; Ko C.C.; Cheung K.K., *J. Chem. Soc. Dalton Trans.* 1911 (2001).
- [76] Yam V.W.W.; Chu B.W.K.; Cheung K.K., *J. Chem. Soc. Chem. Commun.* 2261 (1998).
- [77] Panda B.K., *J. Chem. Sci.* **116**, 245 (2004).
- [78] Kureshy R.I.; Khan N.H.; Abdi S.H.R.; Petel S.T.; Iyer P., *J. Mol. Catal.* **150**, 175 (1999).
- [79] Ama Y.; Kujisawa J.T.; Walanawe T.; Toi A.; Ogashi H., *J. Am. Chem. Soc.* **108**, 943 (1986).
- [80] Sdrawn R.S.; Zamakani M.; Cocho J.L., *J. Am. Chem. Soc.* **108**, 3510 (1986).
- [81] Viswanathamurthi P.; Natarajan K., *Trans. Met. Chem.* **24**, 638 (1999).

-
- [82] Vigato P.A.; Tamburini S., *Coord. Chem. Rev.* **248**, 1717 (2004).
- [83] Miyata A.; Furakawa M.; Irie R.; Katsuki T., *Tetrahedron Lett.* **43**, 3481 (2002).
- [84] Galardon E.; Le Maux P.; Toupet L.; Simonneaux G., *Organometallics* **17**, 565 (1998).
- [85] Zhang. J. L.; Chan P.W.H.; Che C. M., *Tetrahedron Lett.* **44**, 8733 (2003).
- [86] Simonneaux G.; Galardon E.; Paul-Roth C.; Gulea M.; Mas-son S., *J. Organometall. Chem.* **617**, 360 (2001).
- [87] Leung W. H.; Che C. M., *Inorg.Chem.* **28**, 4619 (1989).
- [88] Takeda T.; Irie R.; Katsuki T., *Synlett.* **7**, 1166 (1999).
- [89] Saridha K.; Karvembu R.; Viswanathamurthi P.; Yasodhai S., *Synthesis and Reactivity in Inorganic, Metal-Organic, and Nano-Metal Chemistry* **35**, 707 (2005).
- [90] De Clercq B.; Verpoort F., *Tetrahedron Lett.* **42**, 8959 (2001).
- [91] De Clercq B.; Verpoort F., *J. Mol. Catal. A: Chem.* **180**, 67 (2002)
- [92] Caravan P.; Ellison J.J.; McMurry T.J.; Lauffer R.B., *Chem. Rev.* **99**, 2293 (1999).
- [93] Smith P.H.; Brainarc J.R.; Morris D.I.; Jarvinen G.O.; Ryan R.R., *J. Am.Chem. Soc.* **111**, 7437 (1989).
- [94] Coulais Y.; Cros G. Darbieu M.H.; Tafani J.A.M.; Belhadj Tahar H ; Bellande E.; Pasqualini R.; Guitaud R., *Nucl. Med. Biol.* **21**, 263 (1994).
- [95] Michael W. Basig ; Webster Keogh D.; Brian L. Scott; John G Watkin, *Polyhedron* **20**, 373 (2001).
- [96] Williams R.J.P.; Quart , *Rev. Chem. Soc. (London)* **XXIV**, 231 (1970).
- [97] Morallee K.G.; Nieboer E.; Rossotti F.J.C.; Williams R.J.P.; Xavier A.V., *Chem. Commun.*, 1132 (1970).
- [98] Mayadeo M.S.; Nalgoikar, *J.Inst. Chem. (India)*, **60**, 139 (1988).
- [99] Doreth L.; Sitran S.; Madalssso F.; Bandoli.G.; Palocci, *J.Inorg. Nucl. Chem.* **42**, 106 (1980).
- [100] Tschudisteiner I.; *Pharm. Acta. Helv.* **33**, 105, (1958).
-

-
- [101] Jorgensen C.K.; Baker E.C.; Halstead G.W.; Raymond K.N.; Sinha S.P., Structure and Bonding-25 ; Rare Earths, Springer-Verlag, Berlin Heidelberg, New York (1976).
- [102] Ramachandra B.; Narayana B., Indian J. Chem. **38A**, 1297 (1999).
- [103] Bastida; Rufina; de Blas; Andres; Castro; Pilar; Fenton; David E.; Macias; Alejandro; Rial; Rita; Rodriguez; Adolfo; Rodriguez-Blas; Tereqsa, J.Chem. Soc. Dalton Trans. **8**, 1493 (1996).
- [104] Maurya R.C.; Varma R.; Shukla P.; J. Indian Chem. Soc. **74**, 789 (1997).
- [105] Roig A.; Hettich R.; Schneider H., J.Inorg. Chem. **37**, 751 (1998).
- [106] Oh S.J.; Song K.H.; Whang D.; Kim K.; Yoon T.H.; Moon H.; Park J.W., Inorg. Chem. **35**, 378 (1992).
- [107] Morrow J.R.; Buttrey L.A.; Shelton V.M.; Berback K.A., J. Am.Chem. Soc. **114**, 1903 (1992).
- [108] Takasaki B.K.; Chin J., J. Am. Chem. Soc. **115**, 9337 (1993).
- [109] Jurek P.E.; Jurek A.M.; Martell A.E., Inorg. Chem. **39**, 1016 (2000).
- [110] Komiyama M.; Takeda N.; Shigekawa H., Chem. Commun. 1443 (1999).
- [111] Hurst P.; Takasaki B.K.; Chin J., J. Am. Chem. Soc. **118**, 9982 (1996)
- [112] Wang R.; Liu H.; Carducci M.D.; Jin T.; Zheng C.; Zheng Z., Inorg.Chem. **40**, 2743 (2001).
- [113] Lin Jiyun; Mo.Dejian; Zhong Wenyuan, Peop. Rep. China Zhong guo Xitu Xuebao, **14**, 193 (1996).
- [114] Moeller T.; Martin D.F.; Thompson L.C.; Ferrus R.; Feistel G.R.; Randall W., J. Chem. Rev. **65**, 1 (1965).
- [115] Yan Janangli ; Kong; Fanrong; Mao Xian; Peop. Ep. China, Bopuxue Zazhi **14** (3), 229 (1977).
- [116] Hussain Reddy K.; Lingappa Y., Ind.J.Chem. **37A**, 1133 (1998).
- [117] Singh B.; Praveen K.; Singh, Ind. J. Chem. **37A** (1991).
- [118] Parshall G W.; Ittel S. D., Homogenous catalysis 2nd edition, wiley, New York (1996).
-

-
- [119] ch Elschentreich ; Salzer A., Organometallics, 2nd edition, wiley, New York (1996).
- [120] Ando R.; Ono H.; Yagyu T.; Maeda M., Inorg.Chim.Acta **357**, 817 (2004).
- [121] Ando R.; Mori S. Hayashi M.; Yagyu T.; Maeda M., Inorg.Chim.Acta, **357**, 1177 (2004).
- [122] Maurya M.R.; Jain I.; Titinchi S.J., J. Appl. Catal. A: Gen. **249**, 139 (2003).
- [123] Maurya M.R.; Kumar A.; Manikandan P.; Chand S., Appl. Catal. A; Gen. **277**, 45 (2004).
- [124] Maurya M.R.; Kumar A., J. Mol. Catal. A: Chem. **250**, 190 (2006).
- [125] Sherrington D.C., Pure Appl. Chem. **60**, 401 (1988).
- [126] Karjalainen J.K.; Hormi O.E.O.; Sherrington D.C, Molecules **3**, 51 (1998).
- [127] Sherrington D.C., Catal. Today **57**, 87 (2000).
- [128] Rafelt G.S.; Clark J.H., Catal. Today **57**, 3 (2000).
- [129] Sheldon R.A.; Arends I.W.C.E.; Dijksman A., Catal. Today **57**, 157 (2000).
- [130] Jacob C.R.; Varkey S.P.; Ratnasamy P., Microporous Mesoporous Mater. **22**, 465 (1998).
- [131] Hutchings G.J., Chem. Commun. 301 (1999).
- [132] Maurya M.R.; Titinchi S.J.J.; Chand S., J. Mol. Catal. A: Chem. **214**, 257 (2004).
- [133] Lungford J.H., Catal. Rev. Sci. Eng., **12**, 137 (1975).
- [134] Romanovsky B.V.; Yu Zakharov V.; Borisova T.G., Moscow Univ. Publ., **170** (1982).
- [135] Herron N., Inorg. Chem., **25**, 4714 (1986).
- [136] Bowers C.; Dutta P.K., J. catal. **122**, 271 (1990).
- [137] Gaillon L.; Sajot N.; Bedioui F.; Devynck J.; Balkus K.J. Jr. J. Electroanal. Chem. **345**, 157 (1993).
- [138] Balkus K.J. Jr.; welch A.A.; Gnade B.E., Zeolites **10**, 722 (1990).
- [139] Kowalak S.; Weiss R.C.; Balkus. K.J. Jr, J.Chem.Soc., Chem.Comm. **57** (1991).
- [140] Koner S., Chem. Commun. **595** (1998).
- [141] Varkey S.P.; Jacob C.R., Ind. J. Chem., **37A**, 407 (1998).

-
- [142] Ratnasamy C.; Murugkar A.; Padhye S., *Ind. J. Chem.*, **36A**, 1 (1996).
- [143] Jacob C.R. ; Varkey S.P.;Ratnasamy P., *Appl. Catal.* **168**, 353 (1998).
- [144] Rong-Min Wang; Hui-Xia Feng;Yu-Feng He; Chun-Gu Xia; Ji-Shuan Suo;Yun-Pu Wang, *J. Mol. Catal. A Chem.* **151**, 253 (2000).
- [145] Zsigmond A.; Notheisz F.; Frater Z.; Backvall J.E., in *Heterogeneous Catalysis and Fine Chemicals IV*, (Eds.) Blaser H.U.; Baiker A.; Prins R.; **453** (1997).
- [146] Maurya M.R.; AnilK. Chandrakar; Shri Chand, *J. Mol. Catal. A. Chem.* **263**, 227 (2006).
- [147] Sheldon R A.; Vansnaten R.A., *Catalytic Oxidation, Principles and Applications*, World Scientific, Singapore (1995).
- [148] Taramasso M.; Perego G.; Notari B., *US Patent* **4**, 410, 501 (1983).; Taramasso M.; Manara G.; Fattore V.; Notari B., *US Patent* **4**, 666, 692 (1987).
- [149] Yokoi T.; Wu P.; Tatsumi T., *Catal. Commun.* **4**, 11 (2003).
- [150] Perego C.; Carati A.; Ingallina I.; Mantegazza M.A.; Bellussi G., *Appl. Catal. A.Gen.* **221**, 63 (2001).
- [151] Zhang H.; Zhang X.; Ding Y.; Yan L.; Ren T.; Suo J., *New J. Chem.* **26**, 376 (2002).
- [152] Balkus K.J. Jr.; Gabelov A.G., *J. Inclusion Phenom. Mol. Recogn. Chem.* **21**, 159 (1995).
- [153] Raja R.; Ratnasamy P., *Stud. Surf. Sci. Catal.* **101**, 181 (1996).
- [154] Seelan S.; Sinha A.K.; Srinivas D.; Sivsanker S.,*Bull.Catal. Soc. India* **1**,29 (2002).
- [155] Maurya M.R.; Kumar.M. Titinchi S.J.J.; Abbo H.S.; Chand S., *Catal. Lett.* **86**, 97 (2003).
- [156] Chatterjee D.; Bajai H.C.; Das A.; Bhatt K., *J. Mol. Catal.*, **92**, 235 (1994).
- [157] Thibault-Starzyk F.; Parton R.F.; Jacobs P.A., *Stud. Surf. Sci. and Catal.*, **84B**, 1419 (1994).
- [158] De Vos E.D.; Jacobs P.A., "Proceedings from the Nineth International zeolite Conference", Von Ball Moos R.; Higgins J.B.; Treacy M.M.J., (Eds.)
-

-
- Butterworth-Heinemann, Boston **2**, 615 (1993).
- [159] Zakharov A.N., Mendeleev Commun. **80** (1991).
- [160] Henrici-Olive G.; Olive S., J. Mol. Catal. **76**,1, 121 (1975).
- [161] Jacobs P.A.; Chantillon R.; Dhaet P.;Verdonek J.; Tilem M., ACS. Symp. Ser.,**218**, 439 (1983).
- [162] Auroux A.; Bolis V.; Wierzchowski P.; Gravelle P.; Vedrine J.,J. Chem. Soc. Faraday Trans., **2**, 75, 2544 (1979).
- [163] Iwamoto M.; kusano H.; Kagawa S., Inorg. Chem., **22**, 3366 (1983).
- [164] Mantovani E.; Palladino N.; Zarrobi A., J. Mol. Catal. **3**, 285 (1977).
- [165] Woltinger J.; Backvall E.; Zsigmond A., Chem. Eur. J. **5**, 1460 (1997).
- [166] Bailey D C; Langer S .H., Chem. Rev. **81**, 109 (1981).
- [167] Whitehurst D. D., Chemtech 44 (1980).
- [168] Regen S.L., Angew chem. Int. Ed. Eng. **18**, 421 (1979).
- [169] Hodge P.; Sherrington D. C., "Polymer Supported Reactions in Organic Synthesis"; J. Wiley and Sons, Ltd. : London: (1980).
- [170] Mathur N. K; Narang C.K.; Williams D.R., "polymers as Aids in Organic Chemistry"; Academic Press : New York, (1980).
- [171] Grubbs R.H.; Kroll L.C., J.Am.Chem. Soc. **93**, 3062 (1971).

CHAPTER II

MATERIALS AND METHODS

This chapter provides details of the general reagents and preparation of the ligands used in the present study. A brief account of the various analytical and physicochemical techniques employed in the characterization and catalytic studies are also discussed.

2.1 Reagents

o-Phenylenediamine (Loba Chemie), sodium pyruvate (Loba chemie) bromine, glacial acetic acid, precipitated CaCO_3 (Merck), sodium bicarbonate (Merck), sodium chloride (Merck), salicylaldehyde (Merck), 2-aminobenzimidazole (Merck), 2-aminophenol (Merck), $\text{RuCl}_3 \cdot 3\text{H}_2\text{O}$ (Merck) and neodymium oxide (Indian Rare Earths Ltd.) were used in the present investigation. All materials used were of the highest purity available and were used without further purification.

Phenol, catechol and hydrogen peroxide (30% aqueous solution) used for the catalytic as well as kinetic studies were obtained from Merck. All other reagents employed in the present study were of analytical reagent grade. Solvents employed were either of 99% purity or purified by known laboratory procedures.¹

2.2 Synthesis of Ligands

Crude o-phenylenediamine was dissolved in distilled water. Activated charcoal was added to this, boiled, filtered and allowed to cool. The recrystallized sample was separated by filtration and dried.

3-Hydroxy-2-methyl quinoxaline

Recrystallized o-phenylenediamine (0.1 mol, 10.8 g) and sodium pyruvate (0.1 mol, 11.0 g) were dissolved in 250 mL water each. Concentrated HCl (~11 mL) was

added to convert sodium pyruvate to pyruvic acid. The two solutions were then mixed and stirred for about 30 minutes. The precipitated yellow compound was filtered, washed with water and dried over anhydrous calcium chloride (yield = 90%, m.p. 255°C).

3-Hydroxy-2-dibromo methyl quinoxaline

3-Hydroxy-2-methyl quinoxaline (0.1 mol, 16.2 g) was dissolved in glacial acetic acid (200 mL), and 10% (v/v) bromine in acetic acid (110 mL) was added with stirring. The reaction mixture was then kept in sunlight for 1 h with occasional stirring. This was then diluted to 1 L and the precipitated dibromo derivative was filtered, washed with water and purified by crystallization from 50% alcohol (yield : 95%, m.p. 246°C).

3-Hydroxyquinoxaline-2-carboxaldehyde

The dibromo compound (5 g) was thoroughly mixed with precipitated calcium carbonate (20 g). This mixture was treated with water (1.5 L) in a 3 L RB flask and heated over water bath for 2 h with occasional shaking. As the aldehyde formed is soluble in water, the solution was collected by filtering hot. The yellow aqueous solution thus obtained is very stable and this solution has been used for the preparation of the Schiff bases.

2.2.1 N,N'-Bis(3-hydroxyquinoxaline-2-carboxalidene)-o-phenylenediamine (qpd)

The aldehyde solution was made 0.025 molar with respect to HCl. An aqueous solution of o-phenylenediamine (2 g in 20 mL water) was added to this drop by drop while the solution was stirred. The amine solution was added till the precipitation of Schiff base was completed. The reddish brown compound thus obtained was filtered, washed with methanol and dried in *vacuo* over anhydrous phosphorus(V) oxide (yield: 60-70%, m.p: 225°C).

2.2.2 3-Hydroxyquinoxaline-2-carboxalidene-o-aminophenol (qap)

An aqueous solution of o-aminophenol (2 g in 20 mL of water) was added to the aldehyde solution. The amine solution was added till the precipitation of Schiff base was completed. The orange red compound thus obtained was filtered, washed with methanol and dried in *vacuo* over anhydrous phosphorus(V) oxide (yield = 75% m.p : 140°C).

2.2.3 3-Hydroxyquinoxaline-2-carboxalidene-2-aminobenzimidazole (qab)

Quinoxaline aldehyde was made 0.025 M with respect to HCl. An aqueous solution of 2-aminobenzimidazole (1.5 g in 20 mL hot water) was added to this drop by drop while the solution was stirred for 30 minutes. The precipitated Schiff base was filtered, washed with hot water and dried in *vacuo* over anhydrous phosphorus(V) oxide (yield = 65% m.p : 205°C).

2.2.4 N,N'- Bis(salicylaldimine)-o-phenylenediamine (salpd)

Recrystallized o-phenylenediamine was refluxed with methanolic solution of salicylaldehyde in the ratio 1:2 for 30 minutes. The volume of the solution was reduced by distillation of the solvent. The yellow solid formed was filtered, washed several times with methanol and dried under vacuum over phosphorous(V) oxide (yield : 75% m.p : 145°C).

2.2.5 Salicylaldimine- o-aminophenol (salap)

Amino phenol (10.9 g) was dissolved in methanol (75 mL) by heating on a boiling water bath. Then it was boiled for about 10 minutes and salicylaldehyde (12.2 g) in methanol (25 mL) was added to it. The resulting solution was refluxed on a water bath for a period of 30-40 minutes. The volume of the solution was reduced by distillation of the solvent. The orange red coloured solid formed was filtered, washed several times with methanol and ether. Then it was dried under vacuum over phosphorous(V) oxide (yield : 90% m.p : 175°C).

2.2.6 Salicylaldimine-2-aminobenzimidazole (salab)

Aminobenzimidazole (1.33 g) was dissolved in methanol (25 mL) by heating on a boiling water bath. Then it was refluxed for about 10 minutes and salicylaldehyde (1.22 g) in methanol (25 mL) was added to it. The resulting solution was refluxed on a water bath for a period of 8 h. The volume of the solution was reduced by distillation of the solvent and cooled in ice. The yellow colored solid formed was filtered, washed several times with cold water. Then it was dried under vacuum over phosphorous(V) oxide (yield : 75% m.p : 200°C).

2.3 Supports used

2.3.1 Zeolite-Y

Synthetic Y-zeolite (in powder form) was obtained from Zeolyst International, Netherlands.

Modification of Y-zeolite

Preparation of sodium exchanged zeolite (NaY)

Zeolite-Y (5.0 g) was stirred with a solution of NaCl (0.1 M, 500 mL) for 24 h to convert any other ions if present into Na⁺ ions. It was then filtered and made chloride free by washing with distilled water.² The NaY formed was dried at 100°C for 2 h.

Preparation of metal exchanged zeolite (RuY and NdY)

The incorporation of metal ions into the zeolite matrix is a prerequisite for encapsulation of metal complexes in the zeolite cages. Sodium exchanged zeolite (5 g) was stirred with metal chloride solution (0.001 M) at 70°C for 4 h. Low concentration of metal salt solution was used as dealumination occurs at higher concentrations.³ The slurry was filtered and washed with deionised water to make it free from anions. It was then dried at 120°C for 1h and then at 450°C for 4 h.

2.3.2 Polystyrene beads

Chloromethylated polystyrene beads of 200-400 mesh size cross-linked with 2% divinylbenzene and containing 12% chlorine (Fluka) were functionalized with aldehyde group according to the reported procedure.⁴ A mixture of chloromethylpolystyrene (20.0 g), dimethylsulphoxide (300 mL) and sodium bicarbonate (19.0 g) was stirred at 138-140°C for 12 h. The resultant resin was filtered, washed with hot ethanol and methylene chloride. It was then dried in *vacuo* over anhydrous calcium chloride.

2.4 Preparation of polymer bound Schiff base

2.4.1 Preparation of polymer bound Schiff base with o- phenylenediamine (PS-opd)

Polymer bound aldehyde (10.0 g) was swollen in dioxan (50 mL) for 24 h. Afterwards dioxan was decanted off and o-phenylenediamine (2.0 g) in absolute ethanol was added. This mixture was refluxed on a water bath for 10 h. The polymer bound Schiff base was filtered, washed several times with dioxan and ethanol and dried in *vacuo* over anhydrous calcium chloride.⁵

2.4.2 Preparation of polymer bound Schiff base with o-aminophenol (PS-ap)

Polymer bound aldehyde (10.0 g) was swollen in dioxan (50 mL) for 24 h. Afterwards dioxan was decanted off and o- aminophenol (4.0 g) in absolute ethanol was added. This mixture was refluxed on a water bath for 10 h. The polymer bound Schiff base was filtered, washed several times with dioxan and ethanol and dried in *vacuo* over anhydrous calcium chloride.

2.4.3 Preparation of polymer bound Schiff base with 2-aminobenzimidazole (PS-ab)

Polymer bound aldehyde (10.0 g) was swollen in dioxan (50 mL) for 24 h. Afterwards dioxan was decanted off and 2-aminobenzimidazole (4.0 g) in absolute ethanol was added. This mixture was refluxed on a water bath for 10 h. The polymer

bound Schiff base was filtered, washed several times with dioxan and ethanol and dried in *vacuo* over anhydrous calcium chloride.

2.5 Analytical methods

A variety of techniques have been employed to characterize the synthesized complexes and to follow the course of the catalytic reactions of the prepared compounds.

2.5.1 CHN analysis

CHN analyses of the synthesized ligands, neat complexes and supported complexes were done on an Elementar model Vario EL III at SAIF, Sophisticated Test and Instrumentation Centre, Kochi. These analytical data provide information about the structure of the ligands and help to quantify the organic ligands complexed to the metal ion.

2.5.2 Chemical analysis

The metal percentage present in the neat complexes were determined by ICP-AES spectrometer (Thermo Electron, IRIS Intrepid II XSP DUO) at SAIF, Sophisticated Tests and Instrumentation Centre, Kochi. The solutions of the neat complexes were prepared in nitric acid after digesting it with concentrated nitric acid several times.

Organic part of the polymer samples was decomposed by digesting in microwave digester at high temperature. The metal content was then determined by ICP-AES method.

Chemical analysis was done to determine the composition of the zeolite samples. The dried zeolite sample was accurately weighed ('x' g) and transferred to a beaker. Conc.Sulphuric acid (~ 40 mL) was added and heated until SO₃ fumes were evolved. It was diluted with water (200 mL) and filtered through an ashless filter paper (filtrate A). The residue was dried at 1000°C in a platinum crucible, cooled and weighed ('a' g).

Hydrofluoric acid (10 mL) was then added and evaporated and finally ignited to 1000°C ('b' g). The percentage of silica (SiO₂) was calculated using the equation

$$\% \text{ SiO}_2 = \frac{a-b}{X} \times 100$$

Potassium persulphate was added to this residue and heated until a clear melt was formed. The melt was dissolved in water and this solution was combined with filtrate A. The metals present in this solution were determined by ICP-AES method. The degree of ion exchange in zeolite and the unit cell formula are derived from Si/Al ratio.⁶ The Si/Al ratio of the zeolite complexes was compared with that of pure zeolite to make sure that the frame work was preserved on encapsulating complexes.

2.6 Physico-chemical methods

2.6.1 Surface area analysis

Surface area of the samples was measured by multipoint BET method using a Micromeritics Gemini 2360 surface area analyzer. Nitrogen gas was used as the adsorbate at liquid nitrogen temperature. Surface area measurements have been carried out to know whether the encapsulation of guest molecules inside zeolite cages or anchoring of complexes on polymer supports has occurred. A lower surface area of intrazeolite complex as compared to metal exchanged zeolite indicates the filling of zeolite pores with complexes.

2.6.2 Magnetic susceptibility measurements

Magnetic susceptibility measurements were done at room temperature on a PAR model 155 Vibrating Sample Magnetometer (VSM) at 5.0 kOe field strength at Indian Institute of Technology, Roorkee. The method involves moving the magnetized sample to be measured in a periodic manner at small amplitude and detecting the periodic field change produced by the moving sample. This periodic field change is proportional to the

magnetic moment of the sample. Gram susceptibility is calculated by dividing the susceptibility value by weight of the sample. Molar susceptibility is calculated by using the formula

$$\chi_M = \mu M/W_X .$$

$$\mu_{BM} = 2.828 \sqrt{\chi_M \times T/5 \times 10^3}$$

where T is the temperature in Kelvin and M is the molecular weight.

2.6.3 Thermogravimetry

Thermogravimetric analyses were done on a Perkin Elmer, Diamond TG/DTA at a heating rate of $10^\circ\text{C min}^{-1}$ in an inert atmosphere.

2.6.4 Conductance measurements

The molar conductance of the simple complexes was determined at room temperature in methanol (10^{-3} M) using a Centry CC 601 digital conductivity meter with a dip type cell and a platinum electrode.

2.6.5 SEM

The morphology of the samples was examined using JEOL-JSM-840 A scanning electron microscopy at Indian Institute of Science, Bangalore to determine whether there are any adsorbed materials or any morphological change occurred during the conditions of encapsulation. The samples were coated with a thin film of gold to prevent surface charging and to protect the zeolite material from thermal damage by electron beam.

2.6.6 X-ray diffraction spectroscopy

X-ray diffraction pattern of the parent zeolite and zeolite encapsulated complexes was recorded by Bruker AXSD8 Advance diffractometer. The evaluation of the spectra of host zeolite and zeolite complex was carried out to ensure that zeolite crystallinity is not affected by the encapsulation of the metal complex.⁷

2.6.7 FAB mass spectra

FAB mass spectra were recorded on a JEOL SX 102/DA-6000 mass spectrometer using Argon/Xenon (6k, 10 mA) as the FAB gas. The accelerating voltage was 10 kV and the spectra were recorded at room temperature in thioglycerol matrix. In FAB mass spectrometry, samples in condensed state are ionized by bombardment with energetic xenon or argon atoms. FAB of organic or biochemical compounds produces significant amount of the parent ion even for high molecular weight and thermally unstable samples.⁹

2.6.8 Infra red spectra

Infrared spectra of the ligands, neat complexes and supported complexes in the region 4600-400 cm^{-1} were taken by the KBr pellet technique using Shimadzu 8000 Fourier Transform Infrared Spectrophotometer. FTIR provides valuable evidences for the formation of metal complexes in zeolite pores. The ligand molecules are coordinated to transition metal cations if different spectral patterns for them appear in the free and chelated state or if characteristic bands exhibit shift in frequency up on coordination. The far infrared spectra of the simple complexes were recorded in the region 500-100 cm^{-1} on a Nicolet Magna 550 FTIR instrument at Regional Sophisticated Instrument Facility, Indian Institute of Technology, Bombay.

2.6.9 Electronic spectra

The electronic spectra of the zeolite and polymer supported complexes were recorded on a Varian Cary 5000 UV-Vis-NIR spectrophotometer. UV-visible absorption spectra of polymer anchored complexes were recorded in Nujol by a layering mull of the sample on the inside of one of the cuvettes while keeping the other one layered with Nujol as reference.

Electronic spectra of the neat complexes in methanolic solution were also recorded.

2.6.10 EPR spectroscopy

The EPR spectra of the powdered zeolite and polymer supported samples and of simple complexes in DMF were recorded at liquid nitrogen temperature. In magnetic field the spinning magnetic moment of the spinning electron may align either with or against the applied field. At resonance, absorption of energy causes magnetic moment of the spinning electron to flip from lower to higher energy state. The g values were determined relative to tetracyanoethylene (TCNE, $g = 2.0027$). Value of g depends upon the orientation of the molecule having the unpaired electron with respect to the applied magnetic field. In the case of paramagnetic ion or radical situated in a perfectly cubic crystal site, the value of g is the same in all directions but the value of g in paramagnetic ion or radical situated in a crystal of low symmetry depends upon the orientation of the crystal and in these cases anisotropic g values are obtained. μ_{eff} values were also calculated from EPR parameters by substituting g_{\perp} and g_{\parallel} in the equation⁸

$$\mu_{\text{eff}}^2 = g_{\parallel}^2 / 4 + g_{\perp}^2 / 4 + 3kT/\lambda_0(g-2)$$

where λ_0 is the spin orbit coupling constant for the free metal ion.

2.7 Catalytic studies

2.7.1 Gas chromatography

The catalytic activity studies of the synthesized complexes in phenol oxidation reaction were performed with a Chemito 8510 Gas Chromatograph. The various components of the reactants and products were separated by an SE-30 column.

2.7.2 UV/visible spectroscopy

Catalytic activity of the synthesized complexes in the reaction involving catechol and H_2O_2 was followed spectrophotometrically by measuring absorbance at suitable wavelengths at different time intervals on a Genesys 10 series spectrophotometer. Since

absorbance value is proportional to the concentration, the course of the reaction can be followed.

2.8 Biological activity

Biological activity of the simple complexes was done in DMSO solution against gram positive and gram negative bacteria and *aspergillus* fungus. Details of the experiment are presented in chapter IX.

References

- [1] Brian S. Furniss; Antony J.Hannaford; Peter W.G. Smith; Austin R. Tatchell, Vogel's Text book of Practical Organic Chemistry -5th Edition- ELBS-Longman Singapore publishers (1996).
- [2] Edward H.Yonemoto; Yeong II Kim; Russel H.Schmchl; Jim O.Wallin; Ben A. Shoulders; Benny R.Richardson; James F. Haw; Thomas E. Mallouk, J. Am.Chem. Soc. **116**, 10537 (1994).
- [3] Menon P.G.; "Lectures on Catalysis", 41stAnn. Meeting. Ind. Acad. Sci, Ramasheshan S. (Ed.) (1975).
- [4] Frechet J. M. J.; Haque K. E.; Macromolecules **8**, 130 (1975).
- [5] Varkey S. P.; Jacob C.R., Indian J.Chem. **37A**, 407 (1998).
- [6] Tollman C.; Herron N., Symposium in Hydroc.oxidation, 194th National Meeting of the Am. Chem. Soc. New Orleans, LA, Aug.30-Sept 4 (1987).
- [7] Paez-Mozo E.; Gabriunas N.; Lucaccioni F.; Acosta D.D.; Patrono P.; Laginestra A.; Ruiz P.; Delmon B.; J. Phys. Chem. **97**, 12819 (1993).
- [8] Agarwala B. V.; Inorg.Chim. Acta. **36**, 209 (1979).
- [9] Michael Barber M.; Robert S. Bordoli; Gerald J. Elliott; Donald R. Sedgewick; Andrew N. Tyler, Anal. Chem. **54**, 645A (1982).

CHAPTER III

***SYNTHESIS AND CHARACTERISATION OF SCHIFF BASE
COMPLEXES OF RUTHENIUM***

3.1 Introduction

The growing interest of the chemists in the study of ruthenium¹⁻⁴ is due to the fascinating electron-transfer properties exhibited by the complexes of this metal. Change in coordination environment around ruthenium plays an important role in modulating the redox properties of the complexes. The presence of nitrogen and oxygen donor atoms tunes the properties of the complexes to a great extent as effective and stereo specific catalysts for oxidation⁵, reduction⁶ and hydrolysis.⁷ These type of complexes are also reported to have carcinostatic, antitumour, antiviral and antibacterial activity.⁸

Catalytic activity of metal complexes of salen Schiff base ligands has been highlighted in the past few decades.⁹⁻²⁰ Binuclear complexes have gained considerable interest in recent years.²¹⁻²⁶ The role of multimetallic species is well known in a variety of metalloenzymes and in chemical catalysis. Many theoretical and experimental studies have been carried out in these fields.²⁷⁻³⁰ These complexes are known to serve as models for biologically important species, which contain metal ions in macro cyclic environment.³¹ Schiff bases and their metal complexes have been reported to possess important biological^{32,33} and catalytic activity^{34,35} and also function as oxygen carriers.^{36,37}

The scope of the present investigation is to synthesize and characterize new Schiff base complexes of ruthenium and study their catalytic activity in oxidation reactions. Literature survey highlights the vast application of ruthenium Schiff base complexes in biological field. Hence the study also aims at realizing the biological perspectives of the complexes.

3.2 Synthesis of complexes

Procedure of the synthesis of the ligands qpd, qap, qab, salpd, salap and salab are given in chapter II.

3.2.1 Ruthenium- qpd complex

Ruthenium(III) chloride trihydrate (1 mmol; 0.261 g) was dissolved in methanol(10 mL) and added to refluxed solution of qpd (0.5 mmol; 0.210 g) in methanol (10 mL). This mixture was refluxed for 24 h, concentrated by evaporation and cooled. Precipitated complex was filtered, washed with dichloromethane and dried in *vacuo* over anhydrous calcium chloride (Yield = 65%).

3.2.2 Ruthenium - qap complex

The complex was prepared in a similar manner as in the case of the qpd complex of ruthenium by taking $\text{RuCl}_3 \cdot 3\text{H}_2\text{O}$ (1 mmol: 0.261 g) and qap (1 mmol: 0.265 g) (Yield = 80%).

3.2.3 Ruthenium - qab complex

The qab complex of ruthenium was synthesized in a similar manner except that qab (1 mmol; 0.289 g) was used in the place of qap (Yield = 70%).

3.2.4 Ruthenium - salpd complex

Ruthenium(III) chloride trihydrate (0.5 mmol; 0.131 g) was refluxed with a solution of salpd (0.75 mmol; 0.237 g) in methanol (20 mL) for 8 h. The solution was concentrated and stirred with petroleum ether (60-80°C). The resultant solid was separated, washed with dichloromethane and dried in *vacuo* over anhydrous calcium chloride (Yield = 75%).

3.2.5 Ruthenium - salap complex

$\text{RuCl}_3 \cdot 3\text{H}_2\text{O}$ (1 mmol; 0.261 g) in methanol (10 mL) was refluxed with a solution of salap (2 mmol; 0.426 g) in methanol (10 mL) for 8 h. The solution was concentrated by evaporation to 3 mL, cooled in refrigerator and stirred with petroleum ether. The crystallized complex was filtered, washed with dichloromethane and dried in *vacuo* over anhydrous calcium chloride (Yield = 80%).

3.2.6 Ruthenium - salab complex

The complex was prepared as in the case of salap complex of ruthenium using $\text{RuCl}_3 \cdot 3\text{H}_2\text{O}$ (1 mmol; 0.261 g) and salab (1 mmol; 0.237 g). The crystallized complex was filtered and washed with dichloromethane and dried in *vacuo* (Yield = 75%).

3.3 Results and discussion

Details of analytical and various physico-chemical techniques employed to characterize the prepared complexes are given in chapter II.

3.3.1 Elemental analysis

All the complexes were isolated as nonhygroscopic, amorphous substances and are quite stable in air. They are soluble in dimethylsulphoxide, dimethylformamide and are insoluble in hexane, carbon tetrachloride and water.

The microanalysis data are presented in Table III.1. The analytical data suggest the empirical formula as $\text{Ru}_2(\text{qpd})\text{Cl}_4(\text{H}_2\text{O})_4$ for the qpd complex, $\text{Ru}_2(\text{qap})_2\text{Cl}_2(\text{H}_2\text{O})_3$ for the qap complex, $\text{Ru}_2(\text{qab})_2\text{Cl}_4(\text{H}_2\text{O})_5$ for the qab complex, $\text{Ru}_2(\text{salpd})_3\text{Cl}_2(\text{H}_2\text{O})_2$ for the salpd complex, $\text{Ru}_2(\text{salap})_4\text{Cl}_2(\text{H}_2\text{O})$ for the salap complex and as $\text{Ru}(\text{salab})\text{Cl}_2(\text{H}_2\text{O})_5$ for the salab complex .

TABLE III.1 Analytical data of ligands and complexes

compound	Color	Elements % found/(calc.)			
		%C	%H	%N	%Metal
qpd	Reddish	68.22	3.59	19.72	-
	Brown	(68.56)	(3.84)	(19.99)	-
Ru ₂ (qpd)Cl ₄ (H ₂ O) ₄	Black	38.01	2.68	11.37	25.83
		(34.55)	(2.66)	(10.07)	(24.23)
qap	Orange	67.42	4.53	16.14	-
		(67.92)	(4.18)	(15.84)	-
Ru ₂ (qap) ₂ Cl ₂ (H ₂ O) ₃	Black	43.03	2.78	9.88	22.58
		(42.21)	(2.83)	(9.85)	(23.68)
qab	Orange	65.87	4.04	23.59	-
		(66.43)	(3.83)	(24.21)	-
Ru ₂ (qab) ₂ Cl ₄ (H ₂ O) ₅	Black	39.11	3.16	13.84	22.00
		(38.03)	(2.99)	(13.86)	(20.00)
salpd	Yellow	75.82	5.21	8.70	-
		(75.93)	(5.10)	(8.86)	-
Ru ₂ (salpd) ₃ Cl ₂ (H ₂ O) ₂	Black	56.54	4.15	7.29	15.43
		(57.46)	(3.86)	(6.70)	(16.14)
salap	Orange	72.63	5.23	6.83	-
		(73.22)	(5.20)	6.57)	-
Ru ₂ (salap) ₄ Cl ₂ (H ₂ O)	Black	53.73	3.75	5.12	17.24
		(54.79)	(3.71)	(4.91)	(17.73)
salab	Lemon	70.5	4.63	17.12	-
	Yellow	(70.87)	(4.67)	(17.71)	-
Ru(salab)Cl ₂ (H ₂ O) ₅	Black	34.05	4.22	8.59	20.80
		(33.74)	(4.05)	(8.43)	(20.28)

3.3.2 Mass spectral analysis

The results of FAB mass spectral analyses of all the ligands and complexes agree well with the empirical formula derived from the elemental analyses. The FAB mass

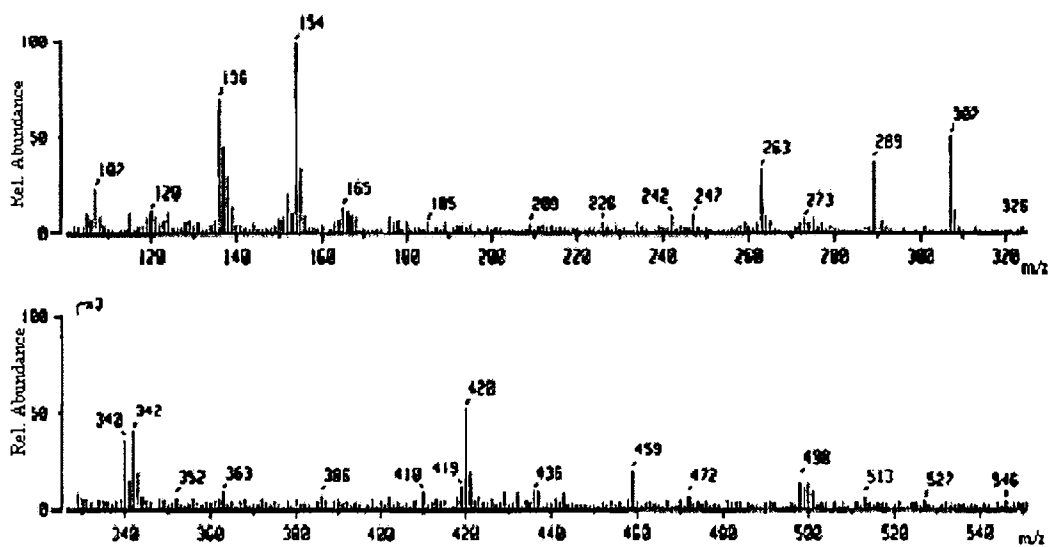


Figure III.1 Mass spectrum of qpD

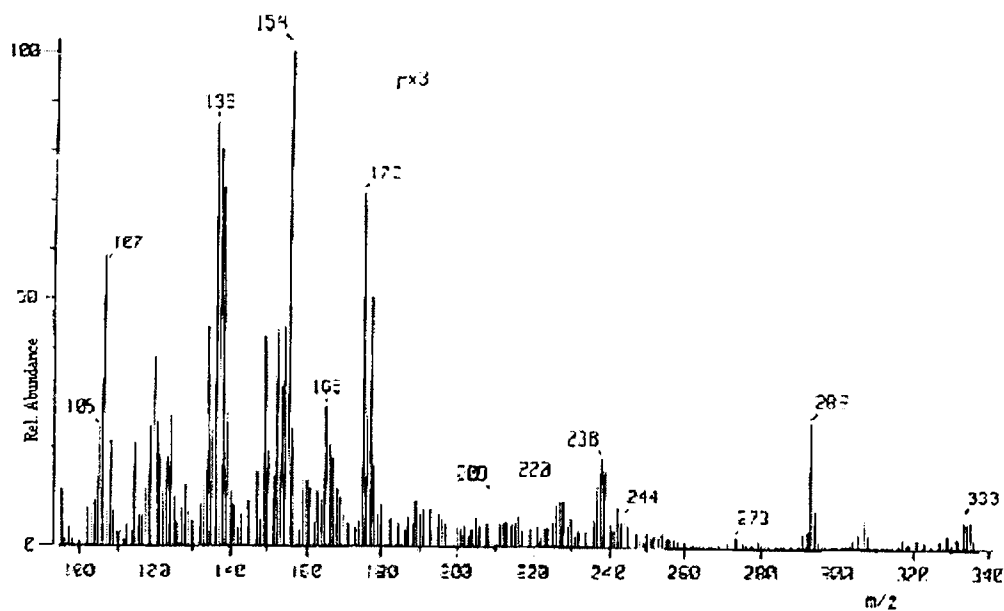


Figure III.2 Mass spectrum of qab

spectrum of ligand qpd shows the molecular ion peak at $m/z = 420$; the other important peaks are assigned as 386 (M-2OH), 263 (M - $C_9N_2H_6O$) and 107 (M- $C_{18}N_4H_{12}O_2$). The peak at $m/z = 342$ may be due to the molecular ion formed by the ring cleavage. Other large peaks at 307, 154 and 136 are assigned as the matrix peaks. The molecular ion peaks of the ligand qap, qab, salpd, salap, salab are seen at 265, 289, 316, 213, 237, respectively. They all show the same type of fragment pattern as given by qpd. FAB mass spectra of the ligands qpd, qab and salab are given in Figure III.1-III.3.

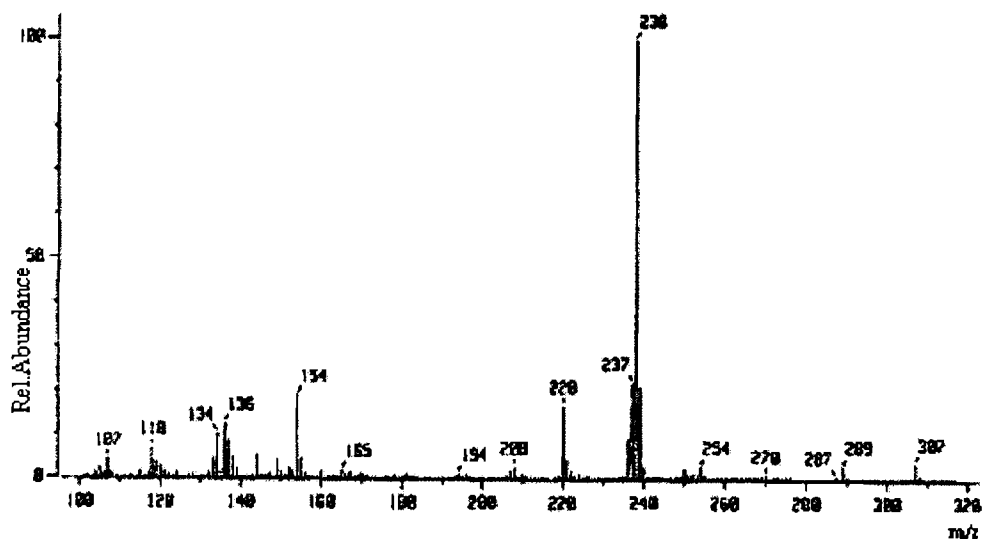
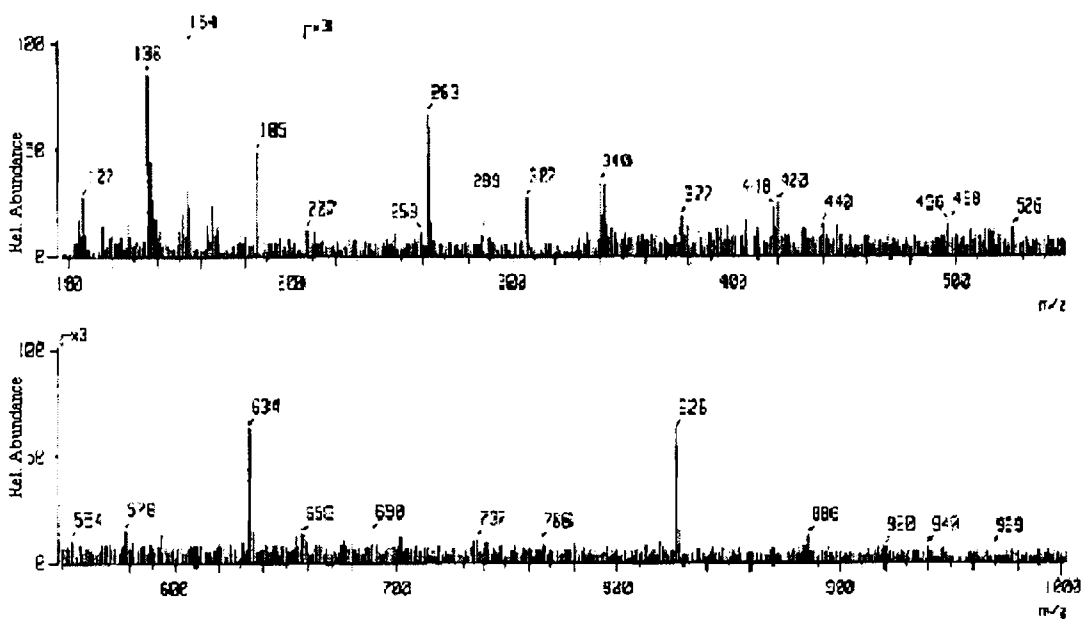


Figure III.3 FAB mass spectra of salab

The FAB mass spectrum of $Ru_2(qpd)Cl_4(H_2O)_4$ (Figure III.4) shows the molecular ion peak at $m/z = 826$. The assignment of other important peaks corresponding to the fragments of the ligand and complexes formed are given in Table III.2.

Table III.2 FAB Mass Spectral Data of $\text{Ru}_2(\text{qpd})\text{Cl}_4(\text{H}_2\text{O})_4$

Fragment ion	m/z (found)	m/z (calculated)
$\text{Ru}_2(\text{qpd})\text{Cl}_4(\text{H}_2\text{O})_4$	826	834
$\text{Ru}_2(\text{qpd})\text{Cl}_4$	766	762
$\text{Ru}_2(\text{qpd})\text{Cl}_2(\text{H}_2\text{O})_2$	737	727
$\text{Ru}_2(\text{qpd})\text{Cl}$	658	656
$\text{C}_{16}\text{H}_{10}\text{Cl}_4\text{N}_4\text{O}_2\text{Ru}_2$	634	634
$\text{Ru}(\text{qpd})\text{Cl}$	554	554
qpd-2H	418	418
$\text{C}_6\text{H}_4\text{N}_2$	105	104

Figure III.4 FAB mass spectrum of $\text{Ru}_2(\text{qpd})\text{Cl}_4(\text{H}_2\text{O})_4$

The FAB mass spectrum of qpd complex of ruthenium presents the molecular ion peak at 840 in agreement with the assigned molecular weight 836. Fragmentation of the complex results in spectral peaks as given in Table III.3

Table III.3 FAB Mass Spectral Data of $\text{Ru}_2(\text{qap})_2\text{Cl}_2(\text{H}_2\text{O})_3$

Fragment ion	m/z (found)	m/z (calculated)
$\text{Ru}_2(\text{qap})_2\text{Cl}_2(\text{H}_2\text{O})_2$	840	836
$\text{Ru}_2(\text{qap})_2\text{Cl}_2$	804	800
$\text{Ru}_2(\text{qap})\text{Cl}_2\text{H}_2\text{O}\cdot\text{O}_2$	586	586
$\text{Ru}_2(\text{qap})\text{Cl}\cdot\text{H}_2\text{O}$	516	518

The results of FAB mass spectral analysis of qap complex of ruthenium conform to the elemental analysis and the molecular weight of the complex is suggested to be 1010. The molecular ion peak is formed with the expulsion of three molecules of lattice water.

Table III.4 FAB Mass Spectral Data of $\text{Ru}_2(\text{qab})_2\text{Cl}_4(\text{H}_2\text{O})_5$

Fragment ion	m/z (found)	m/z (calculated)
$\text{Ru}_2(\text{qap})_2\text{Cl}_4(\text{H}_2\text{O})_2$	954	956
$\text{Ru}_2(\text{qab})_2\text{Cl}_2$	848	849
$\text{Ru}_2(\text{qab})\text{Cl}$	426	424

The FAB mass spectral peak at 1254 (Figure III.5) is assigned as the molecular ion peak of $\text{Ru}_2(\text{salpd})_3\text{Cl}_2(\text{H}_2\text{O})_2$ which corresponds to the molecular weight of the complex. Peaks of other important species are listed in Table III.5.

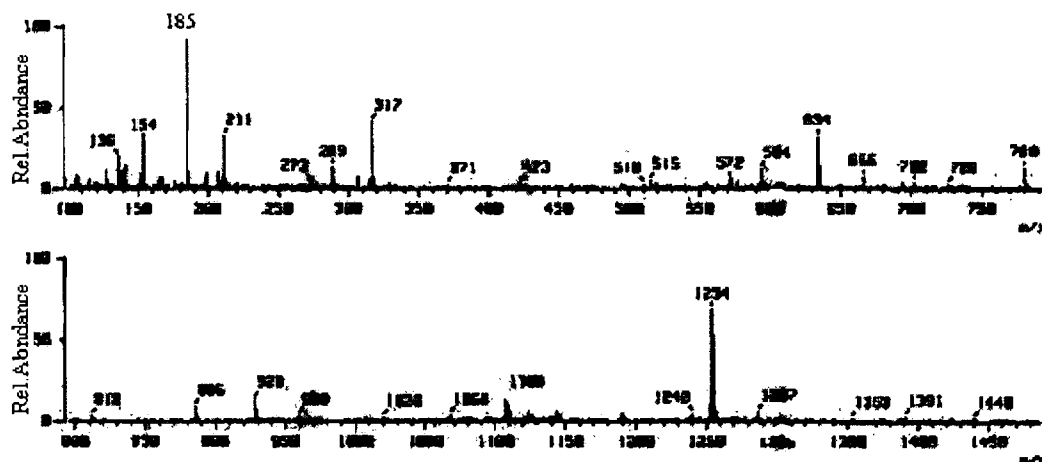


Figure III.5 FAB mass spectrum of $\text{Ru}_2(\text{salpd})_3\text{Cl}_4(\text{H}_2\text{O})_2$

Table III.5 FAB Mass Spectral Data of $\text{Ru}_2(\text{salpd})_3\text{Cl}_4(\text{H}_2\text{O})_2$

Fragment ion	m/z (calculated)	m/z (found)
$\text{Ru}_2(\text{SalPD})_3\text{Cl}_2(\text{H}_2\text{O})_2$	1254	1254
$\text{Ru}_2(\text{SalPD})_2\text{Cl}_2\text{H}_2\text{O}$	922	928
$\text{Ru}(\text{SalPD})_2\text{Cl H}_2\text{O}$	784	780
$\text{Ru}_2(\text{SalPD})\text{O}_2\text{Cl}_2 \text{H}_2\text{O}$	637	634
$\text{Ru}_2(\text{SalPD})\text{Cl H}_2\text{O}$	571	572
SalPD	316	317
$\text{Ru}_2 \text{Cl}_2$	273	273
Ru Cl	136	136

The assignment of the important peaks formed by the FAB spectral analysis of $\text{Ru}_2(\text{salap})_4\text{Cl}_2$ are given in Table III.6. This suggests the molecular weight of the compound to be 1125.

Table III.6 FAB Mass Spectral Data of $\text{Ru}_2(\text{salap})_4\text{Cl}_2(\text{H}_2\text{O})$

Fragment ion	m/z (calculated)	m/z (found)
$\text{Ru}_2(\text{salap})_4\text{Cl}_2$	1122	1125
$\text{Ru}_2(\text{salap})_3\text{Cl}_2$	910	910
$\text{Ru}_2(\text{salap})_2\text{Cl}_2$	684	683
$\text{Ru}(\text{salap})_2\text{Cl}_2$	597	597
$\text{Ru}(\text{salap})_2\text{Cl}$	561	565
$\text{Ru}(\text{salap})$	311	311

The molecular weight of salab complex of ruthenium is calculated to be 498 which conforms with the FAB mass spectral ion peak 497 (Figure III.7). Peaks of other important species are listed in Table III.7.

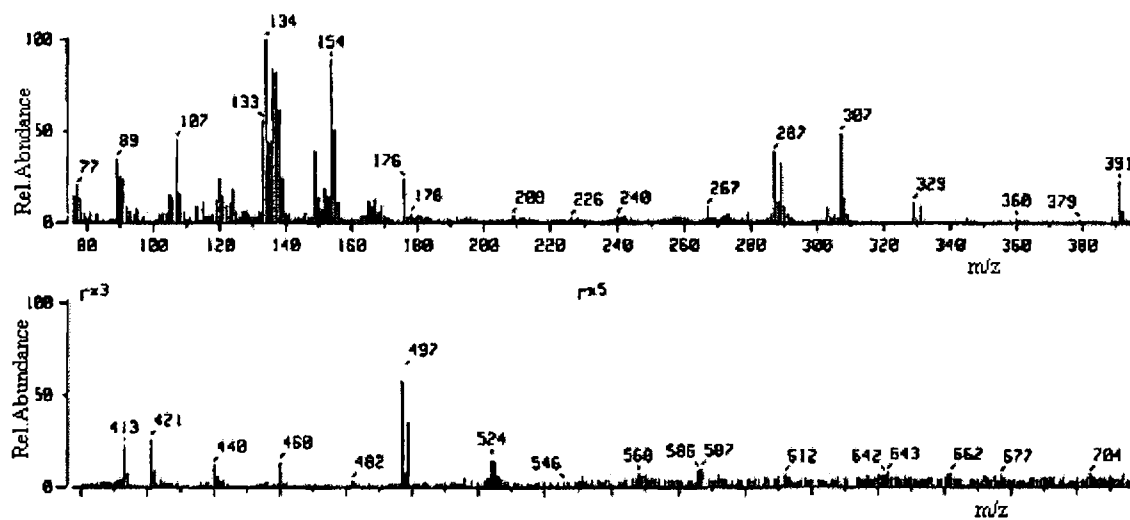
Figure III.6 FAB mass spectrum of $\text{Ru}(\text{salab})\text{Cl}_2(\text{H}_2\text{O})_5$

Table III.7 FAB Mass Spectral Data of Ru(salab)Cl₂(H₂O)₅

Fragment ion	m/z (found)	m/z (calculated)
Ru (salab) Cl ₂ (H ₂ O) ₅	497	498
Ru (salab) Cl ₂ (H ₂ O) ₄	482	480
Ru (salab) Cl ₂	413	409

3.3.3 Molar conductance

TABLE III. 8 Conductance Data of complexes

Complex	Molar Conductance Ohm ⁻¹ cm ² mol ⁻¹
Ru ₂ (qpd)Cl ₄ (H ₂ O) ₄	50.3
Ru ₂ (qap) ₂ Cl ₂ (H ₂ O) ₃	56.0
Ru ₂ (qab) ₂ Cl ₄ (H ₂ O) ₅	55.7
Ru ₂ (salpd) ₃ Cl ₂ (H ₂ O) ₂	0.5
Ru ₂ (salap) ₄ Cl ₂ (H ₂ O)	50.2
Ru (salab) Cl ₂ (H ₂ O) ₅	144.2

The molar conductance value in methanol (10⁻³ solution) suggests non-electrolytic nature for qpd, salpd, qap, qab and salap complexes (Table III.8). The salab complex shows 1:2 electrolytic nature³⁸ indicating the presence of two chlorine atoms outside the coordination sphere. The low values of conductance exhibited by other complexes might be due to the dissociation of the bridged complexes.

3.3.4 Thermo gravimetric analysis

As the complexes contain varying number of water molecules, the TG study was mainly carried out to know the number of coordinated water molecules. The TG/DTG/DSC curves of the complexes are given in Figure III.7-III.12.

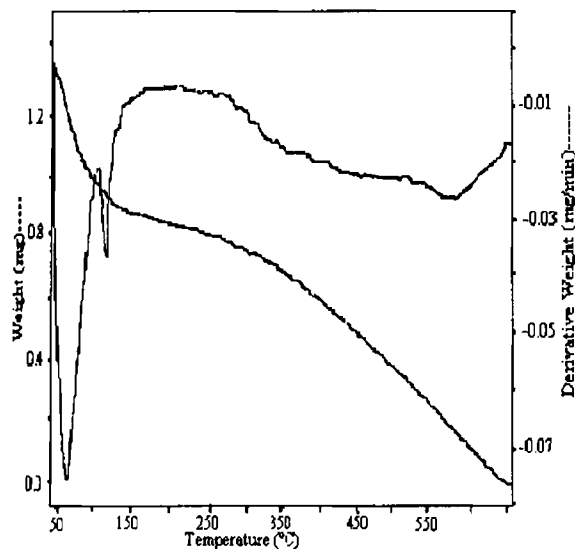


Figure III.7 (a) TG/DTG curve of $[\text{Ru}_2(\text{qpd})\text{Cl}_4(\text{H}_2\text{O})_2] \cdot 2\text{H}_2\text{O}$

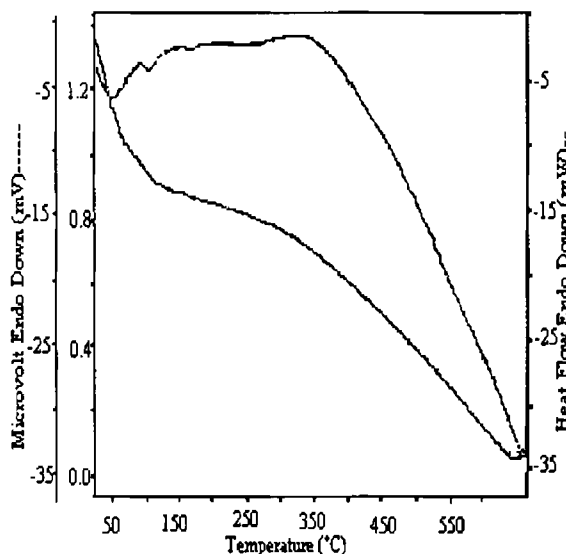


Figure III.7 (b) DSC curve of $[\text{Ru}_2(\text{qpd})\text{Cl}_4(\text{H}_2\text{O})_2] \cdot 2\text{H}_2\text{O}$

TG data (Table III.9) of $\text{Ru}_2(\text{qpd})\text{Cl}_4(\text{H}_2\text{O})_4$ show 4.3% weight loss below 100°C which might be due to the presence of lattice water. The compound experiences weight loss of another 4.3% in the range 120-160°C which corresponds to the removal of two molecules of coordinated water.³⁹ Weight loss of the compound starting from 300°C up to 650°C is due to the decomposition of the organic part of the molecule. Although decomposed fragments of the ligand could not be approximated owing to continuous weight loss, the complete decomposition of the ligand occurred around 650°C.

Water of hydration in $\text{Ru}_2(\text{qap})_2\text{Cl}_2(\text{H}_2\text{O})_3$ loses in the region 50-100°C corresponding to a weight loss of 2.1%. The presence of two molecules of water in the coordination sphere of the complex is indicated by the loss of 4.2% weight loss in the range 120-160°C. Decomposition of the ligand takes place in the range 500-700°C. Complete decomposition of the complex occurs around 960°C.

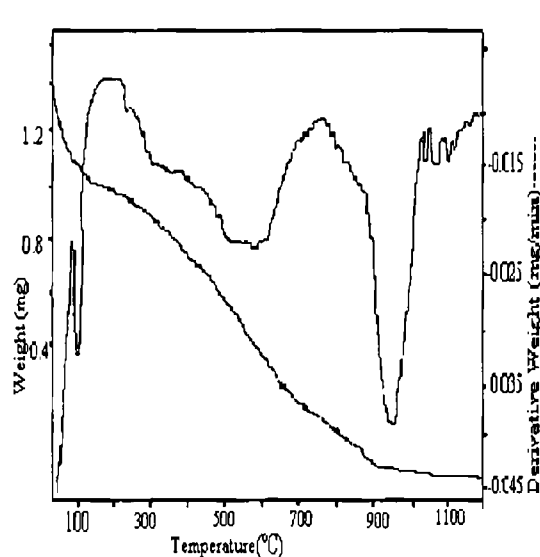


Figure III.8 (a) TG/DTG curve of $[\text{Ru}_2(\text{qap})_2\text{Cl}_2(\text{H}_2\text{O})_2]\cdot\text{H}_2\text{O}$

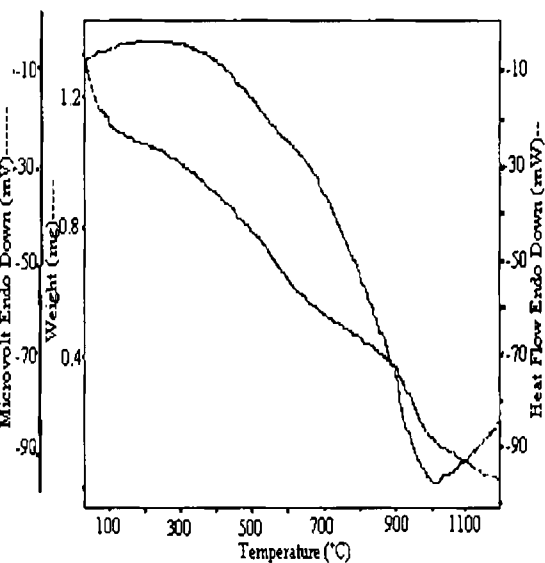


Figure III.8 (b) DSC curve of $[\text{Ru}_2(\text{qap})_2\text{Cl}_2(\text{H}_2\text{O})_2]\cdot\text{H}_2\text{O}$

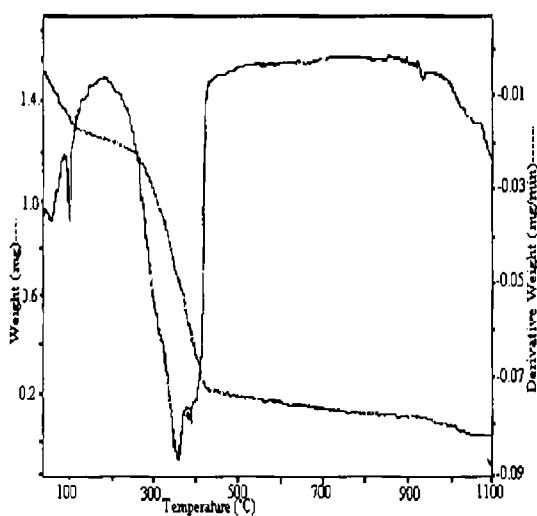


Figure III.9(a) TG/DTG curve of $[\text{Ru}_2(\text{qab})_2\text{Cl}_4(\text{H}_2\text{O})_2]\cdot 3\text{H}_2\text{O}$

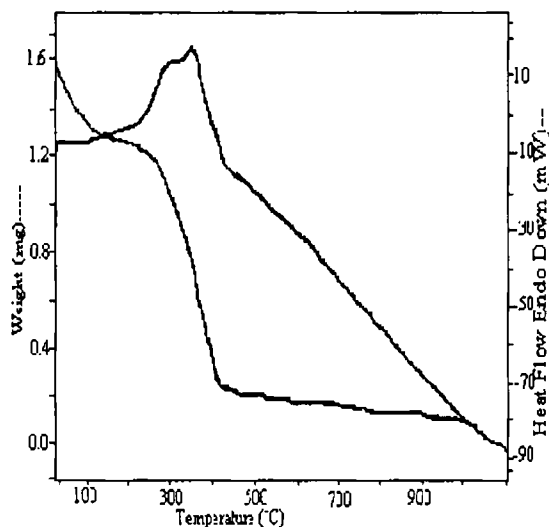


Figure III.9(b) DSC curve of $[\text{Ru}_2(\text{qab})_2\text{Cl}_4(\text{H}_2\text{O})_2]\cdot 3\text{H}_2\text{O}$

TG curve of $\text{Ru}_2(\text{qab})_2\text{Cl}_4(\text{H}_2\text{O})_5$ shows decomposition in two stages. In the first stage removal of water of hydration takes place, which corresponds to the weight loss of 5.3%. Second stage of decomposition occurs between 120°C and 160°C , which corresponds, to 3.5% weight loss of coordinated water. Third stage of decomposition takes place between 280°C and 470°C causing a weight loss of 60% which is due to the complete removal of the ligand part of the molecule. DTG analysis indicates that the decomposition in this region takes place in two steps. From 280°C up to 360°C the mass loss corresponds to the removal of coordinated chlorine followed by the decomposition of the organic moiety of the complex with increase in temperature.

Table III.9 Thermogravimetric data of ruthenium complexes

Complex	Temp. range of decomposition($^\circ\text{C}$)	% weight loss	Nature of DSC curve
$[\text{Ru}_2(\text{qap})_2\text{Cl}_2(\text{H}_2\text{O})_2].\text{H}_2\text{O}$	50-100	2.1	endothermic
	120-160	4.2	endothermic
	300-650	17	exothermic
$[\text{Ru}_2(\text{qab})_2\text{Cl}_4(\text{H}_2\text{O})_2].3\text{H}_2\text{O}$	50-100	5.3	endothermic
	120-160	3.5	endothermic
	280-420	55	exothermic
$[\text{Ru}_2(\text{salpd})_3\text{Cl}_2(\text{H}_2\text{O})_2]$	120-160	2.8	endothermic
	200-500	30	exothermic
$[\text{Ru}_2(\text{salap})_4\text{Cl}_2].\text{H}_2\text{O}$	50-100	1.5	endothermic
	200-280	10	endothermic
	420-550	20	exothermic
$[\text{Ru}(\text{salab})(\text{H}_2\text{O})_4]\text{Cl}_2.\text{H}_2\text{O}$	50-100	3.6	endothermic
	120-170	10.8	endothermic
	310-320	10	exothermic

A weight loss of 2.8% in $\text{Ru}_2(\text{salpd})_3\text{Cl}_2(\text{H}_2\text{O})_2$ due to two molecules of coordinated water occurs from 120°C up to 160°C. Further decomposition of the organic part of the molecule takes place in the region 200-800°C. This corresponds to 70% weight loss. Earlier stages of decomposition might be due to the loss of chlorine followed by decomposition of the organic moiety. Since the weight loss is continuous correct approximation of the decomposed fragments could not be done.

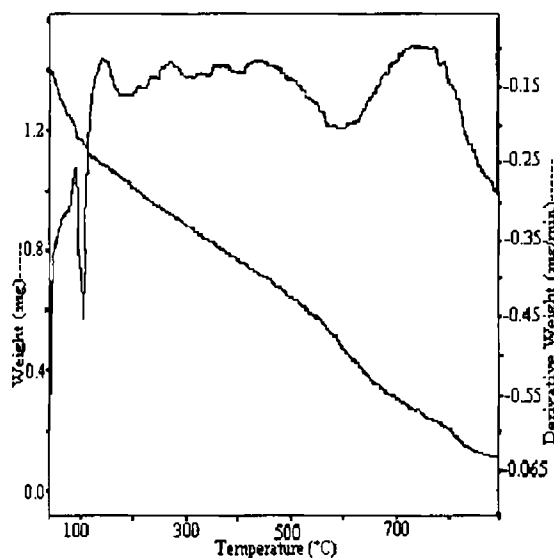


Figure III.10 (a) TG/DTG curve of $[\text{Ru}_2(\text{salpd})_3\text{Cl}_2(\text{H}_2\text{O})_2]$

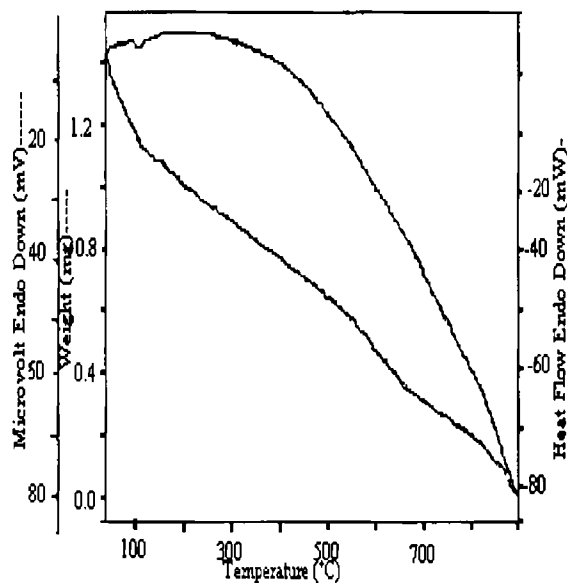


Figure III.10 (b) DSC curve of $[\text{Ru}_2(\text{salpd})_3\text{Cl}_2(\text{H}_2\text{O})_2]$

Around 100°C 1.5% weight loss occurs in $\text{Ru}_2(\text{salap})_4\text{Cl}_2(\text{H}_2\text{O})$ due to removal of lattice water. Ligand part of the molecule decomposes in two stages in the temperature range 200-280°C and 420-650°C.

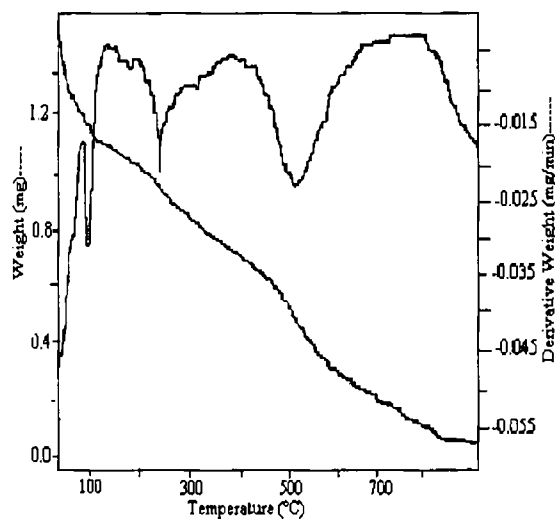


Figure III.11(a) TG/DTG curve of
 $[\text{Ru}_2(\text{salap})_4\text{Cl}_2]\cdot\text{H}_2\text{O}$

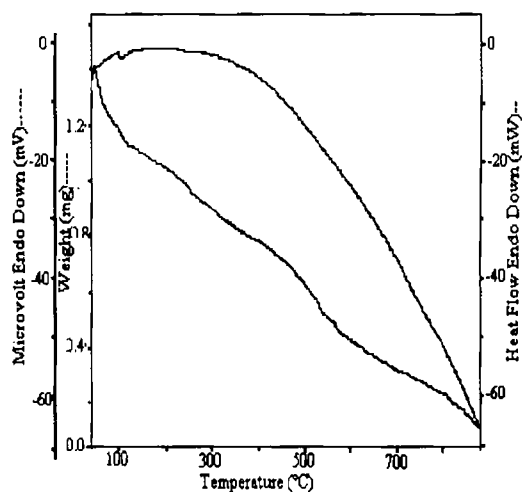


Figure III.11(b) DSC curve of
 $[\text{Ru}_2(\text{salap})_4\text{Cl}_2]\cdot\text{H}_2\text{O}$

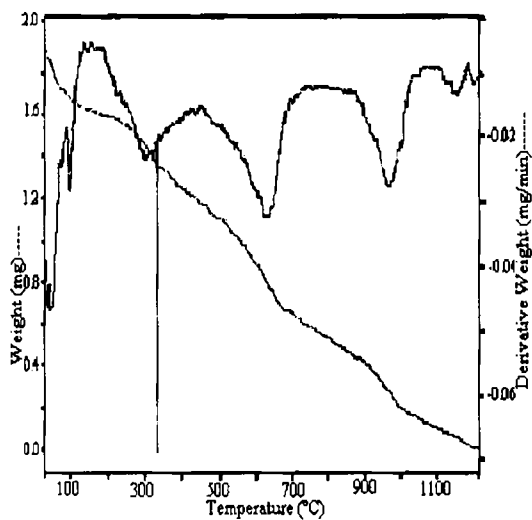


Figure III.12 (a) TG/DTG curve of
 $[\text{Ru}(\text{salab})(\text{H}_2\text{O})_4]\text{Cl}_2\cdot\text{H}_2\text{O}$

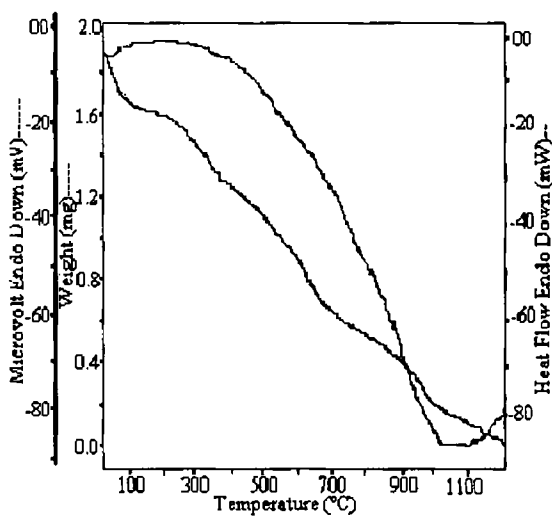


Figure III.12 (b) DSC curve of
 $[\text{Ru}(\text{salab})(\text{H}_2\text{O})_4]\text{Cl}_2\cdot\text{H}_2\text{O}$

Initial weight loss of 3.6% shown in the TG data of the complex $\text{Ru}(\text{salab})\text{Cl}_2(\text{H}_2\text{O})_5$ might be due to the removal of one molecule of lattice held water. The weight loss of 14.4% occurs in the temperature range 120-170°C due to the removal of four molecules of coordinated water. Thereafter major decompositions take place in the temperature range 310-320°C, 550-660°C, 880-1020°C.

DSC study indicates that the organic part of all the synthesized complexes decomposes before the melting point is reached. The study could provide information regarding the actual number of coordinated water molecules and suggests the molecular formulae of the Ru-qpd, Ru-qap, Ru-qab, Ru-salpd, Ru-salap, Ru-salab complexes to be $[\text{Ru}_2(\text{qpd})\text{Cl}_4(\text{H}_2\text{O})_2].2\text{H}_2\text{O}$, $[\text{Ru}_2(\text{qap})_2\text{Cl}_2(\text{H}_2\text{O})_2].\text{H}_2\text{O}$, $[\text{Ru}_2(\text{qab})_2\text{Cl}_4(\text{H}_2\text{O})_2].3\text{H}_2\text{O}$, $[\text{Ru}_2(\text{salpd})_3\text{Cl}_2(\text{H}_2\text{O})_2]$, $[\text{Ru}_2(\text{salap})_4\text{Cl}_2].\text{H}_2\text{O}$, $[\text{Ru}(\text{salab})(\text{H}_2\text{O})_4]\text{Cl}_2.\text{H}_2\text{O}$ respectively.

3.3.5 Infrared spectra

The infrared spectra of all the Schiff base ligands showed a broad band in the region 3390-3480 cm^{-1} which might be due to ν_{OH} . The free hydroxyl group is generally observed between 3500 and 3600 cm^{-1} . The observed low value of this band is due to intra molecular hydrogen bonding between hydrogen of OH and azomethine nitrogen.⁴⁰ The FTIR spectral data of the complexes of ruthenium are given in Table III.10.

IR spectral peaks observed at 1651 cm^{-1} for the free ligand qpd were assigned to $\nu_{\text{C=N}}$ which was shifted to lower frequency 1646 cm^{-1} after complexation in $[\text{Ru}_2(\text{qpd})\text{Cl}_4(\text{H}_2\text{O})_2].2\text{H}_2\text{O}$ (Figure III.13). The low energy shift supports their coordination with metal ion.⁴¹ This can be explained by the donation of electrons from nitrogen to the empty d-orbitals of metal atom. Coordination of the Schiff bases to the metal through nitrogen atom is expected to reduce the electron density in the azomethine

link and lower the frequency of C=N. The presence of coordinated water in the complex is indicated by the band at 820cm^{-1} .³⁹

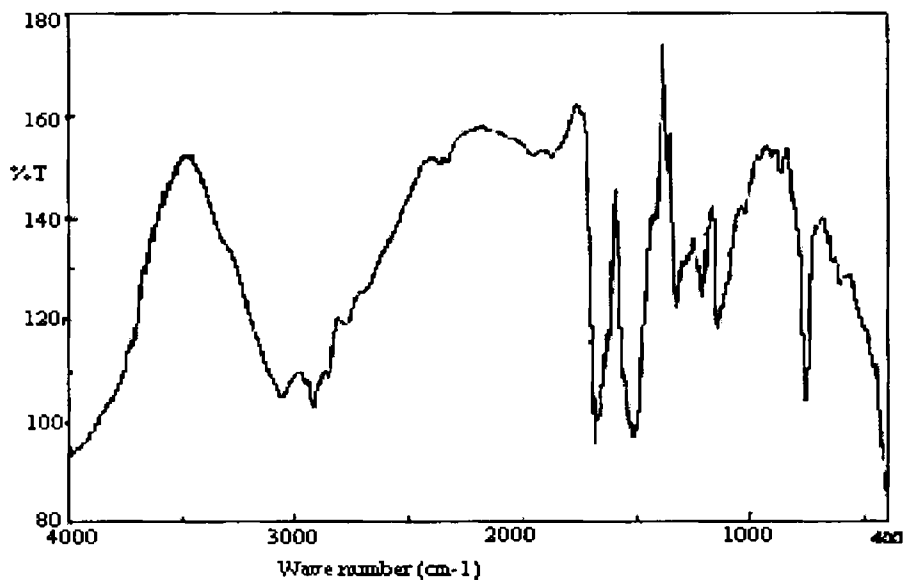


Fig III. 13. Infrared spectrum of $[\text{Ru}_2(\text{qpd})\text{Cl}_4(\text{H}_2\text{O})_2]\cdot 2\text{H}_2\text{O}$

The band at 821 cm^{-1} in $[\text{Ru}_2(\text{qap})_2\text{Cl}_2(\text{H}_2\text{O})_2]$ complex which is not present in the ligand is due to coordinated water. The IR band at 1630 cm^{-1} of the free Schiff base is characteristic of the azomethine ($>\text{C}=\text{N}$) group. In the complex it is shifted to lower frequency 1621 cm^{-1} indicating coordination at this group. A strong band observed at 1316 cm^{-1} in free base due to phenolic C–O stretching, on complexation is shifted to higher frequency 1331 cm^{-1} indicating coordination through phenolic oxygen⁴².

In $[\text{Ru}_2(\text{qab})_2\text{Cl}_4(\text{H}_2\text{O})_2]\cdot 3\text{H}_2\text{O}$, the band at 1642 cm^{-1} due to azomethine ($>\text{C}=\text{N}$) group in ligand is shifted to lower frequency 1630 cm^{-1} , indicating coordination to the metal ion. The presence of a sharp band at 832 cm^{-1} in the IR spectrum of the complex confirms the presence of coordinated water in the molecule. Analogous peak is absent in ligand spectrum.

The IR band at 1651 cm^{-1} in salpd is shifted to lower frequency 1642 cm^{-1} in $[\text{Ru}_2(\text{salpd})_3\text{Cl}_2(\text{H}_2\text{O})_2]$ due to complexation. The band at 3515 cm^{-1} in the ligand is also present in the spectra of the complex indicating the presence of free hydroxyl group in the molecule. The presence of coordinated water in the complex is indicated by the infrared band at 855 cm^{-1} .

In $[\text{Ru}_2(\text{salap})_4\text{Cl}_2]\cdot\text{H}_2\text{O}$ a shift of the band due to $>\text{C}=\text{N}$ group to lower frequency is seen due to the participation of azomethine nitrogen in coordination. The presence of IR band in the region $3550\text{-}3600\text{ cm}^{-1}$ in free ligand and complex ascertains the noninvolvement of OH group in coordination. The absence of spectral band around $820\text{-}860\text{ cm}^{-1}$ indicates coordinated water is not present in the molecule.

In $[\text{Ru}(\text{salab})(\text{H}_2\text{O})_4]\text{Cl}_2\cdot\text{H}_2\text{O}$ all the bands in the region $1700\text{-}1600\text{ cm}^{-1}$ experiences a shift towards lower frequencies in the complex (Figure III.14). This might be due to coordination of azomethine group to the metal atom. The band at 816 cm^{-1} in the complex ascertains the presence of coordinated water. A strong band observed at 1135 cm^{-1} in the free Schiff base has been assigned to phenolic C–O stretching. On complexation the band is shifted to higher frequency 1146 cm^{-1} indicating coordination through phenolic oxygen.

The characteristic phenolic C-O stretching vibrations are observed between $1123\text{ - }1141\text{ cm}^{-1}$ in all the ligands. These are raised by $5\text{ -}24\text{ cm}^{-1}$ in the spectra of the complexes compared to the position of the Schiff bases. This implies deprotonation of enolic group on protonation.⁴³

A broad and medium intensity band around 3400 cm^{-1} in all complexes is due to ν_{OH} of lattice held or coordinated water molecule.⁴⁴ This is in accordance with TG data which reveal the loss of water molecule in the temperature range $50\text{-}100^\circ\text{C}$. For all the

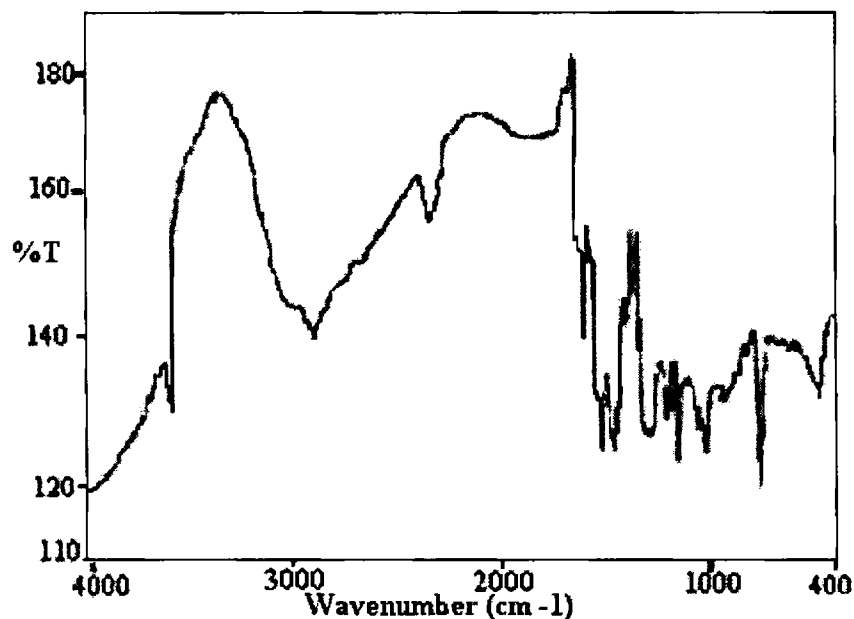
Figure III.14 Infrared spectrum of $[\text{Ru}(\text{salab})(\text{H}_2\text{O})_4]\text{Cl}_2 \cdot \text{H}_2\text{O}$

Table III.10 FTIR Spectral Data the Complexes Of Ruthenium

compound	$\nu_{\text{free O-H}}$	$\nu_{\text{C=N}}$	$\nu_{\text{C=O}}$ (Phenolic)	$\nu_{\text{coord H}_2\text{O}}$	$\nu_{\text{M-N}}$	$\nu_{\text{M-Cl}}$ (terminal)	$\nu_{\text{M-Cl}}$ (bridge)	$\delta_{\text{M-Cl}}$ (bridge)
qpd	3474	1651	1117	-	-	-	-	-
$[\text{Ru}_2(\text{qpd})\text{Cl}_4(\text{H}_2\text{O})_2] \cdot 2\text{H}_2\text{O}$	3428	1646	1125	820	473	365	307	135
qap	3507	1630	1116	-	-	-	-	-
$[\text{Ru}_2(\text{qap})_2\text{Cl}_2(\text{H}_2\text{O})_2] \cdot \text{H}_2\text{O}$	3419	1621	1132	821	468	-	312	134
qab	3461	1642	1123	-	-	-	-	-
$[\text{Ru}_2(\text{qab})_2\text{Cl}_4(\text{H}_2\text{O})_2] \cdot 3\text{H}_2\text{O}$	3410	1630	1147	832	467	370	317	141
salpd	3515	1651	1138	-	-	-	-	-
$[\text{Ru}_2(\text{salpd})_3\text{Cl}_2(\text{H}_2\text{O})_2]$	3515	1642	1148	816	460	-	318	135
salap	3550	1639	1141	-	-	-	-	-
$[\text{Ru}_2(\text{salap})_4\text{Cl}_2] \cdot \text{H}_2\text{O}$	3550	1635	1146	-	445	-	304	135
salab	3571	1641	1135	-	-	-	-	-
$[\text{Ru}(\text{salab})(\text{H}_2\text{O})_4]\text{Cl}_2 \cdot \text{H}_2\text{O}$	3591	1630	1146	816	470	370	-	-

complexes except $[\text{Ru}(\text{salab})(\text{H}_2\text{O})_4]\text{Cl}_2 \cdot \text{H}_2\text{O}$ the $\nu_{\text{Ru-Cl}}$ absorption has been observed in the region $300\text{-}320\text{ cm}^{-1}$ region. In $[\text{Ru}(\text{salab})(\text{H}_2\text{O})_4]\text{Cl}_2 \cdot \text{H}_2\text{O}$ the band at a higher frequency 370 cm^{-1} indicates the presence of terminal chlorine. The absence of band around 310 and 145 cm^{-1} rules out the possibility of metal-chlorine bridging⁴⁵ in $[\text{Ru}(\text{salab})(\text{H}_2\text{O})_4]\text{Cl}_2 \cdot \text{H}_2\text{O}$

3.3.6 Magnetic susceptibility measurements

Magnetic moment of the Ru(III) complexes ranges from 1.4 to 1.8 which is much lower than the spin only value (Table III.11). In dimeric trivalent bridged ruthenium complexes, magnetic interaction between ruthenium atoms takes place and may result in lower magnetic moment values.⁴⁶ The values of μ_{eff} agrees well with the values for octahedral trivalent ruthenium complexes, particularly if some distortion from octahedral symmetry is involved.⁴⁷⁻⁴⁹

3.3.7 Electronic spectra

The electronic spectral data of the complexes suggest octahedral nature of the complexes. The ground state of ruthenium(III) is $^2T_{2g}$, arising from the t_{2g}^5 configuration in an octahedral environment. The excited states corresponding to t_{2g}^5 configuration are $^2A_{2g}$, $^2T_{1g}$, 2E_g . Tentative assignments of the absorption peaks obtained are shown in Table III.11. In the six coordinate ruthenium(III) complexes, charge transfer transition often occurs at relatively low energies (Figure III.15). The hole in the low spin t_{2g}^5 configuration of ruthenium(III) permits relatively low LMCT bands. Electronic spectra of the present complexes in methanol are characterized by charge-transfer bands. Since the crystal field parameter is quite large, some of the d-d bands are obscured by the charge transfer bands.⁵⁰ Though the spin-orbit coupling coefficient is greater, intra-configurational transitions within $^2T_{2g}$ will lie at too low an energy to be conveniently identified. The lowest absorption corresponding to spin-forbidden $^2T_{2g} \rightarrow ^4T_{1g}$ transition was found to occur in some cases as shoulders.

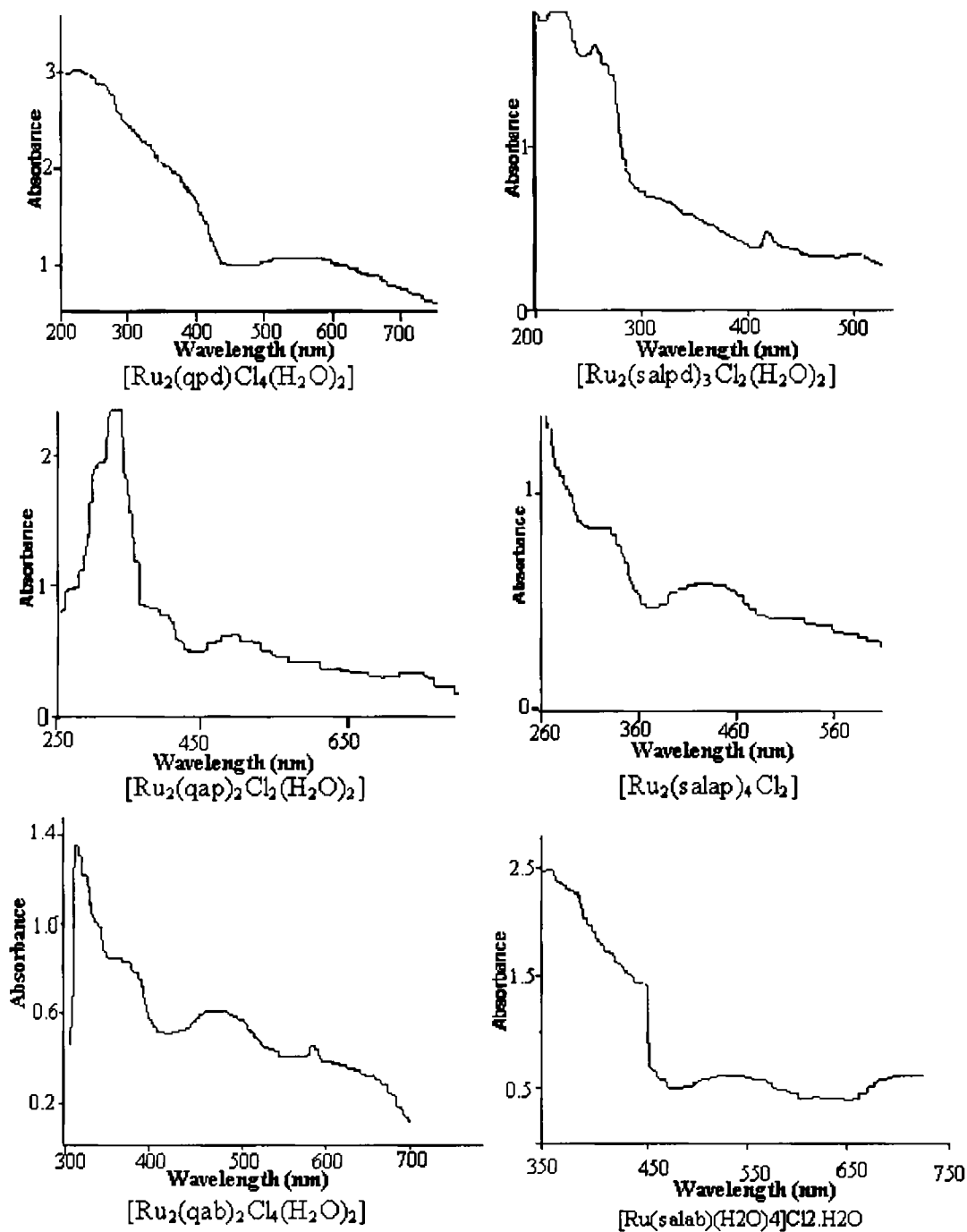


Figure III.15 Electronic spectra of ruthenium complexes

TABLE III.11 Electronic Spectral and Magnetic Moment Data of complexes

Complex	Absorptions(cm^{-1})	Tentative assignments	μ_{eff} (B.M.)
$[\text{Ru}_2(\text{qpd})\text{Cl}_4(\text{H}_2\text{O})_2] \cdot 2\text{H}_2\text{O}$	35700	charge transfer	1.5
	31250 (sh)	${}^2\text{T}_{2g} \rightarrow {}^2\text{A}_{2g}, {}^2\text{T}_{1g}$	
	23500 (sh)	${}^2\text{T}_{2g} \rightarrow {}^2\text{E}_g$	
	15900	${}^2\text{T}_{2g} \rightarrow {}^4\text{T}_{1g}$	
$[\text{Ru}_2(\text{qap})_2\text{Cl}_2(\text{H}_2\text{O})_2] \cdot \text{H}_2\text{O}$	33300	charge transfer	1.4
	25000 (sh)	${}^2\text{T}_{2g} \rightarrow {}^2\text{A}_{2g}, {}^2\text{T}_{1g}$	
	20400	${}^2\text{T}_{2g} \rightarrow {}^2\text{E}_g$	
$[\text{Ru}_2(\text{qab})_2\text{Cl}_4(\text{H}_2\text{O})_2] \cdot 3\text{H}_2\text{O}$	31500	charge transfer	1.6
	26310 (sh)	${}^2\text{T}_{2g} \rightarrow {}^2\text{A}_{2g}, {}^2\text{T}_{1g}$	
	20700	${}^2\text{T}_{2g} \rightarrow {}^2\text{E}_g$	
	16950 (sh)	${}^2\text{T}_{2g} \rightarrow {}^4\text{T}_{1g}$	
	35200	charge transfer	
$[\text{Ru}_2(\text{salpd})_3\text{Cl}_2(\text{H}_2\text{O})_2]$	31500	${}^2\text{T}_{2g} \rightarrow {}^2\text{A}_{2g}, {}^2\text{T}_{1g}$	1.4
	20900 (sh)	${}^2\text{T}_{2g} \rightarrow {}^2\text{E}_g$	
	17700	${}^2\text{T}_{2g} \rightarrow {}^4\text{T}_{1g}$	
$[\text{Ru}_2(\text{salap})_4\text{Cl}_2] \cdot \text{H}_2\text{O}$	37030	charge transfer	1.4
	30950 (sh)	${}^2\text{T}_{2g} \rightarrow {}^2\text{A}_{2g}, {}^2\text{T}_{1g}$	
	22800	${}^2\text{T}_{2g} \rightarrow {}^2\text{E}_g$	
$[\text{Ru}(\text{salab})(\text{H}_2\text{O})_4]\text{Cl}_2 \cdot \text{H}_2\text{O}$	28570	Charge transfer	1.8
	26300 (sh)	${}^2\text{T}_{2g} \rightarrow {}^2\text{A}_{2g}, {}^2\text{T}_{1g}$	
	18200	${}^2\text{T}_{2g} \rightarrow {}^2\text{E}_g$	

3.3.8 EPR spectra

Compounds $[\text{Ru}_2(\text{qpd})\text{Cl}_4(\text{H}_2\text{O})_2] \cdot 2\text{H}_2\text{O}$, $[\text{Ru}_2(\text{qap})_2\text{Cl}_2(\text{H}_2\text{O})_2] \cdot \text{H}_2\text{O}$, $[\text{Ru}_2(\text{qab})_2\text{Cl}_4(\text{H}_2\text{O})_2] \cdot 3\text{H}_2\text{O}$, $[\text{Ru}_2(\text{salpd})_3\text{Cl}_2(\text{H}_2\text{O})_2]$, $[\text{Ru}_2(\text{salap})_4\text{Cl}_2] \cdot \text{H}_2\text{O}$ and $[\text{Ru}(\text{salab})(\text{H}_2\text{O})_4]\text{Cl}_2 \cdot \text{H}_2\text{O}$ are EPR active which suggests the ruthenium exists in +3 oxidation state in all the complexes. $[\text{Ru}_2(\text{qpd})\text{Cl}_4(\text{H}_2\text{O})_2] \cdot 2\text{H}_2\text{O}$, $[\text{Ru}_2(\text{qab})_2\text{Cl}_4(\text{H}_2\text{O})_2] \cdot 3\text{H}_2\text{O}$ and $[\text{Ru}_2(\text{salap})_4\text{Cl}_2] \cdot \text{H}_2\text{O}$ give rise to well resolved rhombic spectra consistent with the low spin $4d^5$ configuration indicating rhombohedral distortion of octahedral geometry.^{51,52} Spectral g values are listed in Table III.12. $[\text{Ru}_2(\text{salpd})_3\text{Cl}_2(\text{H}_2\text{O})_2]$ exhibit a reverse axial spectrum with $g_{\perp} > g_{\parallel}$. This might be due to the positive hole in the t_{2g} subshell. Super hyper fine splitting of the EPR signal ascertains nitrogen coordination in the complex (Figure III.19). The two g values of $[\text{Ru}_2(\text{qap})_2\text{Cl}_2(\text{H}_2\text{O})_2] \cdot \text{H}_2\text{O}$, $[\text{Ru}_2(\text{salpd})_3\text{Cl}_2(\text{H}_2\text{O})_2]$ and $[\text{Ru}(\text{salab})(\text{H}_2\text{O})_4]\text{Cl}_2 \cdot \text{H}_2\text{O}$ indicate distorted octahedral geometry for these axial complexes.

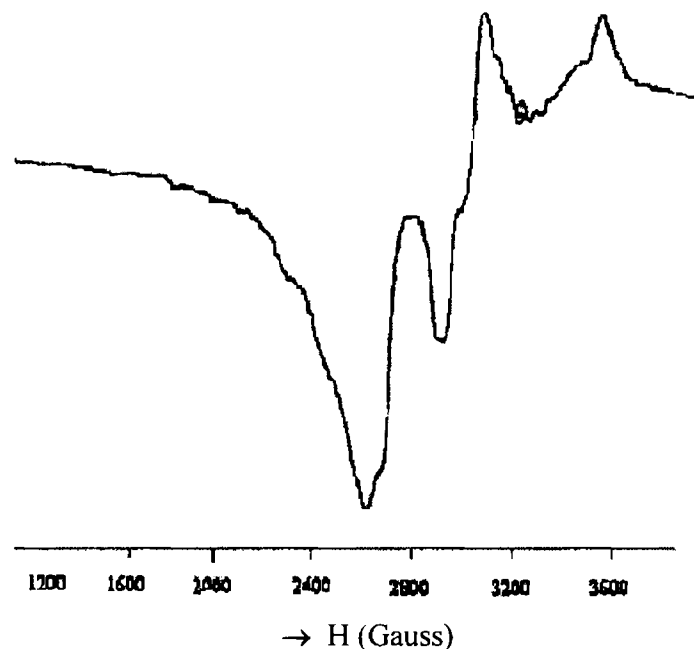


Figure III.16 EPR spectrum $[\text{Ru}_2(\text{qpd})\text{Cl}_4(\text{H}_2\text{O})_2] \cdot 2\text{H}_2\text{O}$

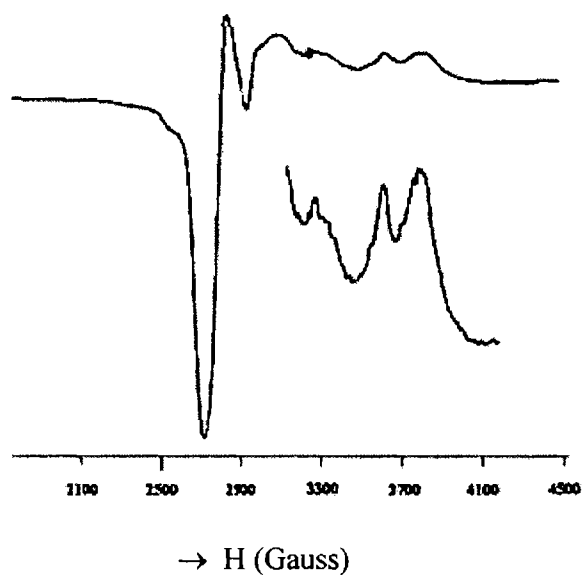


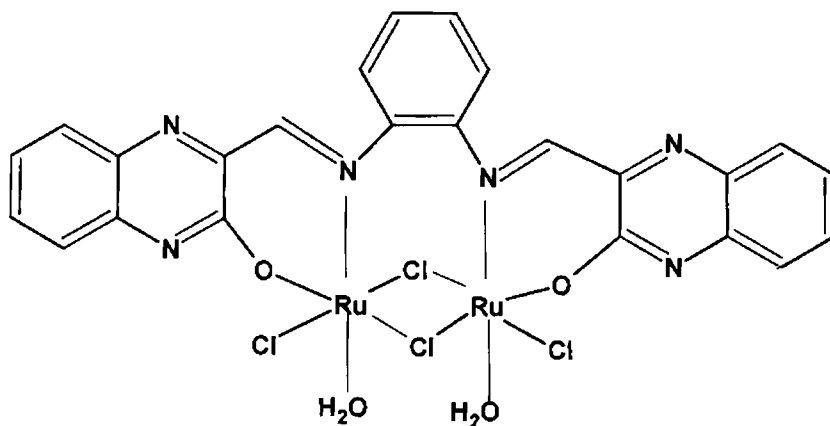
Figure III.17 EPR spectrum of $[\text{Ru}_2(\text{salpd})_3\text{Cl}_2(\text{H}_2\text{O})_2]$



Figure III.18 EPR spectrum of $[\text{Ru}(\text{salab})(\text{H}_2\text{O})_4]\text{Cl}_2 \cdot \text{H}_2\text{O}$

TABLE III.12 EPR Spectral Data of Complexes

Complex	g values
$[\text{Ru}_2(\text{qpd})\text{Cl}_4(\text{H}_2\text{O})_2] \cdot 2\text{H}_2\text{O}$	$g_1 = 2.28, \quad g_2 = 2.11, \quad g_3 = 1.81$
$[\text{Ru}_2(\text{qap})_2\text{Cl}_2(\text{H}_2\text{O})_2] \cdot \text{H}_2\text{O}$	$g_{\parallel} = 2.06, \quad g_{\perp} = 1.97$
$[\text{Ru}_2(\text{qab})_2\text{Cl}_4(\text{H}_2\text{O})_2] \cdot 3\text{H}_2\text{O}$	$g_1 = 2.32, \quad g_2 = 2.1, \quad g_3 = 1.91$
$[\text{Ru}_2(\text{salpd})_3\text{Cl}_2(\text{H}_2\text{O})_2]$	$g_{\parallel} = 1.84, \quad g_{\perp} = 2.34$
$[\text{Ru}_2(\text{salap})_4\text{Cl}_2] \cdot \text{H}_2\text{O}$	$g_1 = 2.12, \quad g_2 = 2.05, \quad g_3 = 1.89$
$[\text{Ru}(\text{salab})(\text{H}_2\text{O})_4]\text{Cl}_2 \cdot \text{H}_2\text{O}$	$g_{\parallel} = 2.03, \quad g_{\perp} = 1.85$

Figure. III.19 Proposed Structure of $[\text{Ru}_2(\text{qpd})\text{Cl}_4(\text{H}_2\text{O})_2]$

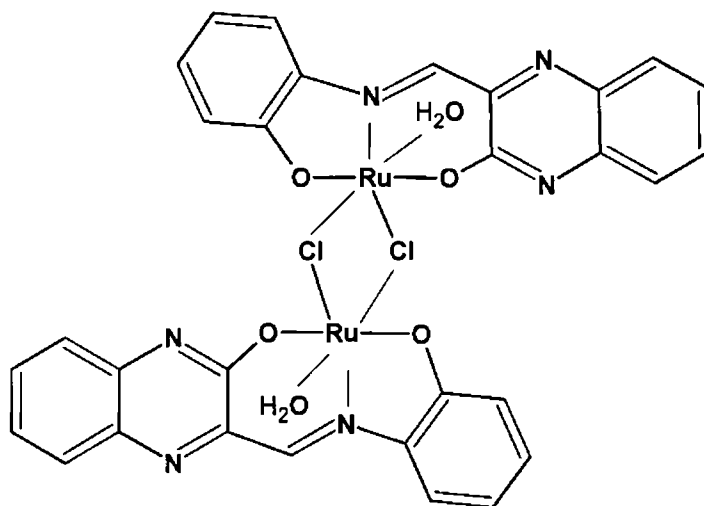


Figure III.20 Proposed Structure of $[\text{Ru}_2(\text{qap})_2\text{Cl}_2(\text{H}_2\text{O})_2]$

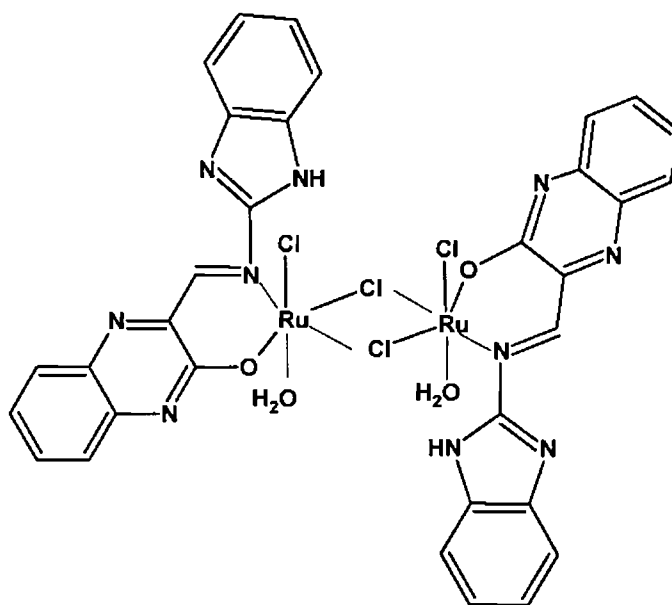


Figure III.21 Proposed Structure of $[\text{Ru}_2(\text{qab})_2\text{Cl}_4(\text{H}_2\text{O})_2]$

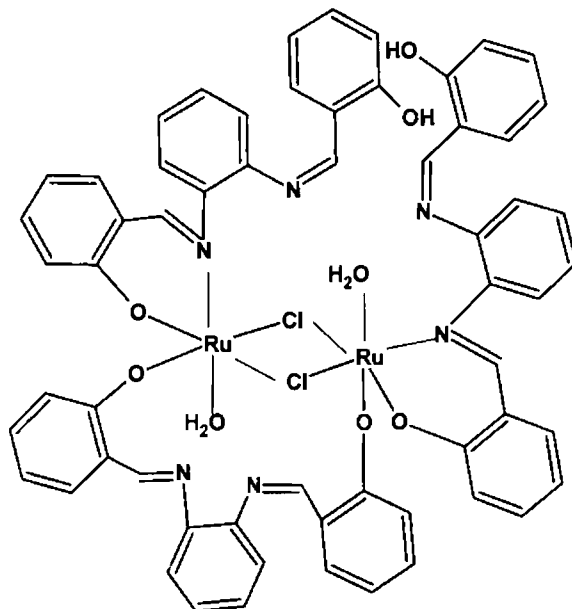


Figure III. 22 Proposed Structure of $[\text{Ru}_2(\text{salpd})_3\text{Cl}_2(\text{H}_2\text{O})_2]$

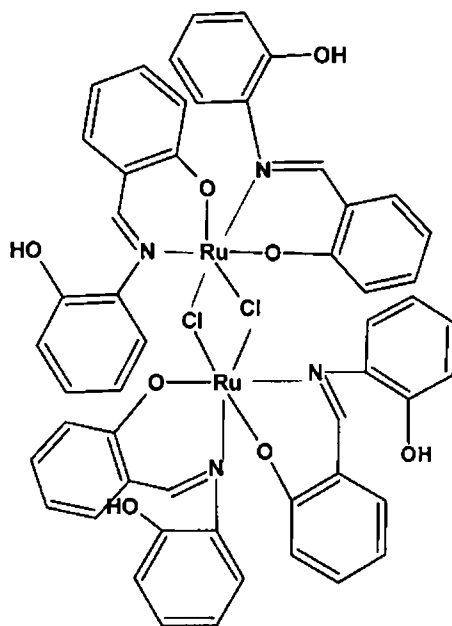


Figure III. 23 Proposed Structure of $[\text{Ru}_2(\text{salap})_4\text{Cl}_2]$

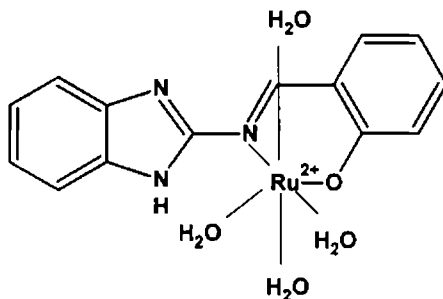


Figure III. 24 Proposed Structure of $[\text{Ru}(\text{salab})(\text{H}_2\text{O})_4]^{2+}$

Conclusion

On the basis of elemental analysis the empirical formula of the complexes were derived. Molar conductance values gave insight into the electrolytic behaviour of the complexes. Number of molecules of water of hydration and nature of ligand decomposition are obtained from the TG data. Molecular ion peaks observed from the FAB mass spectra agree with the empirical formula of the complexes. EPR spectra and magnetic moment values determine the oxidation state and geometry of the molecules. Further evidences were obtained from IR and UV spectral data. In $[\text{Ru}_2(\text{qpd})\text{Cl}_4(\text{H}_2\text{O})_2] \cdot 2\text{H}_2\text{O}$ ruthenium bridges with chlorine atom and the tetradentacy of the ligand is shared by both ruthenium atoms and a stable six membered ring results. The ligand qap acts as tridentate whereas qab, salpd, salap and salab act as bidentate in their complexes. The central metal atom is hexacoordinated. All these point to the octahedral nature of the bridged complexes. Hence it was concluded that the synthesized complexes of ruthenium except $[\text{Ru}(\text{salab})(\text{H}_2\text{O})_4]\text{Cl}_2 \cdot \text{H}_2\text{O}$ form binuclear species in which Ru(III) octahedra are bridged by two chloride ions constituting a common bridge between the octahedra. $[\text{Ru}(\text{salab})(\text{H}_2\text{O})_4]\text{Cl}_2 \cdot \text{H}_2\text{O}$ forms a mononuclear complex with four molecules of water coordinated to the metal in addition to one oxygen and one nitrogen of salab. Thus forms an octahedral geometry. The proposed structures of the complexes are given in Figure III.19-24.

References

- [1] Seddon K. R., *Coord. Chem. Rev.* **35**, 41; **41**, 79; **67**, 171 (1981;1982;1985).
- [2] Wong W. T., *Coord. Chem. Rev.* **131**, 45 (1994).
- [3] Ghosh B. K.; Chakravorty A., *Coord. Chem. Rev.* **25**, 239 (1989).
- [4] Kalyansundaram K., *Coord. Chem. Rev.* **46**, 159 (1982).
- [5] Kureshy R. I.; Khan N. H.; Abdi S H R.; Patel S. T.; Iyer P., *J. Mol Catalysis* **150**, 175 (1999).
- [6] Aoyama Y. K.; Kujisawa J. T; Walanawe T.; Toi A.; Ogashi H., *J. Am. Chem.Soc.* **108**, 943 (1986).
- [7] Sdrawn R.S.; Zamakani M.; Cocho J. L., *J. Am. Chem. Soc.* **108**, 3510 (1986) .
- [8] Viswanathamurthy P.; Natarajan K., *Trans. Met. Chem.* **24**, 638 (1999).
- [9] Groves J.T., "Cytochrome P-450: Structure, Mechanism and Biochemistry", In: P. Ortiz de Montallano (Ed), Plenum Press, New York. **7**, 1 (1986).
- [10] Siddal T.L.; Miyaura N.; Huffman J.C.; Kochi J. K., *J. Chem. Soc., Chem. Commum.* **1185**, (1983).
- [11] Samsel E. G.; Sreenivasan K.; Kochi J. K., *J. Am. Chem.Soc.* **107**, 606 (1985).
- [12] Sreenivasan K.; Kochi J. K., *Inorg. Chem.* **24**, 4671 (1985).
- [13] Sreenivasan K.; Michaud P.; Kochi J. K., *J. Am. Chem.Soc.* **108**, 2309 (1986).
- [14] Yoon H.; Burrows C. J., *J. Am. Chem.Soc.* **110**, 408 (1988).
- [15] Koola J. D.; Kochi J. K., *Inorg. Chem.* **26**, 908 (1987).
- [16] Horwitz C. P.; Creager S. E.; Murray R .W., *Inorg. Chem.* **29**, 106 (1990).
- [17] Zhang W.; Jacobson E .N., *J. Org. Chem.* **56**, 2296 (1991).
- [18] Katsuki T., *Coord. Chem. Rev.* **140**, 189 (1995).
- [19] Fukuda T.; Katsuki T., *Tetrahedron* **53**, 7201 (1997).

-
- [20] Llobt A.; Martel A. E.; Martinez M. A., *J. Mol. Catal.A: Chemical* **129**, 19 (1998).
- [21] Srinivas B.; Arulsamy N.; Zacharias P.S., *Polyhedron* **731**, (1991).
- [22] Gupta A. K.; Poddar R.K.; Choudhury A., *Indian J. Chem.* **39A**, 1191 (2000).
- [23] Gupta A.K.; Poddar R.K.; Gupta A., *Indian J.Chem.* **31**, 1187 (2000).
- [24] Mandal S.K.; Thomson L. K.; Nag K.; Chaland J. P., *Can. J. Chem.* **65**, 2815 (1987).
- [25] Lacroix P.; Khan O.; Theobald F.; Leroy J.; Wal, *Inorg. Chim. Acta* **142**, 129 (1988).
- [26] Casellato U.; Tamburini S.; Vigato P. A.; Destefani A.; Fenton D.E., *Inorg. Chim. Acta* **69**, 45. (1983).
- [27] Casellato U.; Guerriero P.; Tamburini S.; Vigato P.A.; Graziani R., *Inorg. Chim. Acta* **119**, 215 (1986).
- [28] Fenton D. E.; Casellato U.; Vigato P.A.; Vidali M., *Inorg. Chim. Acta* **95**, 187 (1984).
- [29] Halpern J., *Inorg. Chim. Acta* **62**, 31 (1982).
- [30] Poilblanc R., *Inorg. Chim. Acta* **62**, 75 (1982).
- [31] Mohan G.; Sharma R. C.; Parashar R .K., *Polish. J. Chem.* 929 (1992).
- [32] Mishra L.; Jaha A.; Yadav A. K., *Trans. Met. Chem.* **22**, 406 (1997).
- [33] Parashar R. K.; Sharma R C.; Kumar A.; Mohan G., *Inorg. Chim. Acta* **151**, 201 (1988).
- [34] El-Hendawy A. M.; Alkubaisi A. H.; El-Ghany; El-Ko; Shana M.M., *Polyhedron* **12**, 2343 (1993).
- [35] Bhowon M. G.; Li Kam Wah H.; Narain R., *Polyhedron* **341** (1998).
- [36] Niswander R. H.; Martell A. E., *Inorg. Chem.* **17** (1976).
- [37] Tsumaki T., *Bull. Chem.Soc. Japan* **13**, 252 (1938).
-

-
- [38] Geary W. J., *Coord.Chem.Rev.* **7**, 81 (1971).
- [39] Mojumdar S. C.; Melnik M.; Jona E., *Chem. Papers* **53** (5), 309 (1999).
- [40] Ismail A. Patel; Bharat T. Thaker, *Indian J. Chem.* **38A**, 427 (1999).
- [41] Mohammed Yusuff K. K.; Sreekala R., *J. polym.Sci: Part A, Polym.Chem.* **30**, 2595 (1992).
- [42] Chandra S.; Singh R., *Indian J.Chem.* **27A**, 417 (1988).
- [43] Sailaja S.; Radhakrishna Reddy M.; Mohana Raju K.; Hussain Reddy K., *Indian J. Chem.* **38A**, 156 (1999).
- [44] Ismail A. Patel; Thaker B.T.; Thaker P. B., *Indian J. Chem.* **37 A**, 429 (1998).
- [45] Kazuo Nakamoto, *Infrared and Raman Spectra of Inorganic Coordination compounds, Part B*, 5th Edition, Wiley interscience, New York. (1997).
- [46] Figgis B.N.; Lewis J., *The Magnetic Properties of Transition Metal Complexes* (Ed) Cotton F.A., *Progress in Inorganic Chemistry*, Vol. 6, Interscience, New York, 1964.
- [47] Usha; Chandra S., *Synth.React.Inorg. Met. Org.Chem.* **22**, 929, 1565 (1992).
- [48] Kumar A.;Usha; Chandra S., *Synth. React. Inorg. Met. Org.Chem.* **23**, 671 (1993).
- [49] Usha; Kumar A.; Chandra S., *Transition Met. Chem.* **18**, 342 (1993).
- [50] Lever A.B.P., "Inorganic Electronic Spectroscopy", Elsevier, Amsterdam.
- [51] Lahiri C. K.; Bhattacharya S.; Ghosh B.K.; Chakravorthy A., *J. Organomet. Chem.* **674**, 107 (2003).
- [52] Ghosh P.; Pramanik A.; Bag N.; Lahiri C.K.; Chakravorthy A., *J.Organomet. Chem.* **454** 237 (1993).

CHAPTER IV

**STUDIES ON ZEOLITE- Y ENCAPSULATED
COMPLEXES OF RUTHENIUM**

4.1 Introduction

Neat complexes of transition metals are not usually employed in industrial process due to the inability to recover the catalyst from the reaction products. Scientists are in a quest to explore possible solution to the problem. Nowadays researchers are actively engaged in encapsulating the metal complexes in the cavities of zeolites and other suitable molecular sieves which may be used as industrial or biomimetic catalysts.^{1,2} These type of catalysts possess the advantages of both homogeneous and heterogeneous catalytic systems. Since the catalyst is trapped in zeolite cavity, products can be easily separated. Also the lifetime of the catalyst can be increased by encapsulation. Recent reports reveal the importance of zeolite encapsulated complexes in catalysis for the selective oxidation, alkylation, dehydrogenation, cyclization, amination, acylation, isomerisation and rearrangement of various substrates.³⁻⁶

Ruthenium is a very active metal in catalytic field. Since it is expensive it is not advisable to use simple complexes as catalyst. Encapsulation of ruthenium complexes reduces the percentage of metal in the catalyst and thus reduces the cost of catalytic reaction.

4.2 Experimental

Details regarding the synthesis of metal exchanged zeolite, ligands qpd, qap, qab, salpd, salap and salab are given in Chapter II.

4.2.1 Synthesis of Ru(III) zeolite encapsulated complexes of qpd, qap, qab, salpd, salap and salab.

Metal exchanged zeolite (5.0 g RuY) was added to a solution of each ligand (concentration of each ligand was adjusted to have 1:1 metal: ligand mole ratio) in ethanol (50 mL) and refluxed for 10 h to ensure complexation. The ligand penetrates through the pores of the zeolite and complexes with the metal ions already present within the zeolite. The complexed product becomes too large to pass through the aperture of the supercage and will be retained inside the cages. The resultant mass was soxhlet extracted with methanol until the extracting solvent became colourless. It was further soxhlet extracted with acetone, ensuring the complete removal of the surface species. The uncomplexed metal ions in the zeolite and ionisable portions of the ligand were removed by ion exchange with NaCl solution (0.01M, 250 mL) for 24 h. It was filtered, washed free of chloride ions and finally dried at 100°C for 2 h and stored in vacuum over anhydrous calcium chloride.

4.3 Characterization techniques

The various physico-chemical techniques to characterize the prepared complexes are given in Chapter-II.

4.4 Results and discussion

4.4.1 Elemental analysis

Analytical data of metal exchanged zeolite and encapsulated complexes are given in Table IV.1. Elemental analyses reveal a Si/Al ratio of 2.6 for NaY that corresponds to a unit cell formula $\text{Na}_{54}(\text{AlO}_2)_{54}(\text{SiO}_2)_{138.n} \text{H}_2\text{O}$ for NaY.⁷ Almost constant value of Si/Al ratio after the metal exchange and formation of complexes confirm that zeolite framework retains its crystal structure.⁸ This also indicates that dealumination did not take place during metal exchange and encapsulation. Ion exchange takes place according to the equation



where x represents the fraction of M^{3+} ions exchanged with Na^+ in the zeolite.⁹ The unit cell formula of ruthenium exchanged zeolite was derived to be $\text{Na}_{44.14}\text{Ru}_{3.29}(\text{AlO}_2)_{54}(\text{SiO}_2)_{138.n} \text{H}_2\text{O}$ from the metal percentage of RuY. The corresponding degree of ion exchange was calculated as 18.3%. The elemental analysis confirms the formation of metal complexes in the zeolite cavities. However the amount of ruthenium was significantly reduced in encapsulated complexes as compared to RuY. This might be due to dissolution of ruthenium into the solvent while refluxing for complexation process.

TABLE IV.1 Analytical data of metal exchanged zeolites and encapsulated complexes

Compound	Elements % found						
	%C	%H	%N	%Ru	%Si	%Al	%Na
NaY	-	-	-	-	20.9	7.9	9.6
RuY	-	-	-	1.8	20.4	7.6	5.6
RuYqpd	0.979	2.634	0.048	0.3	20.1	7.4	7.8
RuYqap	0.820	1.514	0.032	0.4	19.9	7.7	8.2
RuYqab	1.100	2.584	0.229	0.9	19.6	7.4	3.9
RuYsalpd	0.852	2.610	0.051	0.3	20.3	7.5	8.1
RuYsalap	1.034	2.696	0.053	0.6	20.1	7.4	7.1
RuYsalab	1.798	2.540	0.267	0.5	20.2	7.6	6.1

The analytical data of the encapsulated complexes show that the metal ion percentage is in excess of what is expected for formation 1:1 complexes. This might be because of the unexchanged metal ion present in the cavities. The complex formed or ions trapped within the cages of the zeolite framework may hinder further entry of the ligands, thus preventing the formation of a complex analogous to simple complex. The metal ions trapped in the cages of zeolite prevent the further exchange with Na^+ ions.

Any residual charges left behind after the addition of the ligand to the metal ion in cages would be satisfied by the Cl⁻ of NaCl used during exchange process. The percentage of ruthenium expected from the composition of 1:1 complexes and that actually present in the encapsulated complexes are given in Table IV.2.

TABLE IV.2 Comparison of percentage of metal actually present and calculated from the composition of the 1:1 complexes in zeolite encapsulated complexes

Complex	% Ru for 1:1 complex (calculated)	% Ru (found)
RuYqpd	0.06	0.3
RuYqap	0.08	0.4
RuYqab	0.33	0.9
RuYsalpd	0.18	0.3
RuYsalap	0.38	0.6
RuYsalab	0.64	0.8

4.4.2 Surface area and pore volume

Surface area of the zeolite samples (Table IV.3) was determined by BET method after activating at 350°C in nitrogen atmosphere. A small reduction in surface area was noticed due to metal exchange. Encapsulation of complexes in zeolite pores resulted in decrease in surface area and pore volume to a greater extent.² This is due to the large size of the complex encapsulating in the cage which results in the filling of the pore. Reduction in surface area supports encapsulation of complexes in zeolite cages.

TABLE IV.3 Surface area and Pore volume data

Compound	Surface Area(Sq.m/g)	Pore volume (cc/g)
zeolite	799	0.3978
NaY	692	0.3482
RuY	682	0.3458
RuYqpd	627	0.3195
RuYqap	482	0.2369
RuYqab	567	0.2920
RuYsalpd	662	0.3367
RuYsalap	627	0.3266
RuYsalab	662	0.3520

4.4.3 Thermogravimetric analysis

TG/DTG and DSC/DTA curves of zeolite samples (Figure IV.1-IV.6) were recorded in nitrogen atmosphere from ambient temperature up to 1200°C at a heating rate of 10°C /min. The pattern of decomposition is the same for all encapsulated complexes. The TG curves reveal that there is a continuous weight loss in the early stages, which might be due to deaquation of the samples. Table IV.4 shows the thermogravimetric data of the encapsulated complexes of ruthenium.

RuYqpd loses 28% weight loss till 110°C, the peak temperature being 106°C. Thereafter decomposition takes place slowly and reaches constant weight around 800°C. Weight loss in this stage is only 8%. Zeolite framework is seen to be destroyed only above 900 °C.

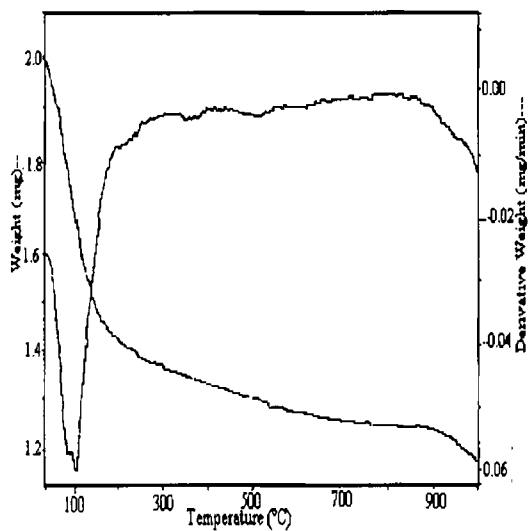


Figure IV.1(a) TG/DTG curve of
RuYqpd

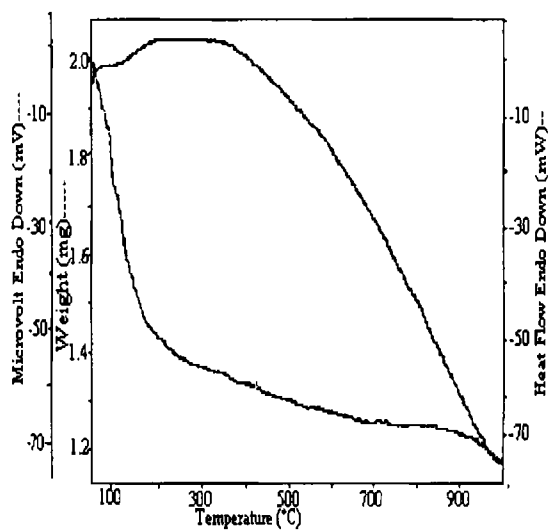


Figure IV.1(b) DSC curve of RuYqpd

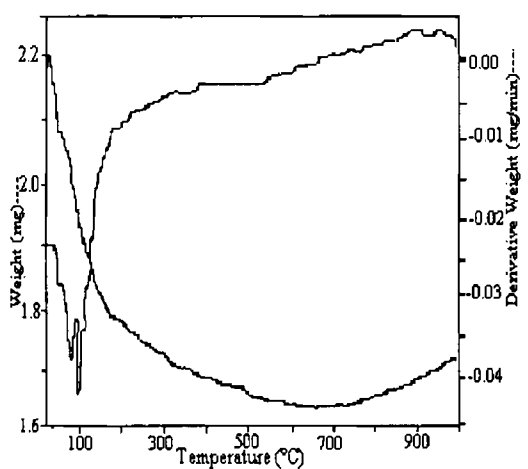


Figure IV.2(a) TG/DTG curve of
RuYqap

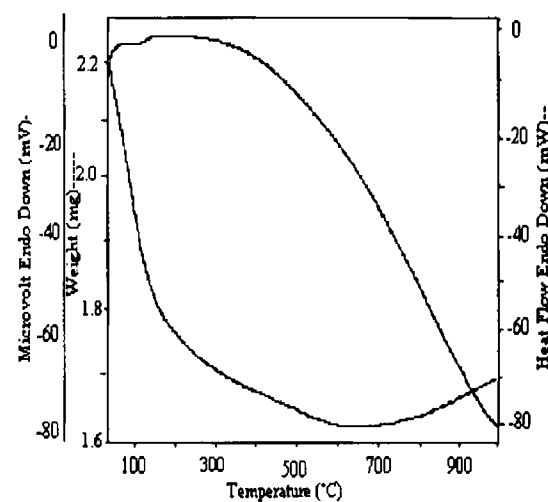


Figure IV.2(b) DSC curve of RuYqap

Upto 200°C a steady mass loss of 21% occurs in RuYqap, the peak temperature being 101°C. This represents deaquation of the complex. Thereafter rate of

decomposition is slow. Weight loss (6%) continues till 600°C. This might be due to decomposition of the organic part of the ligand. Thereafter no decomposition takes place till 800°C. After 800°C destruction of zeolite framework is indicated.

First stage of decomposition in RuYqab occurs till 200°C. Weight loss in this stage corresponds to 25 %, peak temperature being 115°C. Weight loss might be due to the removal of occluded water in addition to the physisorbed water. Weight loss continues till 550°C, peak temperature being 331°C. Destruction of zeolite framework takes place above 800°C.

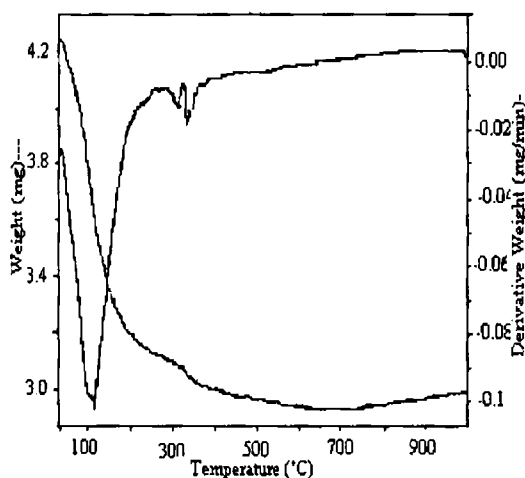


Figure IV.3(a) TG/DTG curve of RuYqab

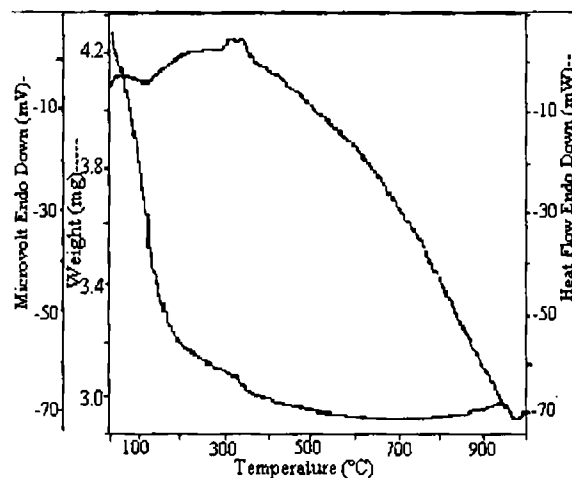


Figure IV.3(b) DSC curve of RuYqab

In RuYsalpd, upto 200°C 28% weight loss occurs, peak temperature being 113°C. Water entrapped in cages would have expelled along with the physisorbed water. Steady weight loss of small percentage occurs till 550°C.

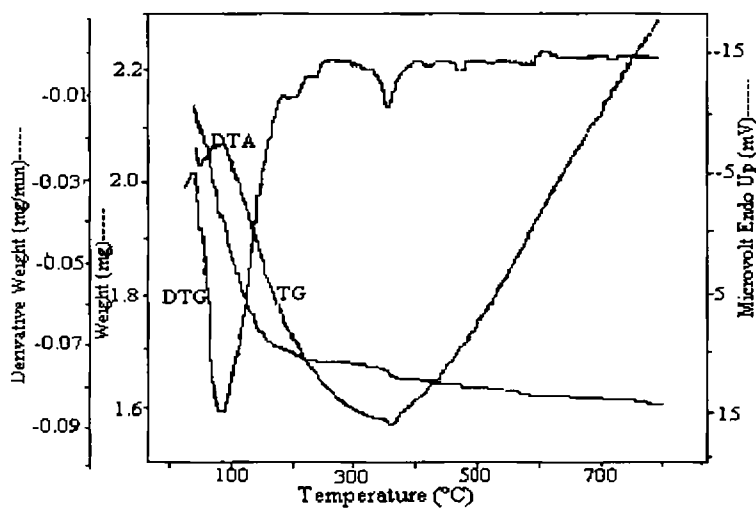


Figure IV.4 TG/DTG/DTA curve of RuYsalpd

RuYsalap undergoes weight loss upto 200°C. 28% weight loss occurs during this stage, peak temperature being 107°C, indicating expulsion of entrapped water along with physisorbed water. Thereafter steady weight loss of about 9% occurs till 550°C. Then constant weight is maintained till 800°C. Thereafter framework is destroyed.

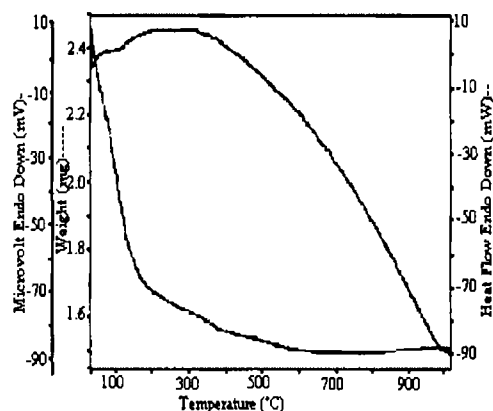
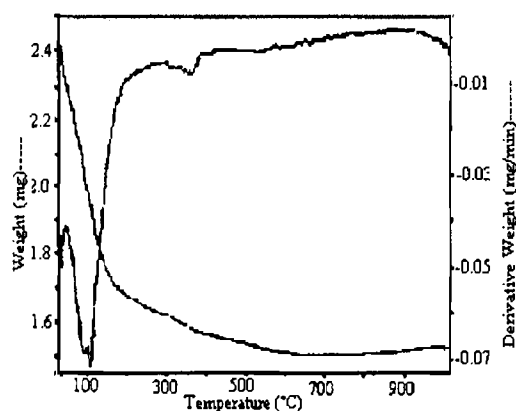
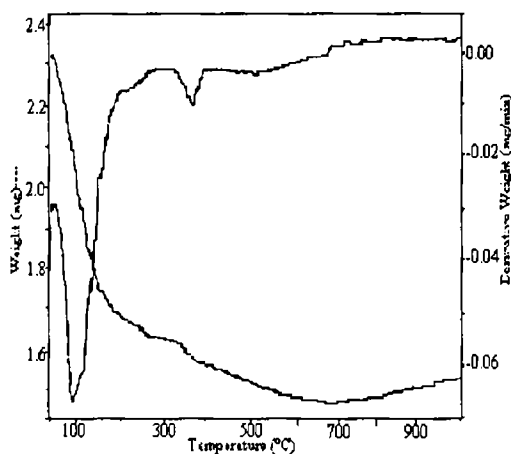


Figure IV.5(a) TG/DTG curve of RuYsalap Figure IV.5(b) DSC curve of RuYsalap

In RuYsalab 28% weight loss occurs till 200°C, peak temperature being 108°C. Physisorbed as well as entrapped water are lost. Decrease in weight continues till 600°C, peak temperature being 367°C.

DSC curve for all complexes presents endothermic peak around 100°C corresponding to the deauration of the sample. This is followed by exothermic maximum with the centre at about 350°C corresponding to the decomposition of the complex. The DTA curve of RuYqab shows two bendings at 320°C and 350°C. They corresponds to the intermediate decomposition products of the complex.¹⁰



**Figure IV.6(a) TG/DTG curve of
RuYsalab**

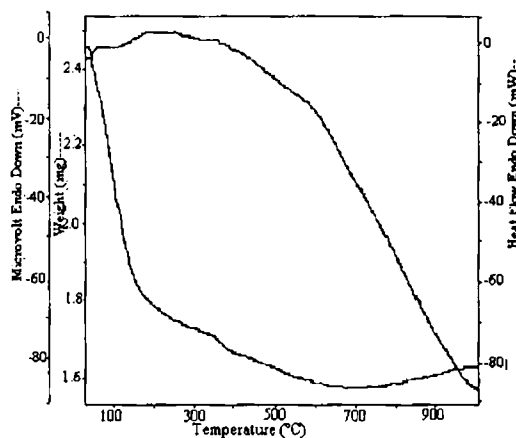


**Figure IV.6(b) DSC curve of
RuYsalab**

Thermal analysis provides a useful tool to study about stability of metal complexes. It is essential to know about the stability of metal complexes in order to apply the synthesized complexes in catalysis. TG curve of RuY also shows a weight loss of 25% in the temperature range 50-200°C. This might be due to loss of intrazeolite water molecules. IR spectra of the complexes after heating to 200°C exhibited similar peaks as that of original complex, indicating that complex is not decomposed till 200°C. In the

second stage of decomposition only very small percentage of weight loss (~7%) occurs. This might be due to the decomposition of the complex within the zeolite cage. Zeolite framework is seen to be destroyed only above 800°C. Thermal analysis shows that the stability of the complexes are enhanced on heterogenization by encapsulation in zeolite pores as suggested by earlier reports.¹¹

TABLE IV. 4 TG/DTG data of encapsulated complexes

Compound	I Stage			II Stage		
	Temperature(°C)	Weight loss(%)	Nature of DSC/DTA curve	Temperature(°C)	Weight loss(%)	Nature of DSC/DTA curve
RuYqpd	40-100°C	28	endothermic	200-800	8	exothermic
RuYqap	40-100°C	21	endothermic	200-600	6	exothermic
RuYqab	40-100°C	25	endothermic	200-550	7	exothermic
RuYsalpd	40-100°C	28	endothermic	200-550	6	exothermic
RuYsalap	40-100°C	28	endothermic	200-550	9	exothermic
RuYsalab	40-100°C	28	endothermic	200-550	8	exothermic

4.4.4 X-Ray diffraction

Powdered X-ray diffraction patterns were obtained for NaY, Metal exchanged zeolites and zeolite encapsulated complexes of o-phenylenediamine. The diffraction patterns of different complexes are given in Figure IV.7. Zeolite framework retains its crystallinity even after encapsulation, which is evidenced by the similar diffraction pattern in all cases. This supports the fact that reduction in surface area observed is not due to collapse of crystalline structure but due to encapsulation of complexes in the cages.

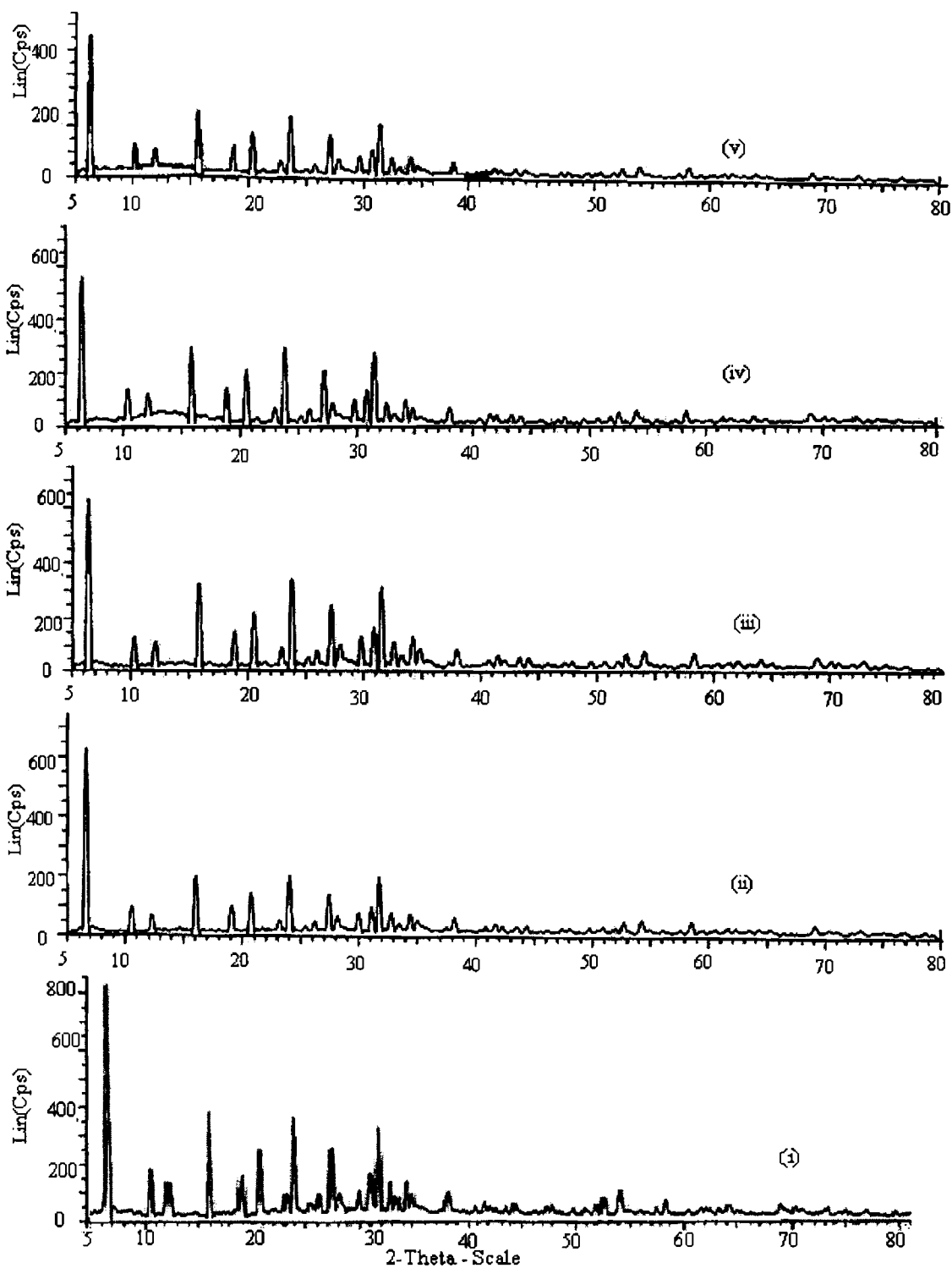


Figure IV. 7 XRD spectra of (i) RuY (ii) RuYqpd (iii) RuYqab (iv) RuYsalpd(v) RuYsalap

4.4.5 SEM analysis

Scanning electron micrographs of encapsulated complexes¹² before and after soxhlet extraction are given in Figure IV.8. This clearly indicates the presence of well defined crystals free from any shadow of metal ions or complexes present on their external surface after soxhlet extraction.

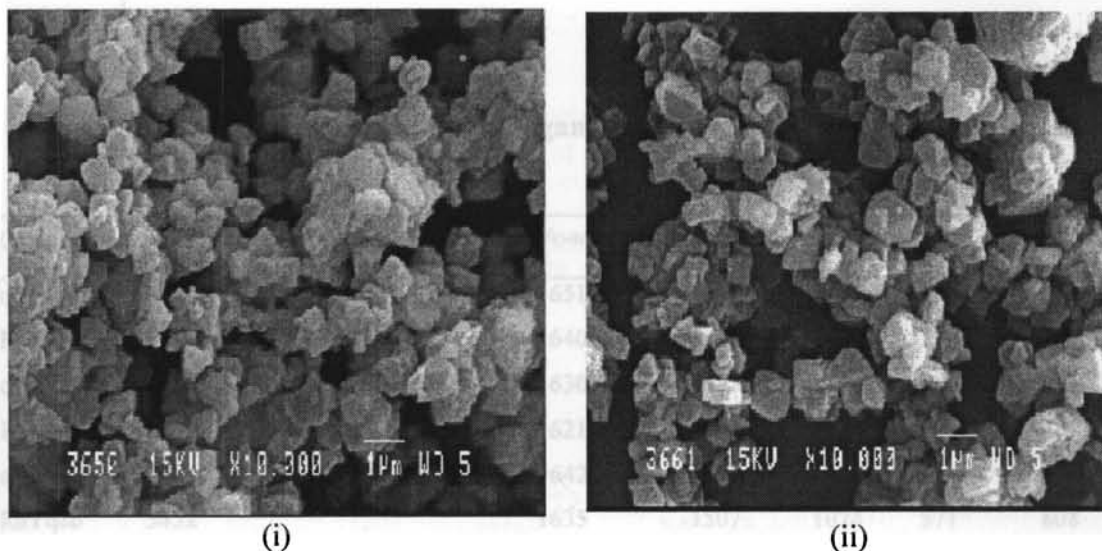


Figure IV.8 Scanning Electron Micrographs of RuYqpd (i) before and (ii) after soxhlet extraction

4.4.6 Infrared spectra

The FTIR spectral bands of the ligands and supported complexes were recorded as KBr pellets in the region $400\text{-}4000\text{ cm}^{-1}$. The IR frequencies were tabulated in Table IV.5. The infrared frequencies of metal exchanged zeolite and the parent zeolite are of almost the same values as reported in earlier studies.¹³⁻¹⁵ This indicates the non destruction of the zeolite framework by the metal exchange. The encapsulation of complexes inside zeolite cavities is confirmed by several workers.¹⁶ Similarity of the spectra of the simple and the encapsulated complex reveals the nature of the complex inside the cages.

For molecules containing benzimidazole ring the region $1660-1550\text{cm}^{-1}$ is very important.¹⁷ The band around 1640cm^{-1} in the ligand are shifted to lower frequencies in all the complexes which confirms complexation at nitrogen of the azomethine group. Band at 3461cm^{-1} in qab and at 3470cm^{-1} in salab are due to N-H of imidazole ring. This experiences slight shift towards lower frequency in RuYqab and RuYsalab which can be attributed to changes in environment due to coordination at other positions. The stretching vibrations of water molecules present in the zeolite lattice can be seen around 3500cm^{-1} .

TABLE IV.5 IR spectral data of ligands and zeolite encapsulated complexes

Compound	$\nu_{\text{N-H}}$	$\nu_{\text{O-H}}$	$\nu_{\text{C-O}}$ phenolic	$\nu_{\text{C=N}}$	$\nu_{\text{C-C}}$	$\nu_{\text{Zeolitic Peaks}}$	$\nu_{\text{Zeolite peaks}}$	$\nu_{\text{Coord. water}}$
qpd		3474	1117	1651	1534			
RuYqpd		3459		1640	1526	1021	579	789
qap			1116	1630	1525			
RuYqap		3448		1621	1513	1026	580	782
qab	3461		1123	1642	1530			
RuYqab	3452			1635	1507	1024	571	808
salpd			1138	1651	1561			
RuYsalpd		3489		1644	1547	1023	579	792
salap			1141	1639	1526			
RuYsalap		3439		1630	1518	1023	579	785
salab	3470		1135	1641	1533			
RuYsalab	3459			1636	1520	1023	576	792

IR spectra of all zeolite encapsulated complexes show bands in the region $1500-1600\text{cm}^{-1}$. These are assigned to C-C stretching vibrations of benzene ring. Since there are no zeolite bands at this position, $\nu_{\text{C-C}}$ of benzene rings indicates encapsulation of complexes.

In the IR spectra of the free ligands, bands occur in the region 1120-1150 cm^{-1} due to $\nu_{\text{C-O}}$ of phenolic group. However this is absent in encapsulated complexes. This might be due to the masking by the broad zeolite band around 1000 cm^{-1} which is not seen in the corresponding ligands. Hence it can be assigned to the zeolite framework vibration. Other major zeolite framework bands appear around 1140, 725 cm^{-1} .¹⁸ Also most of the bands due to ligands are masked by the zeolite peaks in complexes.

4.4.7 Electronic spectra

TABLE IV.6 Electronic Spectral Data of the encapsulated complexes of ruthenium

Complex	Absorbance (cm^{-1})	Tentative assignments
RuYqpd	34720	${}^2T_{2g} \rightarrow {}^2A_{2g}, {}^2T_{1g}$
	17540	${}^2T_{2g} \rightarrow {}^4T_{1g}$
RuYqap	20620	${}^2T_{2g} \rightarrow {}^2E_g$
	17480	${}^2T_{2g} \rightarrow {}^4T_{1g}$
RuYqab	34600	${}^2T_{2g} \rightarrow {}^2A_{2g}, {}^2T_{1g}$
	20700	${}^2T_{2g} \rightarrow {}^2E_g$
	17570	${}^2T_{2g} \rightarrow {}^4T_{1g}$
RuYsalpd	36100	charge transfer
	33350	${}^2T_{2g} \rightarrow {}^2A_{2g}, {}^2T_{1g}$
	36630	Charge transfer
RuYsalap	34360	${}^2T_{2g} \rightarrow {}^2A_{2g}, {}^2T_{1g}$
	20280	${}^2T_{2g} \rightarrow {}^2E_g$
RuYsalab	36000	charge transfer
	17270	${}^2T_{2g} \rightarrow {}^4T_{1g}$

Due to the low concentration of the metal ion species in the zeolite, the absorption bands are of very low intensity. Furthermore ligand absorptions and charge transfer

transitions complicate the assignment of band in the ultraviolet and high energy visible region. However similar spectral patterns were observed with neat as well as encapsulated complexes of ruthenium. Hence an octahedral structure may be suggested for encapsulated complexes and this is possible only on additional coordination of water with the metal. The electronic spectral data of the encapsulated complexes are given in Table IV.6.

4.4.8 EPR spectra

EPR spectra of the encapsulated complexes were recorded at liquid nitrogen temperature. The slight variations in the EPR parameters of the Ru(III) ions in the metal exchanged zeolite (RuY) with the addition of the ligand is due to the change in environment of the ion and hence supports the encapsulation of the complex in the zeolite cavities.

EPR spectrum of encapsulated complex RuYsalap gives three g values (Table IV.7) indicating rhombohedral distortion of octahedral geometry. RuYqab and RuYsalab present an axial symmetry giving two g values. The presence of paramagnetically active Ru(III) in the complex is consistent with the axial symmetry of the complex.¹⁹ A well resolved EPR spectra could not be obtained for other complexes. This might be due to the impact imposed by the zeolite matrix.

TABLE IV.7 EPR spectral parameters of zeolite encapsulated complexes

Complex	EPR parameters
RuYqab	$g_{\parallel} = 2.12$; $g_{\perp} = 2.14$
RuYsalap	$g_1 = 2.17$; $g_2 = 2.12$; $g_3 = 2.00$
RuYsalab	$g_{\parallel} = 2.16$; $g_{\perp} = 2.05$

Conclusion

Zeolite encapsulated Ru(III) complexes of Schiff bases have been synthesized and characterized with a view to understand the chemical and physical properties, the nature of coordination and thermal stability of complexes. Chemical analyses reveal that the percentage of metal in encapsulated complexes is greater than that expected for 1:1 complexes, which might be due to the inclusion of unexchanged metal in the cavities. The similarity in XRD pattern of NaY, RuY and encapsulated complexes reveal that the framework retains its crystal structure even after complexation. The removal of surface species was ascertained by SEM analyses. The lower surface area and pore volume of complexes as compared to metal exchanged zeolite suggest encapsulation. The coordination of ligands with metal ion was ascertained in all cases by IR spectra. On the basis of magnetic moment, electronic spectra and EPR, an octahedral geometry was suggested for all the complexes.

References

- [1] Raja R.; Ratnasamy P., *J. Mol. Catal.* **100**, 93 (1995).
- [2] Balkus K.J.Jr.; Gabrielov A.G., *J. Inclusion Phenom. Mol. Recogn. Chem.*, **21**, 159. (1995).
- [3] Rafelt G.S.; Clark J. H., *Catal. Today* **57**, 3 (2000).
- [4] Sheldon R.A.; Arends I.W.C.E.; Dijkstra A., *Catal Today* **57**, 157. (2000).
- [5] Jacob C.R.; Varkey S.P.; Ratnasamy P., *Microporous Mesoporous Mater.* **22**, 465 (1988).
- [6] Hutchings G.J., *Chem. Commun.* **301**, (1999).
- [7] Tollman C.; Herron N., Symposium on Hydroc. Oxidation, 194th National Meeting of the American Chemical Society, New Orleans, LA, Aug. 30-Sept.4,(1987).
- [8] Menon P.G., "Lectures on Catalysis", 41st Ann. Meeting. Ind. Acad. Sci; S.Ramasheshan (Ed.); (1975).
- [9] Carol A Bessel ; Debra R. Rolison, *J. Phys.Chem. B* **101**, 1148 (1997).
- [10] Mojumdar S.C.; Melnik M.; Jona E., *Chem. Papers* **53 (5)**, 314 (1999).
- [11] Diegruber H.; Plath P.J.; Schulz-Ekloff G.; Mohl M., *J. Mol. Catal.*, **24**, 115. (1984).
- [12] Thomas J.M., Calton C.R.A, *Prog. Inorg. Chem.* **35**, 1 (1988).
- [13] Flanigen E.M. in *Zeolite Chemistry and Catalysis*, Rabo J.A. (Ed), ACS Monograph, American Chemical Society, Washington D C (1976).
- [14] Jacobs P. A.; Beyer H. K.; valyon J., *Zeolites* **1**, 161 (1981).
- [15] Bindu Jacob, Ph.D Thesis, Cochin University of Science and Technology (1998).

- [16] Edgardo P.M; Nyole G.; Fabio L; Acosta D.D.; Pasquale P.; Aldo L.G.; Patricio R.; Bernard D., *J. Phys. Chem.* **97**, 12819 (1993).
- [17] Morgan J., *J.Chem.Soc.* 2343 (1961).
- [18] Egerton T.A.; Hagan A.; Stone F. S.; Vikerman J.C., *J.Chem .Soc. Faraday Trans.* **168**, 723 (1972).
- [19] Quêite A. de Paula; Alzir A. Batista; Otaciro R. Nascimento; Antônio J. da Costa-Filho; Mário S. Schultz; Marcos R. Bonfadini; Glaucius Oliva J. *Braz. Chem. Soc.***11 (5)** (2000).

CHAPTER V

**SYNTHESIS AND CHARACTERISATION OF NEAT AND
ENCAPSULATED SCHIFF BASE COMPLEXES OF NEODYMIUM**

5.1 Introduction

Recently coordination chemistry of lanthanides has achieved much progress. Over the past ten years lanthanide ions and lanthanide complexes have been proposed and used in several biological and medicinal applications. The interaction of lanthanide ions with biologically active ligands is of the utmost relevance to understand and develop new complexes.¹ Studies on neodymium Schiff base complexes have been carried out with a view to understand correctly the role of donor atoms, their relative position, size of the chelating rings formed and shape of the coordinating moiety on the selective binding of charged or neutral species.²⁻⁹ In this chapter, the results of our study on the synthesis and characterization of some new neodymium complexes are presented.

5.2 Simple complexes of neodymium

5.2.1 Synthesis

5.2.1.1 Neodymium - qpd complex

Neodymium(III) chloride hexahydrate (5 mmol ; 1.79 g) in methanol (25 mL) was added to refluxed solution of qpd (10 mmol; 4.2 g) in methanol (25mL). Resulting mixture was refluxed for 6 hours, concentrated to 5 mL and cooled in refrigerator. Crystalline yellowish brown compound separated was filtered, washed with hexane. It is then dried in *vacuo* over anhydrous calcium chloride (yield 92%).

5.2.1.2 Neodymium - qap complex

A similar synthetic procedure to that described for qpd complex of neodymium was followed for the synthesis of qap complex of neodymium with the ligand qap (10mmol; 2.65g). Resulting mixture was refluxed for 6 h. The solution was concentrated to 5mL and stirred magnetically in ice cold bath for 30 mts. Reddish brown crystalline compound separated was filtered, washed with hexane. It was then dried in *vacuo* over anhydrous calcium chloride (yield 85 %).

5.2.1.3 Neodymium - qab complex

The complex Nd- qab was synthesized in a similar manner except that qab (10mmol ; 2.89g) was used in the place of qap. Reddish brown crystalline compound separated was filtered, washed with hexane. It was then dried in *vacuo* over anhydrous calcium chloride (yield 85 %).

5.2.2 Results and discussion

Details of analytical and various physico-chemical techniques employed to characterize the prepared complexes are given in chapter II.

5.2.2.1 Elemental analysis

All the complexes were isolated as nonhygroscopic, amorphous substances and are quite stable in air. They are soluble in dimethyl sulphoxide, dimethyl formamide and are insoluble in hexane, carbon tetrachloride and water.

The microanalytical data of the ligand and the complexes are presented in Table V.2.1. CHN data indicate 1:2 coordination of the metal ion to the ligand qpd in the Nd-qpd complex. ICP-AES metal analysis of the complex gives an equivalent percentage of neodymium in the sample indicating the empirical formula of the complex to be $\text{Nd}(\text{qpd})_2\text{Cl}(\text{H}_2\text{O})_3$. Elemental analyses of Nd-qap complex suggest the empirical formula

of the complex to be $\text{Nd}(\text{qap})_2\text{Cl}(\text{H}_2\text{O})_4$ and that of Nd-qab complex to be $\text{Nd}(\text{qab})_2\text{Cl}(\text{H}_2\text{O})_5$.

TABLE V.2.1 Analytical Data of ligands and complexes

Compound	colour	Elements % found / (Calculated)			
		%C	%H	%N	%Nd
qpd	Reddish	68.22	3.59	19.72	
	brown	(68.56)	(3.84)	(19.99)	
$\text{Nd}(\text{qpd})_2\text{Cl}(\text{H}_2\text{O})_3$	Light	54.47	4.18	15.60	13.05
	brown	(53.75)	(3.38)	(15.67)	(13.45)
qap	Orange	67.42	4.53	16.14	
	red	(67.92)	(4.18)	(15.84)	
$\text{Nd}(\text{qap})_2\text{Cl}(\text{H}_2\text{O})_4$		47.13	3.48	11.09	17.68
	brown	(46.18)	(3.62)	(10.77)	(18.49)
qab		65.87	4.04	23.59	
	orange	(66.43)	(3.83)	(24.21)	
$\text{Nd}_2(\text{qab})_2\text{Cl}(\text{H}_2\text{O})_5$	Reddish	48.94	3.32	16.71	17.20
	brown	(46.4)	(3.41)	(16.91)	(17.40)

5.2.2.2 Molar conductance

TABLE V.2.2 Conductance Data of complexes in methanol (10^{-3}M)

Complex	Molar Conductance
$\text{Nd}(\text{qpd})_2\text{Cl}(\text{H}_2\text{O})_3$	26.4
$\text{Nd}(\text{qap})_2\text{Cl}(\text{H}_2\text{O})_4$	16.4
$\text{Nd}(\text{qab})_2\text{Cl}(\text{H}_2\text{O})_5$	32.7

The molar conductance value (Table V.2.2) in methanol (10^{-3} solution) suggests non-electrolytic nature for all the complexes of neodymium.¹⁰

5.2.2.3 Thermogravimetric analysis

The TG/DTG and DSC curves of neodymium complexes are given in Figure V.2.1-V.2.3. TG analysis of $\text{Nd}(\text{qpd})_2\text{Cl}(\text{H}_2\text{O})_3$ shows 3.4% weight loss around 60°C which might be due to the removal of two molecules of lattice water (Table V.2.3). Further 1.7% weight loss due to removal of one molecule of coordinated water takes place at 130°C . The compound is stable up to 312°C . Decomposition in the range $312\text{--}385^\circ\text{C}$ represents removal of ligand part of the molecule. Thereafter only very slight change in weight is observed till 800°C . DSC curve shows two small endothermic peaks below 150°C , one at 60°C indicating the removal of lattice held water and other at 130°C indicating removal of coordinated water. The broad endothermic dip at 950°C indicates large energy requirement for the decomposition process that starts at 720°C .

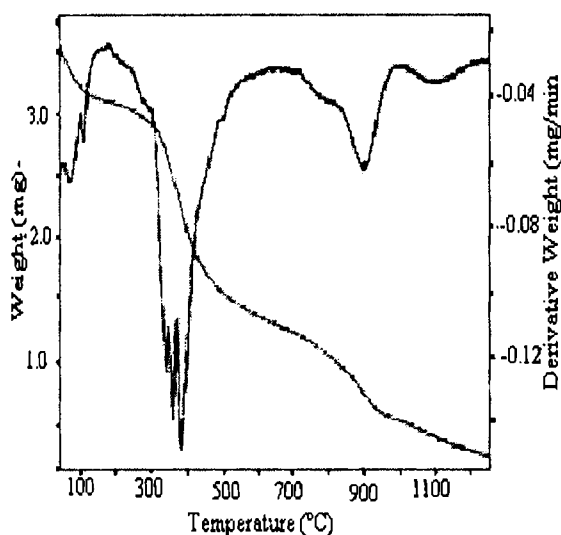


Figure V.2.1 (a) TG/DTG curve of $\text{Nd}(\text{qpd})_2\text{Cl}(\text{H}_2\text{O})_3$

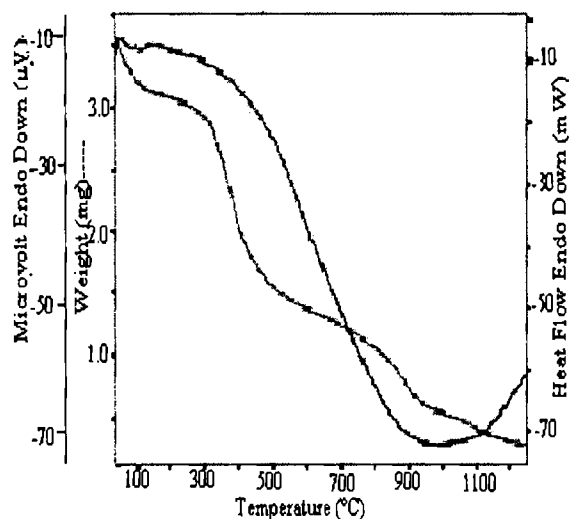


Figure V.2.1 (b) DSC curve of $\text{Nd}(\text{qpd})_2\text{Cl}(\text{H}_2\text{O})_3$

The weight loss of 2.3% around 60°C represents removal of one molecule of lattice water in $\text{Nd}(\text{qap})_2\text{Cl}(\text{H}_2\text{O})_4$. Further weight loss of 7.1% in the range 120-160°C is due to the removal of coordinated water. Gradual decomposition of ligand takes place thereafter. DSC curve shows two endothermic dips below 160°C corresponding to the removal of lattice held and coordinated water. Thereafter the exothermic peak around 300°C representing the decomposition of the organic moiety in the complex is followed by endothermic peaks indicating energy requirement for the decomposition process at high temperature.

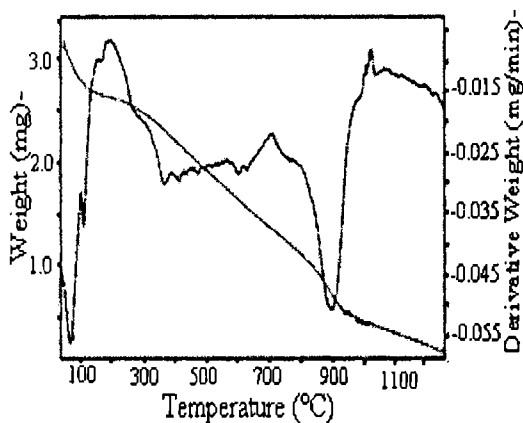


Figure V.2.2(a) TG/DTG curve of
 $\text{Nd}(\text{qap})_2\text{Cl}(\text{H}_2\text{O})_4$

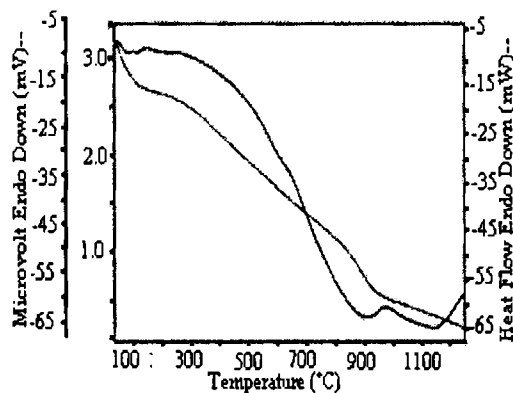


Figure V.2.2(b) DSC curve of
 $\text{Nd}(\text{qap})_2\text{Cl}(\text{H}_2\text{O})_4$

TG curve of $\text{Nd}(\text{qab})_2\text{Cl}(\text{H}_2\text{O})_5$ shows decomposition in two stages. In the first stage at 62°C removal of lattice water (2.1%) takes place. Second stage corresponds to the removal of coordinated water which corresponds to the weight loss of 6.5% in the range 120-150°C. This is indicated by the endotherms at 60°C and 130°C in the DSC curve.

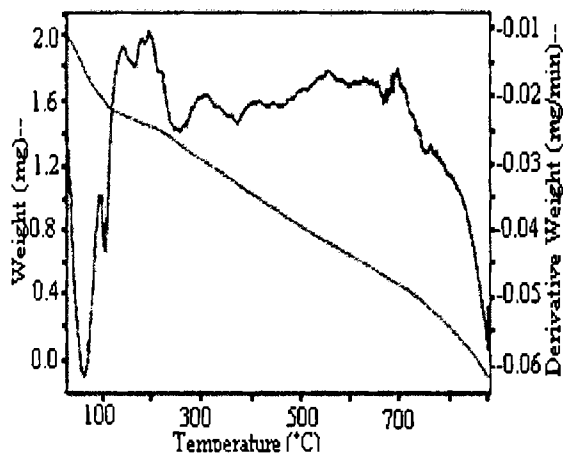


Figure V.2.3(a) TG/DTG curve of
 $\text{Nd}(\text{qab})_2\text{Cl}(\text{H}_2\text{O})_5$

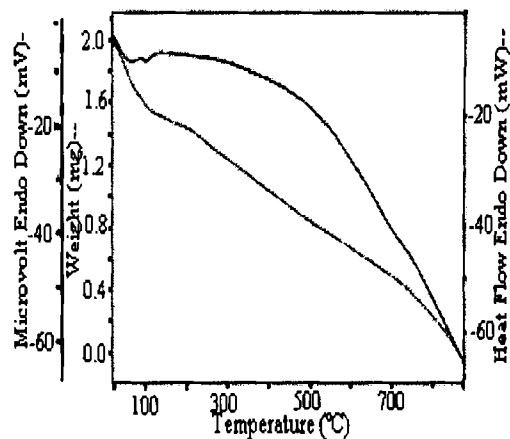


Figure V.2.3(b) DSC curve of
 $\text{Nd}(\text{qab})_2\text{Cl}(\text{H}_2\text{O})_5$

TABLE V.2.3 Thermogravimetric data of neodymium complexes

Complex	Temp. range of decomposition ($^{\circ}\text{C}$)	% weight loss	Nature of DSC curve
$\text{Nd}(\text{qpd})_2\text{Cl}(\text{H}_2\text{O})_3$	50-130	5.1	endothermic
	312-410	27	exothermic
$\text{Nd}(\text{qap})_2\text{Cl}(\text{H}_2\text{O})_4$	50-160	9.4	endothermic
	260-490	18	exothermic
$\text{Nd}(\text{qab})_2\text{Cl}(\text{H}_2\text{O})_5$	60-150	8.6	endothermic

5.2.2.4 Infrared spectra

The broad band in the region $3400\text{-}3500\text{cm}^{-1}$ in all the complexes is due to the free hydroxyl group of water molecule present. IR spectral peaks observed in the region $1600\text{-}1650\text{cm}^{-1}$ for the free ligand due to C=N stretch were shifted to lower frequency (Table V.2.4). This low energy shift supports their coordination with metal ion at

azomethine group.¹¹ The C-O stretching band observed around 1110-1130 cm^{-1} in the ligands undergoes a positive shift indicating coordination of phenolic oxygen to the metal ion.

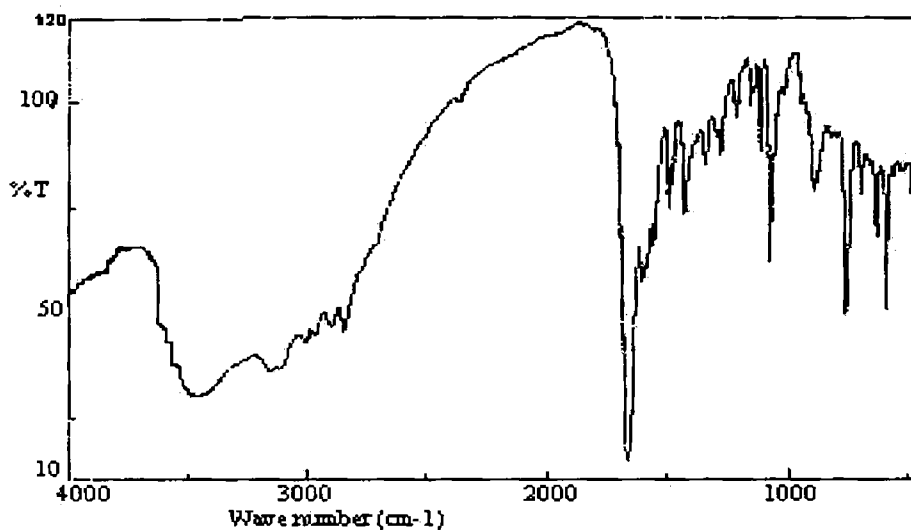


Fig V.2.4 Infrared spectrum of qab

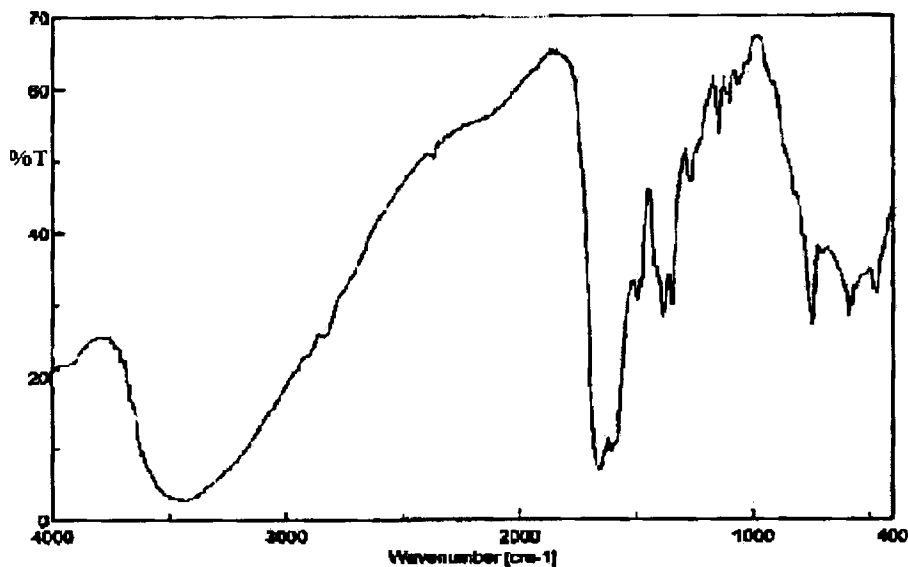


Fig V.2.5 Infrared spectrum of $\text{Nd}(\text{qab})_2\text{Cl}(\text{H}_2\text{O})_5$

The spectral band due to coordinated water is present in all complexes around 820 cm^{-1} . The sharp band in the region $360\text{-}365\text{ cm}^{-1}$ in all complexes, indicates the presence of M-OH bond. The M-N stretching band in the region $470\text{-}475\text{ cm}^{-1}$, further ascertains the formation of the complexes. Representative infrared spectra are given in Figure V.2.4 and V.2.5.

TABLE V.2.4 IR spectral data of simple complexes of neodymium

Compound	$\nu_{\text{O-H}}$	$\nu_{\text{C=N}}$	$\nu_{\text{C-O}}$ (Phenolic)	ν_{coord} H_2O	$\nu_{\text{M-Cl}}$ (terminal)	$\nu_{\text{M-N}}$
qpd	3474	1651	1117	-	-	-
$[\text{Nd}(\text{qpd})_2(\text{H}_2\text{O})\text{Cl}]\cdot 2\text{H}_2\text{O}$	3421	1645	1128	818	367	472
qap	3507	1630	1116	-	-	-
$[\text{Nd}(\text{qap})_2(\text{H}_2\text{O})_3\text{Cl}]\cdot \text{H}_2\text{O}$	3419	1620	1125	836	363	475
qab	3461	1642	1123	-	-	-
$[\text{Nd}(\text{qab})_2(\text{H}_2\text{O})_3\text{Cl}]\cdot 2\text{H}_2\text{O}$	3436	1632	1130	828	365	471

5.2.2.5 Magnetic susceptibility measurements

Magnetic moment of the Nd(III) complexes are found to be ~ 3.5 B.M. as expected for Nd(III) complexes.

5.2.2.6 Electronic spectra

The electronic spectra of the complexes are in Figure V.2.6-V.2.8 and the tentative assignments are given in Table V.2.5. The tripositive neodymium ion is characterized by having unfilled 4f-orbital with electronic configuration $4f^3 5s^2 5p^6 5d^0$. The spectroscopic properties of the lanthanide ions and their complexes are mainly due to the internal f-f transitions.¹² In lanthanides the 4f transitions are normally forbidden, but are observed indicating d-f orbital mixing occurring due to external crystal field.^{13,14} A few $f \leftrightarrow f$ transitions of lanthanide ions are very sensitive to the environment and are more intense

when the ion is coordinated than they are in the corresponding aquo ions. Most of the electronic spectra of neodymium complexes in methanol are characterized by charge-transfer bands and the hypersensitive transition ${}^4G_{5/2} \rightarrow {}^4I_{9/2}$ due to complexation.¹⁵

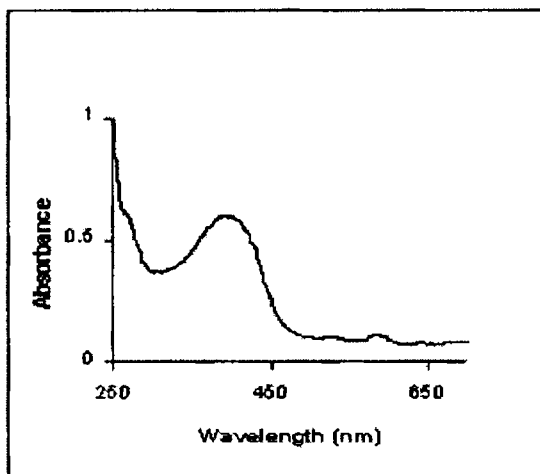


Figure V.2.6 Electronic spectrum of $[\text{Nd}(\text{qpd})_2(\text{H}_2\text{O})\text{Cl}]$

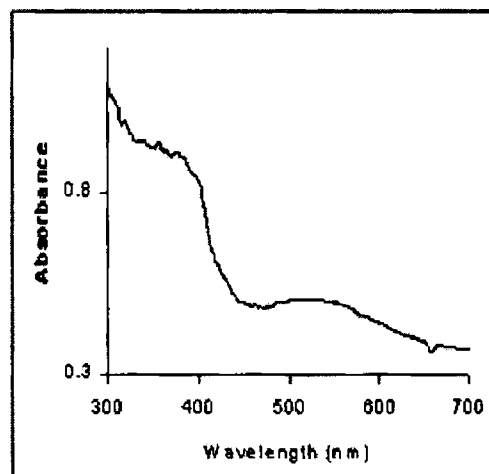


Figure V.2.7 Electronic spectrum of $[\text{Nd}(\text{qap})_2(\text{H}_2\text{O})_3\text{Cl}]$

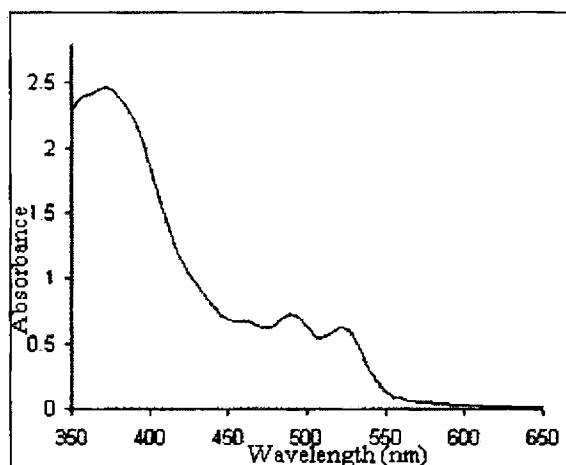
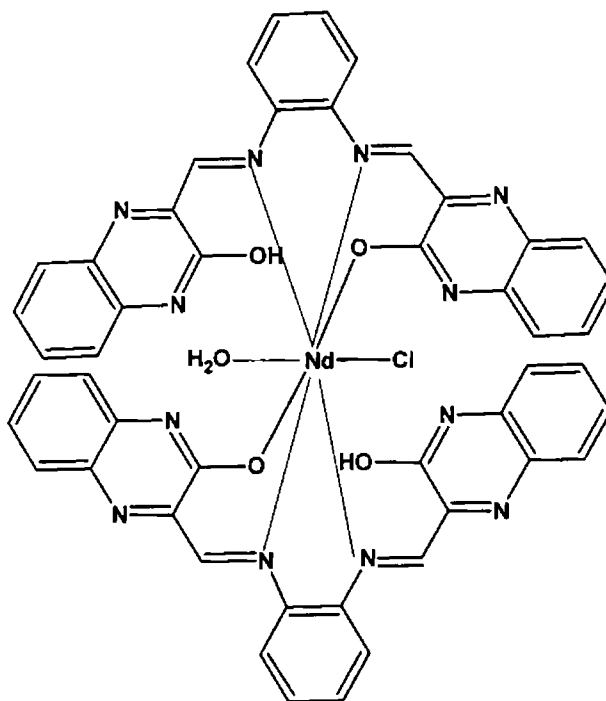


Figure V.2.8 Electronic spectrum of $[\text{Nd}(\text{qab})_2(\text{H}_2\text{O})_3\text{Cl}]$

TABLE V.2.5 Electronic Spectral Data of complexes

Complex	Absorptions (cm^{-1})	Tentative assignments
$[\text{Nd}(\text{qpd})_2(\text{H}_2\text{O})\text{Cl}]$	24810 16950	Charge Transfer ${}^4\text{G}_{5/2} \rightarrow {}^4\text{I}_{9/2}$
$[\text{Nd}(\text{qap})_2(\text{H}_2\text{O})_3\text{Cl}]$	25840 18500	Charge Transfer ${}^4\text{G}_{5/2} \rightarrow {}^4\text{I}_{9/2}$
$[\text{Nd}(\text{qab})_2(\text{H}_2\text{O})_3\text{Cl}]$	26590 20280 18800	Charge Transfer Charge Transfer ${}^4\text{G}_{5/2} \rightarrow {}^4\text{I}_{9/2}$

Figure V.2.9 Proposed structure of $[\text{Nd}(\text{qpd})_2(\text{H}_2\text{O})\text{Cl}]$

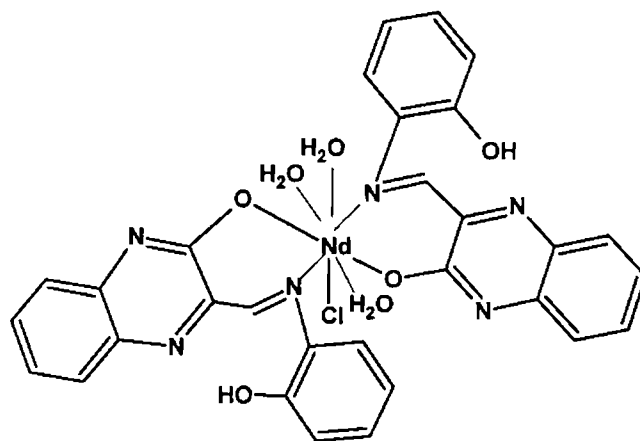


Figure V.2.10 Proposed structure of $[\text{Nd}(\text{qap})_2(\text{H}_2\text{O})_3\text{Cl}]$

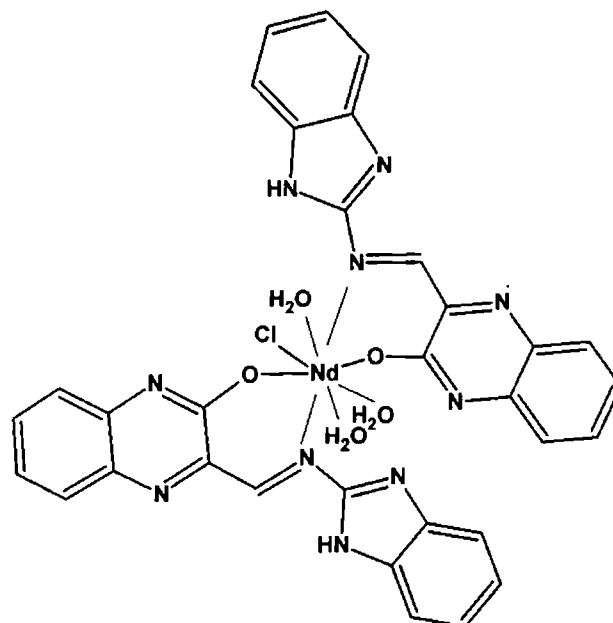


Figure V.2.11 Proposed structure of $[\text{Nd}(\text{qab})_2(\text{H}_2\text{O})_3\text{Cl}]$

Conclusion

On the basis of elemental analysis the empirical formula of the complexes were derived. Molar conductance values suggest non-electrolytic nature of the complexes. Number of water molecules coordinated to the neodymium ion and nature of ligand decomposition are obtained from the TG data. IR data indicate that two nitrogen and one oxygen of the ligand qpd are coordinated while qap and qab act as bidentate ligand with one nitrogen and one oxygen coordinated to the metal in their complexes. The central metal atom is eight coordinated and the complex is proposed to have bicapped trigonal prismatic geometry.¹² The proposed structures of the complexes are given in Figure V.2.9-V.2.11.

5.3 Encapsulated complexes of neodymium

5.3.1 Synthesis

The ligands qpd, qap, qab, salpd, salap and salab used in the present study were prepared as explained in chapter II. Neodymium exchanged zeolite (5 g) was added to ethanolic solution(50 mL) of each ligand (1:1 metal : ligand mole ratio) and refluxed for 10 h. The resultant material was suction filtered and then extracted with methanol using soxhlet extractor until the complex was free from unreacted ligand. It was further soxhlet extracted with acetone to ensure complete removal of the surface species. After filtering, the uncomplexed neodymium ions present in the zeolite was removed by stirring with aqueous solution of NaCl (0.01 M) for 24 h. Finally the resultant solid was washed with water until free from chloride ions, dried at 100°C for 2 h and stored in vacuum over anhydrous calcium chloride.

5.3.2 Results and discussion

5.3.2.1 Elemental Analysis

Elemental analyses of the metal exchanged zeolite NdY indicate the unit cell formula to be $\text{Na}_{45.1}\text{Nd}_{2.95}(\text{AlO}_2)_{54}(\text{SiO}_2)_{138}\cdot n\text{H}_2\text{O}$. The analytical data of the complexes are given in Table V.3.1. The degree of ion exchange of neodymium is calculated from the percentage of neodymium in the sample and found to be 16.37. Further the presence of carbon, hydrogen and nitrogen suggest the formation of metal complexes in the zeolite cages.

TABLE V.3.1 Analytical data of encapsulated complexes

compound	%C	%H	%N	%Nd	%Si	%Al	%Na
NaY	-	-	-	-	20.9	7.9	9.6
NdY	-	-	-	2.3	20.6	7.9	1.7
NdYqpd	2.6	2.8	1.0	1.8	20.4	7.8	2.0
NdYqap	7.9	2.5	1.7	2.2	19.8	7.8	1.9
NdYqab	4.6	2.3	1.8	1.9	19.8	7.8	2.2
NdYsalpd	4.8	2.4	0.7	1.2	20.2	7.8	1.8
NdYsalap	10.0	2.7	0.8	2.1	19.9	7.6	2.0
NdYsalab	6.2	2.9	1.9	2.2	19.7	7.4	1.9

5.3.2.2 Surface area

Surface area of the neodymium exchanged zeolite is smaller than sodium exchanged zeolite (Table V.3.2). This can be attributed to the large size of neodymium compared to sodium. Encapsulation resulted in decrease in surface area due to the large size of the complex encapsulating in the cage. This results in filling of the pores of zeolite thereby reducing surface area.

TABLE V.3.2 Surface area data of encapsulated complexes of neodymium

Compound	Surface area (m ² /g)
Zeolite	799
NaY	692
NdY	605
NdYqpd	509
NdYqap	404
NdYqab	418
NdYsalpd	461
NdYsalap	462
NdYsalab	507

5.3.2.3 X-ray diffraction studies

The powder X-ray diffraction patterns of NaY, NdY and encapsulated complexes exhibit similar pattern, though slight change in the intensity of the bands were noticed. These observations indicate that the framework of the zeolite has not undergone any significant structural change on complexation. This suggests that the crystallinity of the zeolite Y is preserved during encapsulation. No new peaks could be detected in zeolite encapsulated complexes probably due to poor loading of the complex in zeolite framework.

5.3.2.4 SEM analysis

The scanning electron micrographs (SEM) of the complexes before and after encapsulation indicate that surface species are completely removed by soxhlet extraction.

5.3.2.5 Thermogravimetric analysis

The thermogravimetric data of the encapsulated complexes of neodymium are given in Table V.3.3 and the curves are given in Figure V.3.1-V.3.6. The thermal decomposition of the zeolite encapsulated complexes occurs in two major steps. An endothermic weight loss of about 6-18% is observed in the temperature range 30-150°C in all complexes. Such a weight loss is observed in the case of metal exchanged zeolite also. Hence this might be due to the removal of intrazeolite water. The second step of exothermic weight loss occurs in a single step and starts immediately after the first step and continues till 800°C in all complexes. A weight loss of about 10% due to the slow decomposition of the metal complex is observed in this wide temperature range. This type of weight loss is not seen in the thermal decomposition curve of metal exchanged zeolite, which provides additional evidence of the formation of metal complex in the

Table V.3.3 Thermogravimetric data of encapsulated complexes

Compound	Temp. range of decomposition (°C)	% weight loss	Nature of DSC/DTA curve
NdYqpd	30-140	18	endothermic
	160-400	9	exothermic
NdYqap	30-125	6.5	endothermic
	180-480	5	exothermic
NdYqab	30-125	10.5	endothermic
	180-415	8	exothermic
NdYsalpd	30-140	8	endothermic
	160-430	2.5	exothermic
NdYsalap	30-140	8	endothermic
	150-500	4	exothermic
NdYsalab	30-115	18	endothermic
	200-600	5	exothermic

zeolite matrix. The variation in the thermal decomposition pattern exhibited by different complexes is indicative of the formation of metal complexes. The small percentage of weight loss indicates the insertion of only small amount of metal complexes in the cavity of the zeolite. This is in agreement with the observed low percentage of metal content in encapsulated complexes.

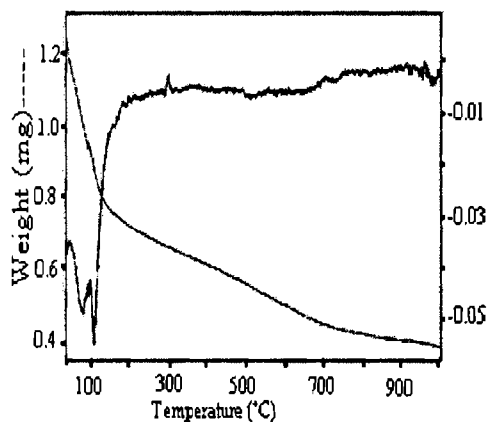


Figure V.3.1 (a) TG/DTG curve of NdYqpd

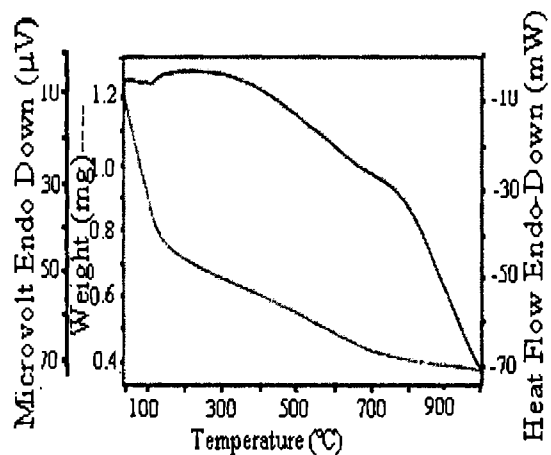


Figure V.3.1 (b) DSC curve of NdYqpd

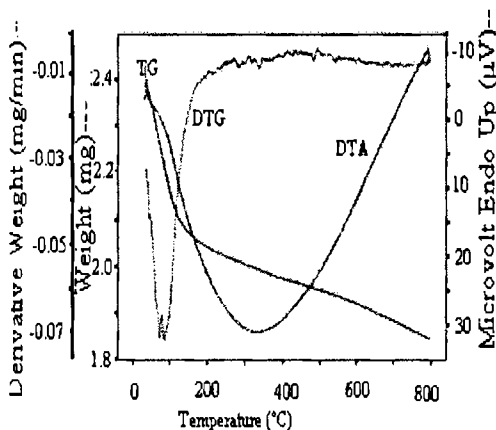


Figure V.3.2 TG/DTG/DTA curve of NdYqap

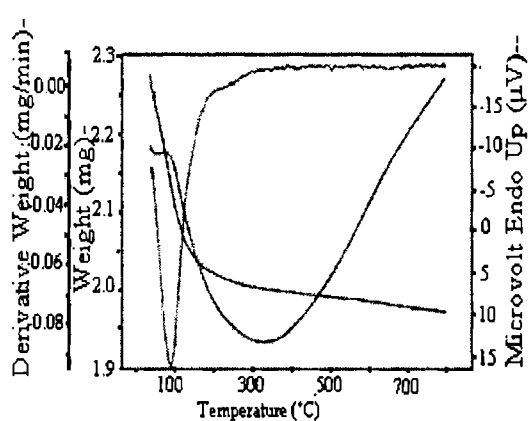
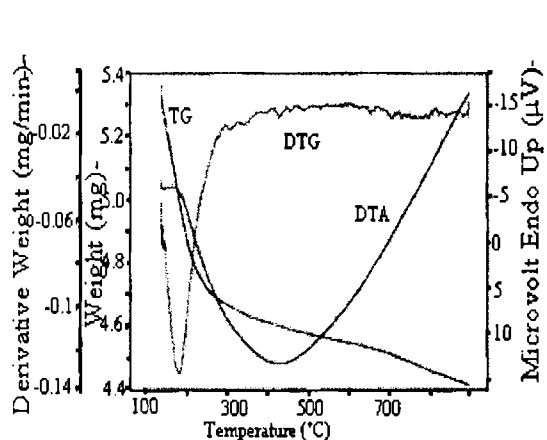
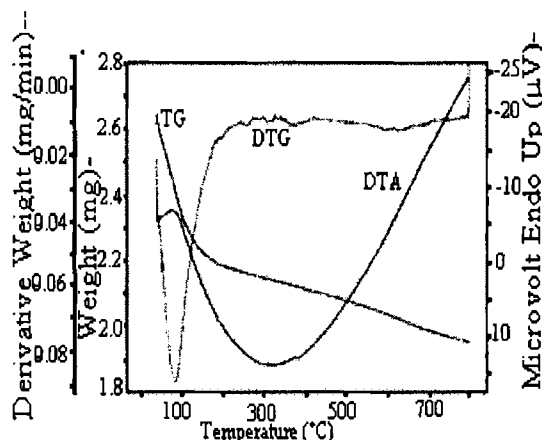


Figure V.3.3 TG/DTG/DTA curve of NdYqab



**Figure V.3.4 TG/DTG/DTA
curve of NdYsalpd**



**Figure V.3.5 TG/DTG/DTA
curve of NdYsalab**

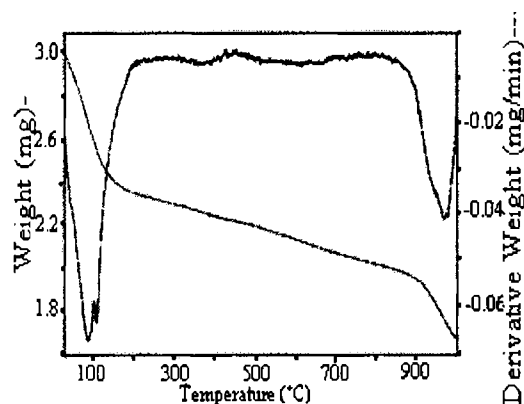


**Figure V.3.6 (a) TG/DTG
curve of NdYsalab**

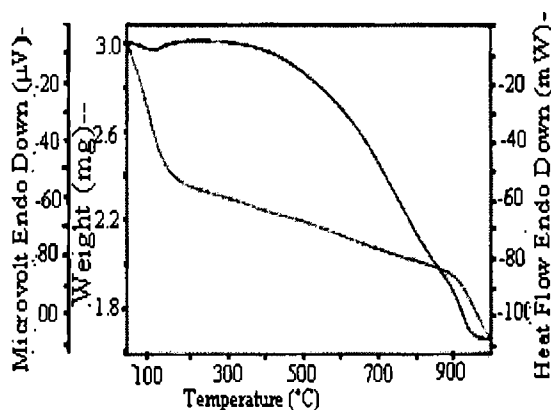


**Figure V.3.6 (b) DSC
curve of NdYsalab**

5.3.2.6 Infrared spectra

IR spectra of all ligands exhibit sharp band in the region $1620-1640\text{ cm}^{-1}$ due to $\nu_{\text{C=N}}$ of azomethine group. This band moves to lower wave number on coordination of azomethine nitrogen to the metal. The coordination of the phenolic oxygen could not be ascertained due to the appearance of broad band in the region $3400-3500\text{ cm}^{-1}$ due to free hydroxyl group which might be due to the water molecule present in the complexes. The

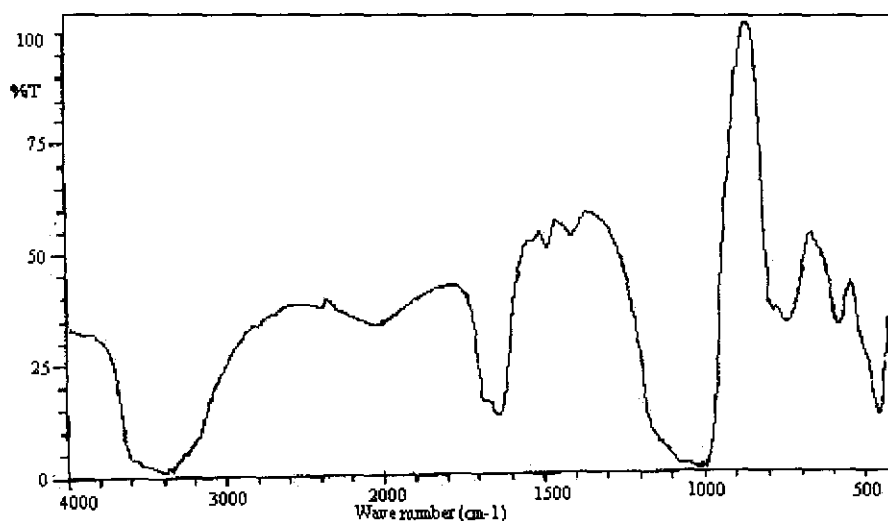


Fig V.3.7 Infrared spectrum of NdYqab

Table V.3.4 IRspectral data of encapsulated complexes of neodymium

Compound	ν_{OH}	$\nu_{C=N}$	$\nu_{Zeolitic\ peaks}$	$\nu_{Zeolitic\ peaks}$
qpd	3474	1651	-	-
NdYqpd	3418	1635	1040	578
qap	3507	1630	-	-
NdYqap	3427	1621	1038	578
qab	3461	1642	-	-
NdYqab	3410	1637	1010	574
salpd	3515	1651	-	-
NdYsalpd	3408	1633	1041	576
salap	3550	1639	-	-
NdYsalap	3410	1633	1030	576
salab	3571	1641	-	-
NdYsalab	3464	1637	1040	576

band in the region $1120-1150\text{ cm}^{-1}$ in free ligands due to ν_{C-O} of phenolic group could not be seen in encapsulated complexes. This might be due to the appearance of strong and

broad band around 1000 cm^{-1} of zeolite framework. Table V.3.4 shows the IR spectral data of the complexes.

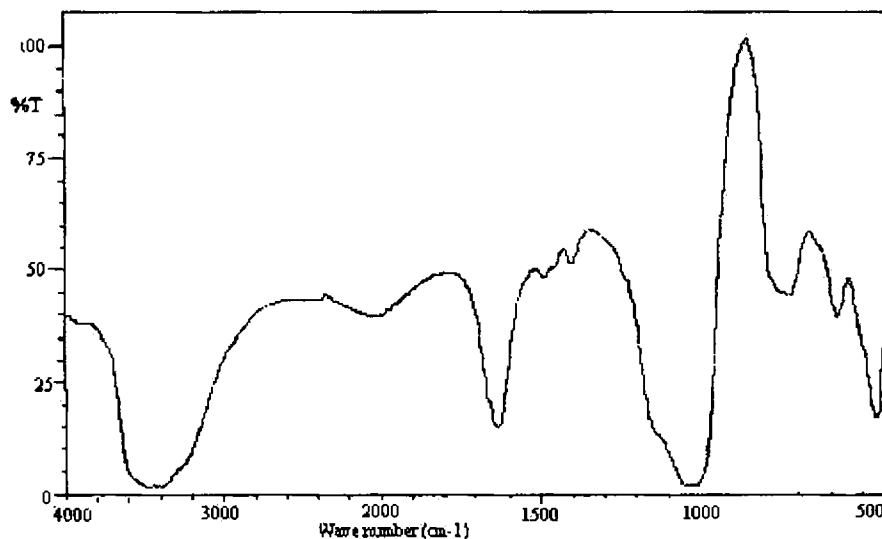


Fig V.3.8 Infrared spectrum of NdYsalap

5.3.2.7 Electronic spectra

The electronic spectral data (Table V.3.5) of encapsulated complexes exhibit charge transfer transitions. Absorption spectra of lanthanide ions result from $f \leftrightarrow f$ transitions. Since these transitions are Laporte forbidden, they are expected to give weak narrow bands. Hypersensitive transition due to ${}^4G_{5/2} \rightarrow {}^4I_{9/2}$ is observed in the case of encapsulated complexes of neodymium. NdYqpd and NdYsalap complexes exhibit a spectral band around 22000 cm^{-1} which might be due to the hypersensitive transition ${}^4I_{9/2} \rightarrow {}^2K_{13/2}$ or ${}^4I_{9/2} \rightarrow {}^4G_{7/2}$.¹⁶ However zeolite encapsulated neodymium complexes of qap do not give a spectral band corresponding to these hypersensitive transitions probably due to the effect of the ligand environment or might have masked by high intensity charge transfer bands. Figure V.3.7-V.3.12 represent the electronic spectra of the complexes.

Electronic Spectra of Encapsulated Complexes of Neodymium

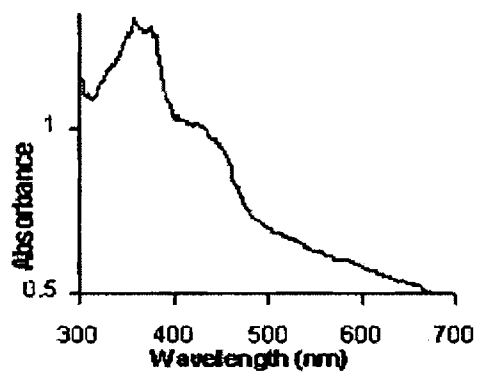


Fig.V.3.9 Electronic spectrum of NdYqpd

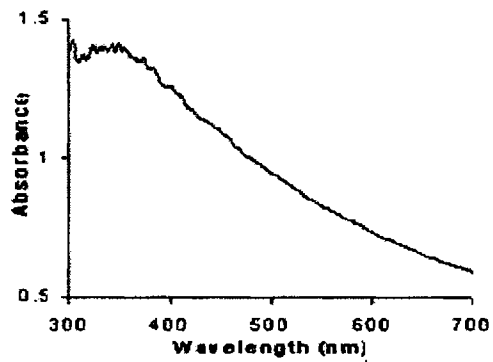


Fig.V.3.10 Electronic spectrum of NdYqap

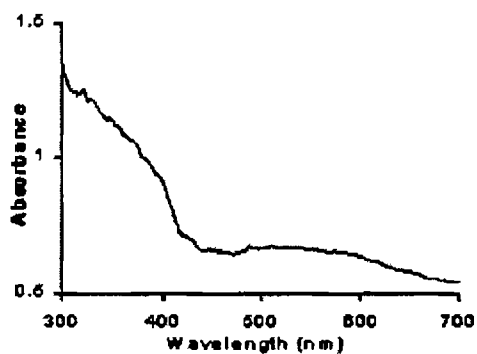


Fig.V.3.11 Electronic spectrum of NdYqab

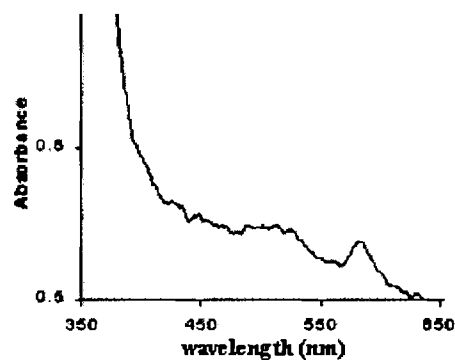
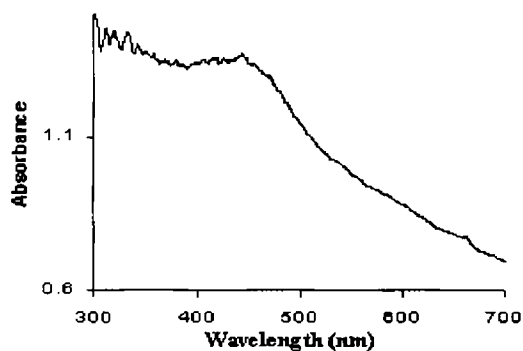
Fig.V.3.12 Electronic spectrum of
NdYsalpd

Fig.V.3.13 Electronic spectrum of NdYsalap

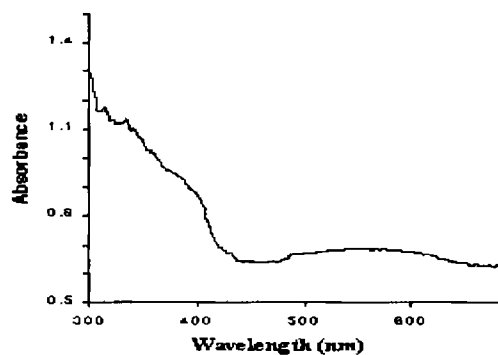


Fig.V.3.14 Electronic spectrum of NdYsalab

TABLE V.3.5 Electronic spectral data of encapsulated complexes of neodymium

Compound	Absorption (cm ⁻¹)	Tentative assignments
	26520	Charge Transfer
NdYqpd	22200	$^4I_{9/2} \rightarrow ^2K_{13/2}$ or $^4I_{9/2} \rightarrow ^4G_{7/2}$
	17060	$^4I_{9/2} \rightarrow ^4G_{5/2}$
NdYqap	28330	Charge Transfer
NdYqab	30860	Charge Transfer
	17760	$^4I_{9/2} \rightarrow ^4G_{5/2}$
NdYsalpd	27020	Charge Transfer
	17060	$^4G_{5/2} \rightarrow ^4I_{9/2}$
NdYsalap	22320	$^4I_{9/2} \rightarrow ^2K_{13/2}$ or $^4I_{9/2} \rightarrow ^4G_{7/2}$
NdYsalab	28850	Charge Transfer
	17500	$^4G_{5/2} \rightarrow ^4I_{9/2}$

Conclusion

The analytical data of the encapsulated complexes indicate the formation of monomeric complexes in zeolite cavities. The Si/Al ratio and XRD pattern show that the crystalline structure of the zeolite has remained intact during encapsulation. The lower surface area and pore volume of the zeolite complexes as compared to zeolite is an evidence for encapsulation of complexes. IR spectral data also indicate encapsulation of complexes. The thermal stability of the complexes are explained on the basis of TG/DTG data. Since in the case of neodymium complexes f electrons are buried deep within the atoms, electronic spectra could not give much information on the structure of the complexes.

References

- [1] Carlos Kremer; Julia Torres; Sixto Dom'inguez; Alfredo Mederos, Coord. Chem. Rev. **249**, 567 (2005).
- [2] Beer P.D.; Smith D.K.; in: Karlin (Ed.), K.D., Progress in Inorganic Chemistry, JohnWiley & Sons, New York, USA, **39**, 1 (1982).
- [3] Beer P.D.; Smith D.K.; in: Karlin K.D. (Ed.) Progress in Inorganic Chemistry, John Wiley & Sons, New York, USA, **46**, 1 (1997).
- [4] McKee V.; in: Sikes A.G. (Ed.), Advanced in Inorganic Chemistry, Academic Press, S. Diego, USA, **40**, 323 (1993).
- [5] Nelson J.; McKee V.; Morgan G., in: Karlin K.D.(Ed.), Progress in Inorganic Chemistry, John Wiley & Sons, NewYork, USA, **47**, 167 (1998).
- [6] Brooker S., Coord. Chem. Rev. **222**, 33 (2001).
- [7] Inone Y.; Gokel G.W.(Eds.), Cation Binding by Macrocycles, Marcel Dekker Inc., New York, USA, (1990).
- [8] Branchi A.; Bowman-James K.; Garcia-Espana E. (Eds.) Supramolecular Chemistry of Anions, Wiley-VCH, New York, USA (1997).
- [9] Amendola V.; Fabbrizzi L.; Mangano C.; Pallavicini P.; Poggi A.; Taglietti A.; Coord. Chem. Rev. **821**, 219 (2001).
- [10] Geary W. J., Co ord.Chem.Rev. **7**, 81 (1971).
- [11] Mojumdar S.C.; Melnik M.; Jona E., Chem. Papers. **53 (5)**, 309 (1999).
- [12] Jorgensen C.K.; Baker E.C.; Halstead G.W.; Raymond K.N.; Sinha S.P., Structure and Bonding-25 ; Rare Earths, Springer-Verlag, Berlin Heidelberg, New York (1976).

- [13] Crosswhite W.M.; Crosswhite H.; Camall W.T.; Paszek A.P., *J. Chem. Phys.* **72** 5103 (1980).
- [14] Lapotakaya A.V.; Pirkes S.B., *Neorg. Khim Zh.* **16**, 369 (1971).
- [15] Nieboer E.; Jorgensen C.K.; Peacock R.D.; Reisfeld R., *Structure and Bonding – 22; Rare Earths*, Springer-Verlag, Berlin Heidelberg, New York (1975).
- [16] Kononenko K.I.; Poluektov W.S., *Russ. J. Inorg. Chem.* **7**, 965 (1962).

CHAPTER VI

**POLYMERBOUND SCHIFF BASE COMPLEXES OF
RUTHENIUM AND NEODYMIUM**

6.1 Introduction

Cross-linked polymers with specific properties are widely used as catalyst supports¹ as they are inert, non-toxic, non-volatile and often recyclable. It can induce specific control over catalytic and complexing ability of the ligand. The ease of separation from the reaction products leads to operational flexibility.² Moreover, the amount of metal present on the surface of such catalysts is very small which is of economic significance in the case of expensive metals like ruthenium, Rhodium and palladium. Thus polymer supported catalysts have generated a lot of interest in research. Earlier reports of catalytic activity of various metal ions such as Rh(I), Ru(III) and Pd(II) anchored to different cross-linked polymers with N-donor ligands³⁻⁵ prompted us to use ligands with nitrogen and oxygen as donor groups. Although Schiff bases are the most widely used ligands, only a few Schiff bases have been immobilized to polystyrene matrix.^{1-2,6-8} Immobilization onto polymer supports through covalent attachment is one of the important means to solve the problem of decomposition of many complexes during catalytic reaction.⁹ Chloromethylated polystyrene cross-linked with divinylbenzene is one of the most widely employed macromolecular supports.¹⁰⁻¹⁴ Ruthenium complex of a pyridine-benzimidazole based polymer poly[2-(2-pyridyl)-bibenzimidazole] shows that the complex is very robust¹⁵ remaining stable under considerable thermal and chemical stress. Ru(II) and Ru(III) are widely known for their catalytic activity.¹⁶⁻¹⁹ Earlier reports reveal that lanthanide complexes are also known for their importance in biological field, as NMR shift reagents, in agriculture and medicine.²⁰⁻²²

In view of the pronounced coordinating properties, the synthesis of multidentate Schiff bases anchored to polystyrene matrix is described here. The newly synthesized

polymer supported Schiff bases have been used for synthesizing the polymer anchored complexes of ruthenium and neodymium. Although complete characterization of the polymer supported complexes is impossible, attempts were made to understand the environment surrounding the metal ion using FTIR, electronic, EPR spectroscopy, magnetic moment measurements, thermogravimetry and surface area analyses. These studies are necessary for the proper understanding of their involvement in catalytic reactions.

Schiff bases are formed by condensing polymer supported aldehyde with o-phenylenediamine, o-aminophenol and 2-aminobenzimidazole respectively. Details on the synthesis and characterization of Ru(III) and Nd(III) complexes of these ligands are presented in this chapter.

6.2 Synthesis of complexes

Details regarding the synthesis of polymer supported Schiff bases are given in chapter II.

6.2.1 Ru(III) and Nd(III) complexes of PS-opd

The polymer bound Schiff base PS-opd (3 g) was swelled in chloroform for 1h. It was filtered and refluxed with a solution of metal chloride (1mmol: 0.261 g $\text{RuCl}_3 \cdot 6\text{H}_2\text{O}$ or 0.357 g $\text{NdCl}_3 \cdot 6\text{H}_2\text{O}$) in methanol (100 mL) for about 6 h. The resultant complexes were separated by filtration, washed repeatedly with methanol, chloroform, acetone and dried *in vacuo* over anhydrous CaCl_2 .

6.2.2 Ru(III) and Nd(III) complexes of PS-ap

The polymer bound Schiff base PS-ap (3 g) was swelled in chloroform for 1h. It was filtered and an excess of metal chloride (1 mmol: 0.261 g $\text{RuCl}_3 \cdot 6\text{H}_2\text{O}$ or 0.357 g $\text{NdCl}_3 \cdot 6\text{H}_2\text{O}$) was added and the reaction vessel was sealed. The mixture was shaken for 5h on a mechanical shaker. The resulting polymer bound metal complex was filtered,

washed with methanol, chloroform and acetone and dried *in vacuo* over anhydrous calcium chloride.

6.2.3 Ru(III) and Nd(III) complexes of PS-ab

Polymer bound Schiff base PS-ab (3.0g) was swollen in chloroform for 1h. An excess of the metal salt (1mmol: 0.261g RuCl₃.6H₂O or 0.357 g NdCl₃.6H₂O) was added and the reaction vessel was sealed. The mixture was shaken for 5 h on a mechanical shaker. The resulting polymer bound complexes was filtered, washed with methanol, chloroform and acetone and dried *in vacuo* over anhydrous calcium chloride.

6.3 Results and discussion

Chloromethylated polystyrene was converted to polymer bound aldehyde on treatment with dimethylsulphoxide and sodium bicarbonate at 138-140^oC. The very low content of chlorine in the sample suggests that almost all chloromethylated groups have been converted to the aldehyde. The formation of aldehyde was further supported by the IR spectrum, which showed a peak at 1648 cm⁻¹. The characteristic peaks of azomethine linkage after condensation with the corresponding amines confirm the formation of Schiff bases.

6.3.1 Elemental analysis

Polymer bound Schiff bases were converted to the corresponding complexes on treatment with metal chloride. Elemental analyses confirm the formation of complexes.

Metal binding capacity (Table VI.1) of the complexes were calculated from observed value of metal ion percentage in the resin using the formula

$$\text{Binding capacity} = \frac{\text{Metal\% (observed)} \times 1000}{\text{Atomic weight of metal}}$$

Metal binding capacity of ruthenium and neodymium is very high compared to transition metals like cobalt, copper and nickel²³.

TABLE VI.1 Elemental analyses data of polymer supported ligands and complexes

Compound	Elements (%) found				Metal binding capacity of resins
	Metal	C	H	N	
PS-opd	-	63.55	7.19	1.88	-
[PS-opdRuCl ₃ (H ₂ O)]	4.00	62.04	6.79	1.65	39.60
[PS-opdNdCl ₃ (H ₂ O) ₃]	4.48	46.06	4.76	0.69	31.11
PS-ap	-	66.81	7.25	2.48	-
[PS-apRuCl ₂ (H ₂ O) ₂]	1.53	65.75	6.26	1.79	15.15
[PS-apNdCl ₂ (H ₂ O) ₄]	3.09	67.40	6.42	0.49	21.45
PS-ab	-	61.87	6.37	2.88	-
[PS-abRuCl ₃ (H ₂ O) ₂]	2.26	60.86	5.81	2.75	22.38
[PS-abNdCl ₃ (H ₂ O) ₄]	3.23	70.02	6.57	0.31	22.43

6.3.2 Magnetic susceptibility measurements

All the Polymer supported Schiff base complexes of ruthenium show a negative value for magnetic susceptibility probably due to the low concentration of the metal and the very large diamagnetic susceptibility of the atoms present in the poly nuclear complex. However neodymium complexes reported a positive value contrary to the ruthenium complexes. Approximate molecular weight of the polymer supported complexes and empirical formula of the repeating complex unit containing one metal atom was calculated. The magnetic moment values are calculated according to the reported procedure.²⁴ The values are tabulated in Table VI.2. A value of ~2 B.M was obtained for the ruthenium complexes which is as expected for Ru(III) low spin

octahedral complexes.²⁵ For neodymium complexes the values are ~3.5 B.M. as reported for Nd(III) complexes.²⁶ However it is difficult to arrive at the structure of the complexes from the data.

Table VI.2 Magnetic moment values of polymer supported complexes of ruthenium and neodymium

Complex	Magnetic moment (B.M)
[PS-opdRuCl ₃ (H ₂ O)]	1.8
[PS-apRuCl ₂ (H ₂ O) ₂]	2.1
[PS-abRuCl ₃ (H ₂ O) ₂]	1.9
[PS-opdNdCl ₃ (H ₂ O) ₃]	3.4
[PS-apNdCl ₂ (H ₂ O) ₄]	3.2
[PS-abNdCl ₃ (H ₂ O) ₄]	3.5

6.3.3 Surface area and pore volume

TABLE VI. 3 Surface area and pore volume data of polymer supported complexes

Compound	Surface Area (m ² /g)	Pore volume (cc/g)
PA	142	0.1479
[PS-opdRuCl ₃ (H ₂ O)]	46	0.1174
[PS-apRuCl ₂ (H ₂ O) ₂]	33	0.0989
[PS-abRuCl ₃ (H ₂ O) ₂]	39	0.1098
[PS-opdNdCl ₃ (H ₂ O) ₃]	14	0.0089
[PS-apNdCl ₂ (H ₂ O) ₄]	33	0.0261
[PS-abNdCl ₃ (H ₂ O) ₄]	33	0.0553

The surface area and pore volume of the polymer aldehyde and anchored complexes were determined at low temperature in nitrogen atmosphere. The loading of the complexes on polymers results in reduction in surface area and Pore volume to large extent (Table VI.3). This might be due to the inclusion of the complexes in the pores of the polymer.²⁷

6.3.4 Thermogravimetric analysis

Thermo gravimetric analysis shows stability of polymer-anchored ruthenium complexes up to ~ 340°C as shown in Table VI.4. Below 100°C, the weight loss observed is due to physisorbed water. As the molecular weight of the polymer supported complexes are very large, only a very small percentage of coordinated water is expected (1% in [PS-opdRuCl₃(H₂O)], 0.5% in [PS-apRuCl₂(H₂O)₂] and 1.5% in [PS-abRuCl₃(H₂O)₂]). A corresponding mass loss has been observed in the thermal decomposition range 120-200°C.²⁸ The first stage of decomposition starts at 389°C in the case of [PS-opdRuCl₃(H₂O)] and at 344°C in the case of [PS-apRuCl₂(H₂O)₂], the peak temperature being 373°C. In [PS-abRuCl₃(H₂O)₂] first stage of decomposition starts at 369°C, the peak temperature being 410°C. However second stage of decomposition is almost complete at 450°C, the peak temperature being 418°C in the case of [PS-opdRuCl₃(H₂O)]. A similar kind of decomposition takes place in the case of [PS-opdNdCl₃(H₂O)₃], in which the peak temperature of the second stage is 423°C. At 343°C a very small decrease in weight is observed. A third stage of decomposition takes place in [PS-opdNdCl₃(H₂O)₃] at 912°C. [PS-apNdCl₂(H₂O)₄] and [PS-abNdCl₃(H₂O)₄] complexes show similar thermal decomposition pattern. Up to 200°C only a very small percentage of weight loss is observed which might be due to the expulsion of coordinated water. The complexes start to decompose around 300°C. In the first stage only a very small part of the complex undergoes decomposition, while around 440°C the decomposition of the complex is almost complete. Thereafter constant weight is

maintained till 800°C. The thermogravimetric curves of the complexes are given in Figure VI.1-VI.6.

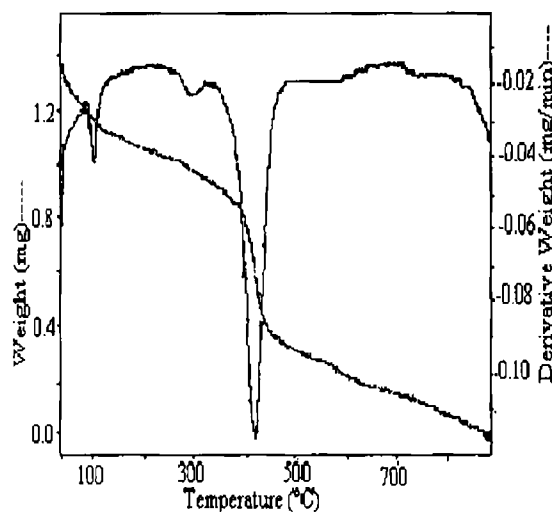


Figure VI. 1(a) TG/DTG curve of [PS-opdRuCl₃(H₂O)]

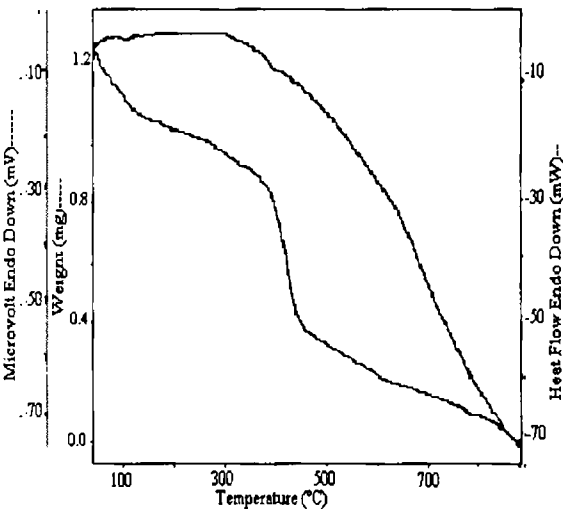


Figure VI. 1(b) DSC curve of [PS-opdRuCl₃(H₂O)]

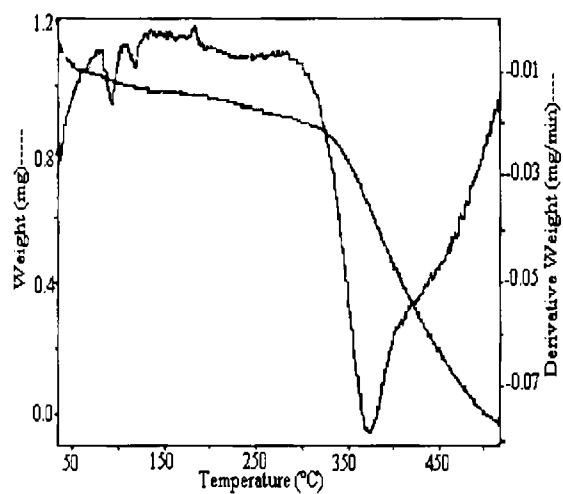


Figure VI. 2(a) TG/DTG curve of [PS-apRuCl₂(H₂O)₂]

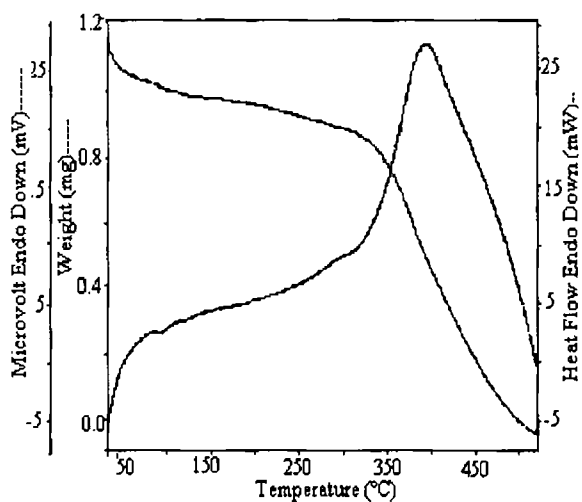


Figure VI. 2(b) DSC curve of [PS-apRuCl₂(H₂O)₂]

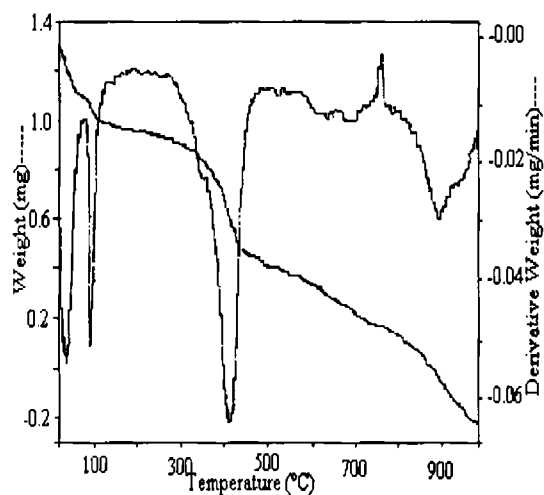


Figure VI. 3 (a) TG/DTG curve of
[PS-abRuCl₃(H₂O)₂]

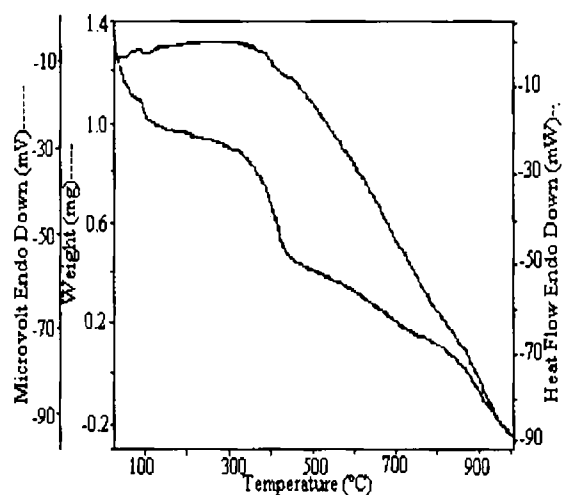


Figure VI. 3 (b) DSC curve
of [PS-abRuCl₃(H₂O)₂]

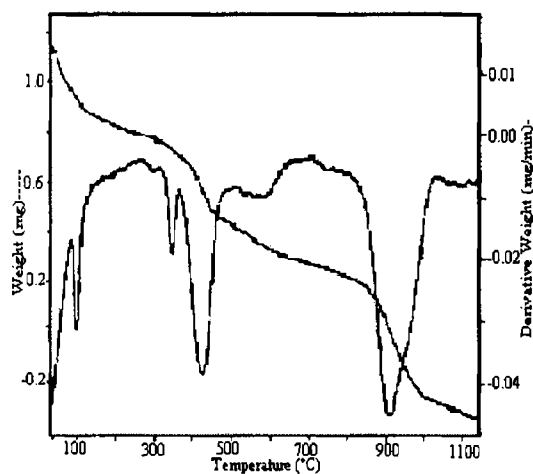


Figure VI.4.(a) TG/DTG curve of
[PS-opdNdCl₃(H₂O)₃]

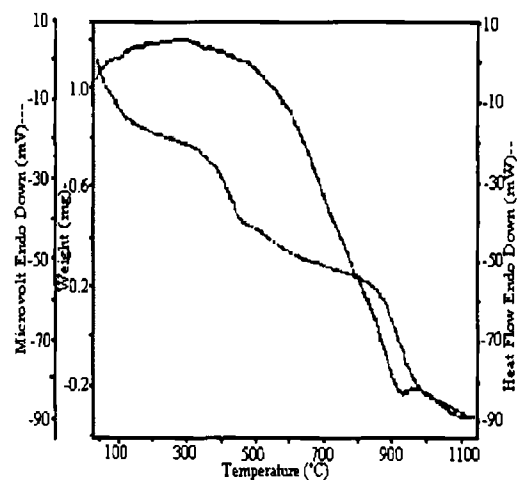


Figure VI. 4.(b) DSC curve of
[PS-opdNdCl₃(H₂O)₃]

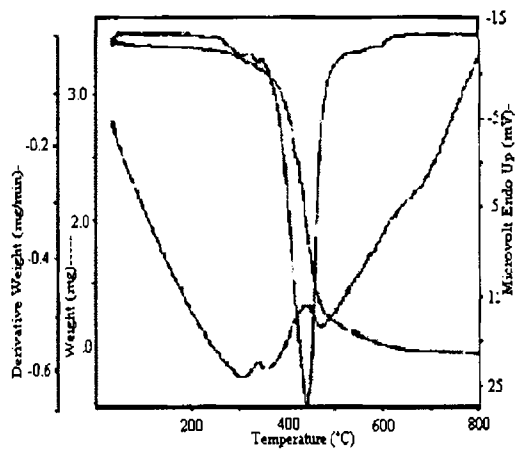


Figure VI. 5 TG/DTG/DTA curve of
[PS-apNdCl₂(H₂O)₄]

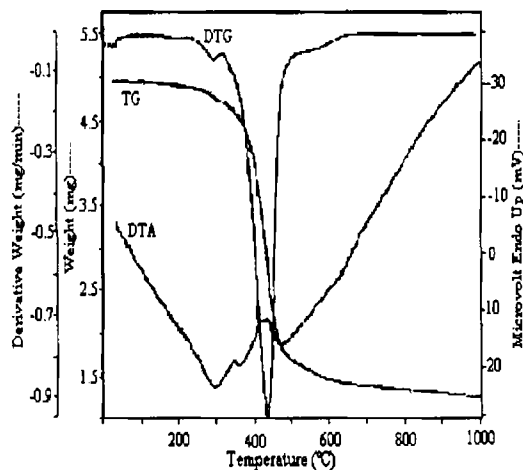


Figure VI. 6 TG/DTG/DTA curve of
[PS-abNdCl₃(H₂O)₄]

Table VI. 4 Thermogravimetric data of polymer supported complexes

complex	Temperature range(°C)	% weight loss	Peak temperature(°C)	Nature of DSC/DTA curve
[PS-opdRuCl ₃ (H ₂ O)]	50-200	17	96	endothermic
	389-450	32	418	endothermic
[PS-apRuCl ₂ (H ₂ O) ₂]	50-200	13	92, 117	endothermic
	344-500	35	393	exdothermic
[PS-abRuCl ₃ (H ₂ O) ₂]	50-200	21	98	endothermic
	369-440	30	369	endothermic
[PS-opdNdCl ₃ (H ₂ O) ₃]	50-200	12	97	endothermic
	350-450	20	343	endothermic
[PS-apNdCl ₂ (H ₂ O) ₄]	50-310	2.0	300	endothermic
	375-450	50	440	endothermic
[PS-abNdCl ₃ (H ₂ O) ₄]	50-310	4	300	endothermic
	380-450	37	435	exdothermic

6.3.5 Infrared spectra

IR spectra of the ligands and polymer supported complexes were taken as KBr pellets in the region $500 - 4000\text{cm}^{-1}$. The IR frequencies are given in Table VI.4-VI.6. Ligand PS-opd exhibit a band at 1650cm^{-1} which can be assigned to the azomethine $>\text{C}=\text{N}$ linkage²⁹ of the Schiff base. The band is observed to show a negative shift by $12-15\text{cm}^{-1}$ in the complexes. This indicates coordination of nitrogen to the metal in the complexes. Bands around 1350cm^{-1} due to C-N stretch is shifted to lower frequencies which supports coordination to the metal. Bands below 600cm^{-1} are assigned to the metal-nitrogen bond arising due to the coordination of the ligand to the metal ion. Other bands may be due to the polymer part, which are not much affected by coordination.

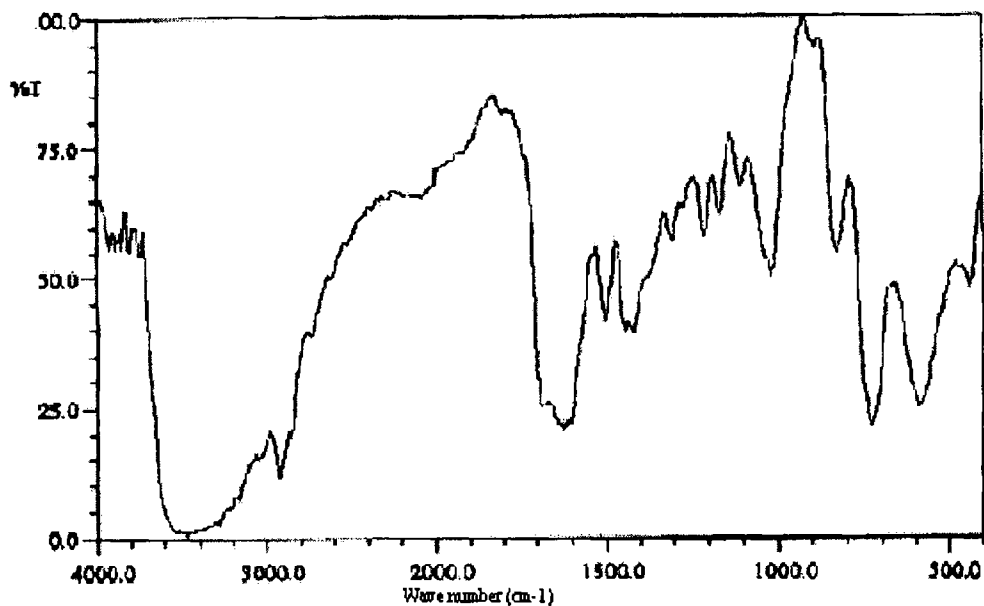


Fig VI.7 Infrared spectrum of $[\text{PS-opdNdCl}_3(\text{H}_2\text{O})_3]$

TABLE VI.5 IR spectral data of polymer supported complexes of PS-opd(cm^{-1})

PS-opd	[PS-opdRuCl ₃ (H ₂ O)]	[PS-opdNdCl ₃ (H ₂ O) ₃]	Assignments
3463	3465	3465	$\nu_{\text{N-H}}$
1650	1638	1635	$\nu_{\text{C=N}}$
1350	1332	1312	$\nu_{\text{C-N}}$
-	594	586	$\nu_{\text{M-N}}$

Polymer supported Schiff base of aminophenol exhibits a band at 3492cm^{-1} due to free hydroxyl group. Band at 1653cm^{-1} due to azomethine group in the ligand on complexation is shifted to lower frequencies as seen in the corresponding PS-opd complexes. This confirms the coordination of the azomethine nitrogen to the metal atom. C-C stretching frequency due to ring carbon atom experiences small positive shift in the [PS-apRuCl₂(H₂O)₂] complex. The polymer anchored ligands show a band at 1502cm^{-1} due to the $\nu_{\text{C-O}}$ (phenolic) which undergoes a positive shift by $\leq 10\text{cm}^{-1}$ in the spectra of the polymer anchored complexes. This is indicative of the coordination of phenolic oxygen atom of the ligand.^{30, 31} Bands at lower frequencies due to M-N stretch confirms the coordination of the ligand to the metal.³²

TABLE VI.6 IR spectral data of polymer supported complexes of PS-ap(cm^{-1})

PS-ap	[PS-apRuCl ₂ (H ₂ O) ₂]	[PS-apNdCl ₂ (H ₂ O) ₄]	Assignments
3492	3468	3468	$\nu_{\text{O-H}}$
1653	1644	1637	$\nu_{\text{C=N}}$
1502	1511	1512	$\nu_{\text{C-O}}$
1382	1384	1387	$\nu_{\text{C-N}}$
-	544	571	$\nu_{\text{M-N}}$

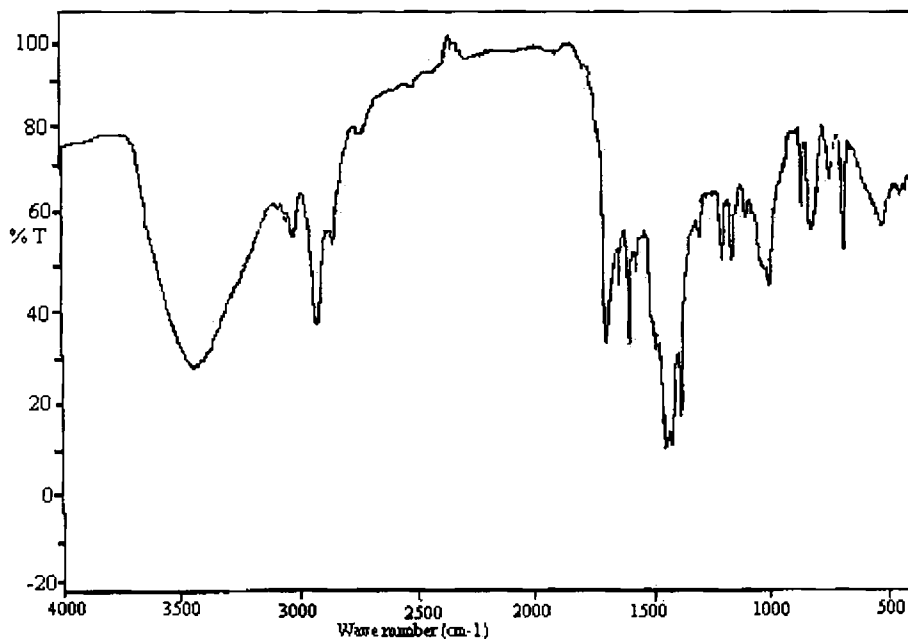


Fig VI.8 Infrared spectrum of [PS-apRuCl₂(H₂O)₂]

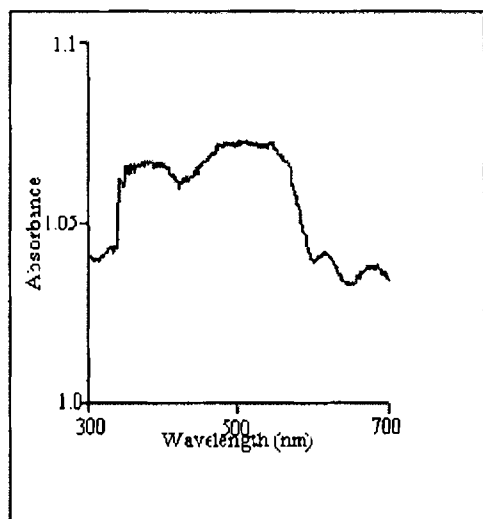
PS-ab complexes experiences negative shift for the stretching frequency band at 1641 cm⁻¹ in the ligand. This is due to the coordination of the nitrogen of the azomethine group to the metal atom. A sharp band seen in all complexes in the region 860-880 cm⁻¹ indicates presence of coordinated water.³³ The broad band in the region 3400-3500 cm⁻¹ observed in all the complexes is due to the presence of water molecule.

TABLE VI.7 IR spectral data of polymer supported complexes of PS-ab(cm⁻¹)

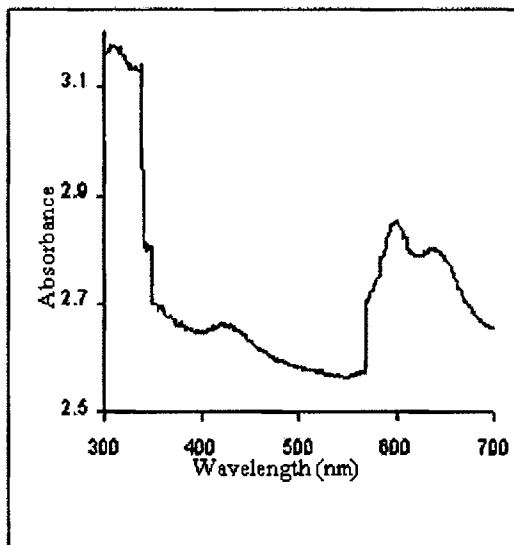
PS-ab	[PS-abRuCl ₃ (H ₂ O) ₂]	[PS-abNdCl ₃ (H ₂ O) ₄]	Assignments
3496	3481	3488	ν_{N-H}
1641	1637	1627	$\nu_{C=N}$
1512	1521	1519	$\nu_{ring\ nitrogen}$
-	545	559	ν_{M-N}

6.3.6 Electronic spectra

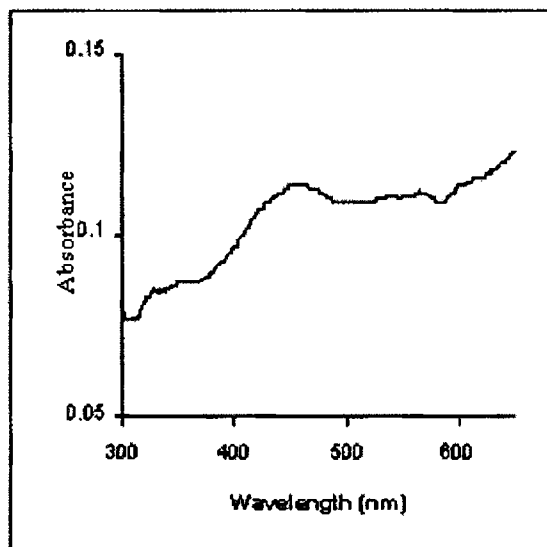
Electronic spectra of polymer anchored complexes were recorded in Nujol on a Varian Cary 5000 UV-Vis-NIR spectrophotometer by a layering mull of the sample on the inside of one of the cuvettes while keeping the other one layered with Nujol as reference. The electronic spectral data (Table VI.8) of the ruthenium complexes suggest the octahedral nature of the complexes. It has been reported that in a number of ruthenium complexes charge transfer absorptions occur at relatively low energies. In the present complexes the high intensity transitions around 20,000 and 30,000 cm^{-1} are assigned as charge transfer bands.^{34, 35} The ground state for the low spin octahedral complexes is $^2T_{2g}$ and the excited states are $^2A_{2g}$, $^2T_{1g}$, 2E_g . In [PS-apRuCl₂(H₂O)₂] the absorption peak seen as shoulder on the high intensity charge transfer band at 29070 cm^{-1} , is assigned to the transition $^2T_{2g} \rightarrow ^2A_{2g}$, $^2T_{1g}$. As the crystal field parameters are quite large, the expected electronic transitions $^2T_{2g} \rightarrow ^2E_g$, usually occur in the region of absorptions of the charge transfer bands and are frequently obscured in all the complexes.³⁶ However, two spin forbidden transitions, $^2T_{2g} \rightarrow ^4T_{1g}$, $^2T_{2g} \rightarrow ^4T_{2g}$ can frequently be observed in the octahedral complexes. The bands occurring in the region 12,000-18,000 cm^{-1} have been assigned to the spin forbidden transitions.^{36,37} Figure VI.7-VI.12 represent the electronic spectra of the complexes.



FigureVI.9 Electronic spectrum of
[PS-opdRuCl₃(H₂O)]

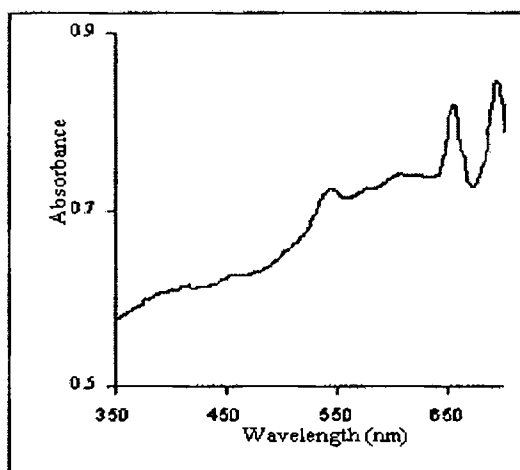


FigureVI.10 Electronic spectrum of
[PS-apRuCl₂(H₂O)₂]

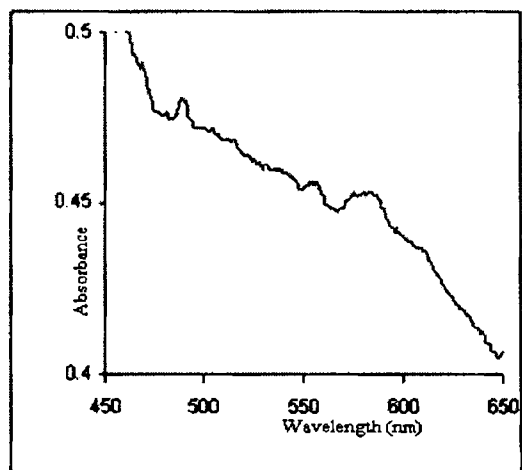


FigureVI.11 Electronic spectrum of
[PS-abRuCl₃(H₂O)₂]

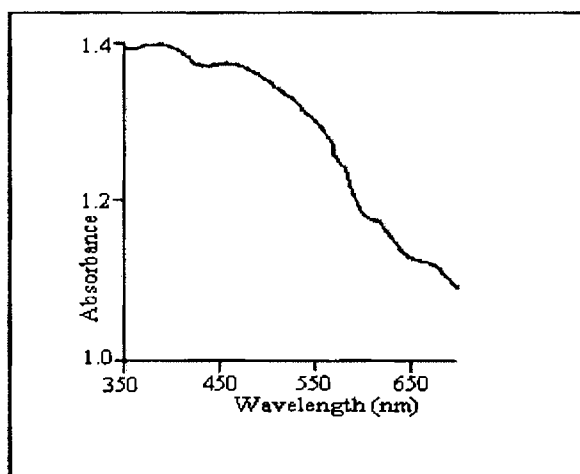
All the synthesized polymer supported neodymium complexes are characterized by ligand to metal charge transfer transition and hypersensitive transition due to ${}^4G_{5/2} \rightarrow {}^4I_{9/2}$. The additional band observed around 18000 cm^{-1} in the case of $[\text{PS-opdNdCl}_3(\text{H}_2\text{O})_3]$ and $[\text{PS-ap NdCl}_2(\text{H}_2\text{O})_4]$ might be due to the probable hypersensitive transition ${}^4I_{9/2} \rightarrow {}^2K_{13/2}$ or ${}^4I_{9/2} \rightarrow {}^4G_{7/2}$ ¹⁶ induced by the ligand environment.



FigureVI.12 Electronic spectrum of
 $[\text{PS-opdNdCl}_3(\text{H}_2\text{O})_3]$



FigureVI.13 Electronic spectrum of
 $[\text{PS-ap NdCl}_2(\text{H}_2\text{O})_4]$



FigureVI.14 Electronic spectrum of $[\text{PS-abNdCl}_3(\text{H}_2\text{O})_4]$

Table VI.8 Electronic spectral data of polymer supported complexes

Complex	Absorptions (cm ⁻¹)	Tentative assignments
[PS-opdRuCl ₃ (H ₂ O)]	30300	Charge Transfer
	26110 (sh)	${}^2T_{2g} \rightarrow {}^2A_{2g}, {}^2T_{1g}$
	19920	${}^2T_{2g} \rightarrow {}^4T_{2g}$
	16130	${}^2T_{2g} \rightarrow {}^4T_{1g}$
[PS-ap RuCl ₂ (H ₂ O) ₂]	29070	Charge Transfer
	24510 (sh)	${}^2T_{2g} \rightarrow {}^2A_{2g}, {}^2T_{1g}$
	16660	${}^2T_{2g} \rightarrow {}^4T_{1g}$
[PS-ab RuCl ₃ (H ₂ O) ₂]	30860	Charge Transfer
	28490 (sh)	${}^2T_{2g} \rightarrow {}^2A_{2g}, {}^2T_{1g}$
	17540	${}^2T_{2g} \rightarrow {}^4T_{1g}$
[PS-opdNdCl ₃ (H ₂ O) ₃]	24570	Charge Transfer
	16480	${}^4I_{9/2} \rightarrow {}^4G_{5/2}$
[PS-ap NdCl ₂ (H ₂ O) ₄]	20400	Charge Transfer
	17120	${}^4I_{9/2} \rightarrow {}^4G_{5/2}$
[PS-ab RuCl ₃ (H ₂ O) ₃]	25640	Charge Transfer
	17330	${}^4I_{9/2} \rightarrow {}^4G_{5/2}$

6.3.7 EPR spectra

All the polymer supported ruthenium complexes are seen to be EPR active giving two *g* values (Table VI.9). This attributes to the axial symmetry of the octahedral molecule (Figure VI.15). EPR spectra of neodymium complexes could not be detected at LNT because of very fast spin lattice relaxation.³⁸ Figure VI.16 and VI.17 represent probable structures of the complexes isolated by this method.

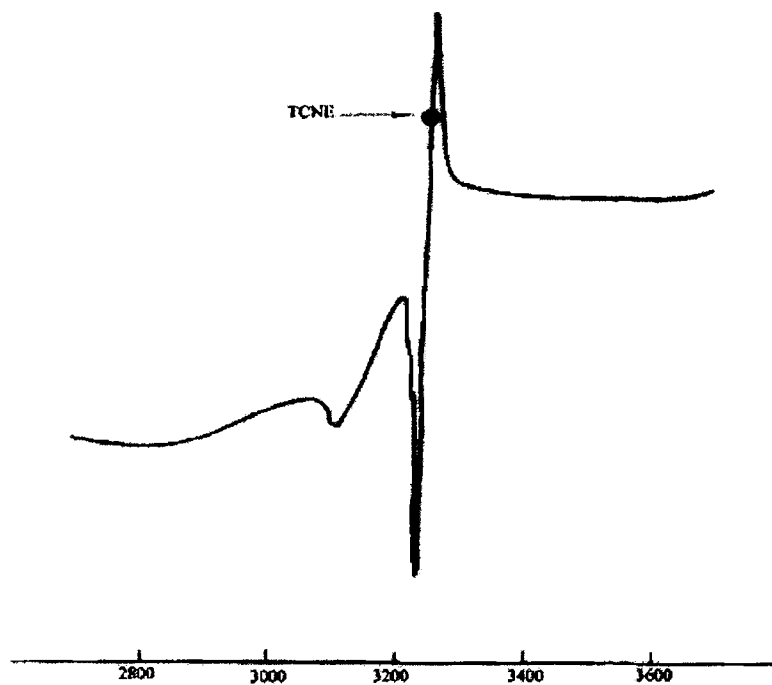


Figure VI.15 EPR spectrum of $[\text{PS-ap RuCl}_2(\text{H}_2\text{O})_2]$

Table VI.9 EPR spectral data of polymer supported complexes

Complex	g_{\parallel} values	g_{\perp} values
$[\text{PS-opdRuCl}_3(\text{H}_2\text{O})]$	2.1	1.99
$[\text{PS-ap RuCl}_2(\text{H}_2\text{O})_2]$	2.1	2.01
$[\text{PS-ab RuCl}_3(\text{H}_2\text{O})_2]$	2.1	1.99

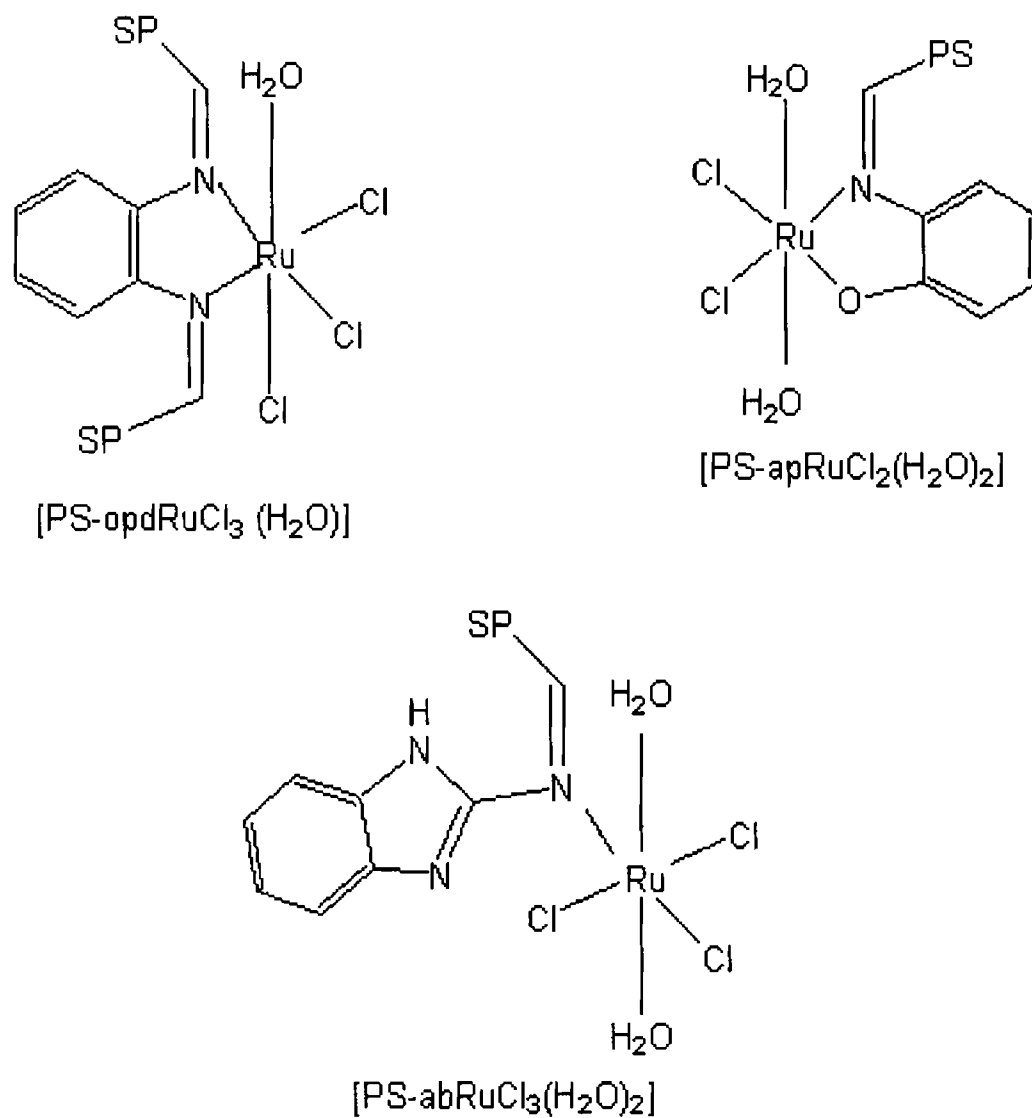


Figure VI.16 Proposed structures of Ruthenium complexes

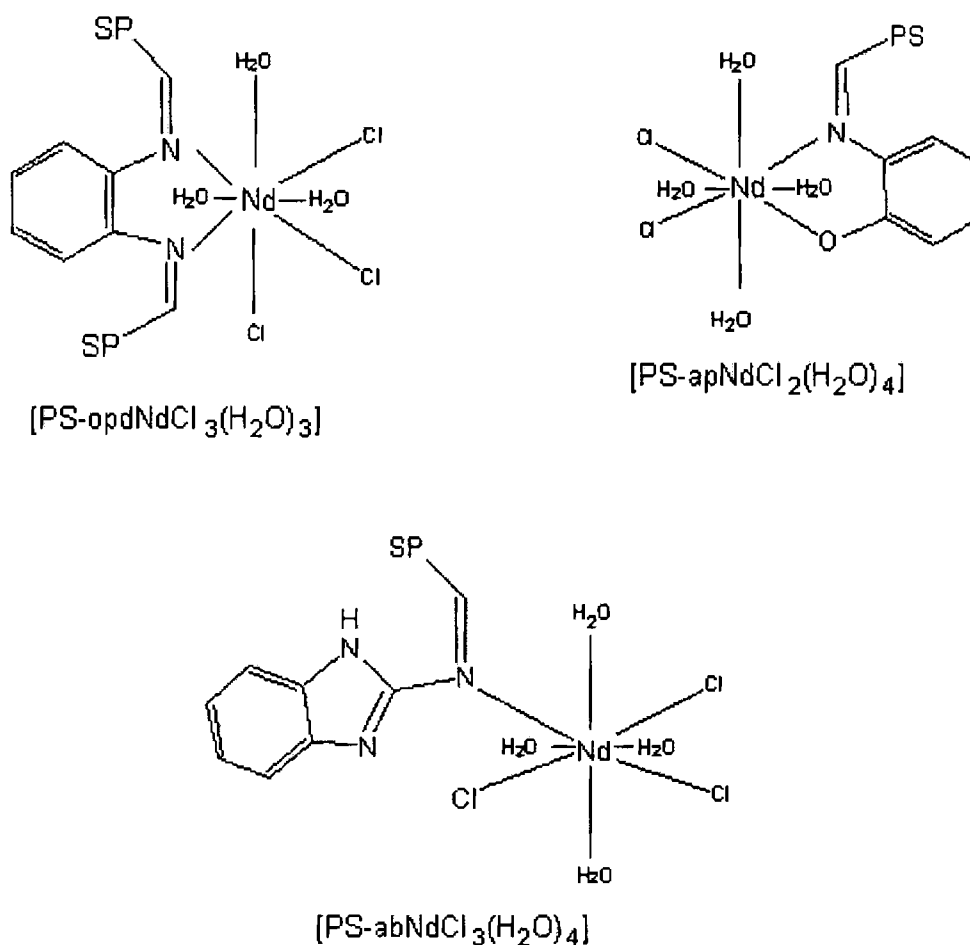


Figure VI.17 Proposed structures of Neodymium complexes

Conclusion

Ru(III) and Nd(III) complexes of polymer supported Schiff bases PS-opd, PS-ap and PS-ab were synthesized and characterized by elemental analyses, Magnetic susceptibility measurements, thermogravimetric analyses, IR, Electronic and EPR spectral studies. Ruthenium(III) complexes with polymer-anchored Schiff base ligands have been suggested to have an octahedral structure with axial symmetry while Nd(III) complexes are supposed to form an eight coordinated bicapped trigonal prismatic structure.

References

- [1] Maurya M.R.; Umesh Kumar.; Manikandan. P., Dalton Trans. **3561** (2006).
- [2] Maurya M.R.; Maneesh Kumar.; Sweta Sikarwar B., React. Funct. Polym. **66**, 808 (2006).
- [3] Gokak D.T.; Kamath B.V.; Ram R.N., J. Appl. Polym. Sci. **35**, 1523 (1988).
- [4] John J.; Dalal M.K.; Patel D.R.; Ram R.N., J. Macromol. Sci. Pure Appl. Chem. A **34**, 489 (1997).
- [5] John, J.; Dalal M.K.; Ram R.N., J. Mol. Catal. A: Chem. **137**, 183 (1999).
- [6] Mehmet T.; Celik C.; Huseyin K.; Selahattin S., Transition Met. Chem. **24**, 525 (1999).
- [7] Suja, N.R.; Yusuff K.K.M., J. Appl. Polym. Sci. **91**, 3710 (2004).
- [8] Drago R.S.; Gaul J.; Zombeck A.; Straub D.K., J. Am. Chem. Soc. **102**, 1033 (1980).
- [9] Maurya M.R.; Sweta Sikarwar.; Trissa Joseph.; Halligudi S.B., J. Mol. Catal. A: Chem. **236**, 132 (2005).
- [10] Sherrington D.C.; Pure Appl. Chem. **60**, 401 (1988).
- [11] Annis D.A.; Jacobson E.N.; J. Am. Chem. Soc. **121**, 4147 (1999).
- [12] Karjalainen J.K.; Hormi O.E.O.; Sherrington D.C., Molecules **3**, 51 (1998).
- [13] Canali L.; Sherrington D.C., Chem. Soc. Rev. **28**, 8 (1999).
- [14] Sherrington D.C., Catal. Today **57**, 87 (2000).
- [15] Chan X.; Wu Y.; Yingyong Hauxue., **6**, 13 (1989). Chem Abstr. **111**, 8252 (1989).
- [16] Jhaumeer-Laulloo B.S.; Minu G. Bhowon Indian J. chem. **42A**, 2536 (2003).
- [17] Debabrata Chatterjee.; Anannya Mitra., J. Coord. Chem. **57**, 175 (2004).
- [18] Mahesh K. Dalal.; Ram R.N., Bull. Mater Sci. **24**, 237 (2001).

-
- [19] Meijer R.H.; Ligthart G.B.W.L.; Meuldijk J.; Vekemans J.A.J.M.; Hulshof L.A., *J. Mol. Catal. A: Chem.* **218**, 29 (2004).
- [20] Mayadeo M S.; Nalgoikar., *J. Inst. Chem. India* **60**, 139 (1988).
- [21] Doreth L.; Sitran S.; Madalosso F.; Bandoli G.; Palocci., *J. Inorg. Nucl. Chem.* **42**, 106 (1980).
- [22] Tschudisteiner I., *Pharm. Acta. Helv.* **33**, 105 (1958).
- [23] Suja.N.R., Ph.D. Thesis, Cochin University of Science and Technology (2002).
- [24] Syamal A.; Singh M M., *Indian J. Chem* **33A**, 58 (1994); **32A**, 42, 431 (1993).
- [25] Figgis B.N.; Lewis., J. *The Magnetic Properties of Transition Metal Complexes*, (Ed.) Cotton, F.A. *Progress in inorganic chemistry Interscience*, New York. **6** (1964).
- [26] Dutta R.L.; Syamal. A., *Elements of Magnetochemistry*, 2nd Edn, East west press, New Delhi.
- [27] Shah J.N.; Gokak D.T.; Ram R.N., *J. Mol.Catal.* **60**, 141 (1990).
- [28] Vinod K.; Sharma.; Shipra Srivastava., *Indian J. Chem.* **45A**, 1368 (2006).
- [29] Yusuff, K.K.M.; Sreekala R., *J. Polym. Sci., Part A; Polym. Chem.* **30**, 2595 (1992).
- [30] Syamal .A.; Singhal O.P., *Transition Met. Chem.* **4**, 179 (1979).
- [31] Miners J.O.; Sinn E.; Coles R.B.; Harris C.M., *J. Chem. Soc. Dalton Trans.* 1149 (1972).
- [32] Durig J.R.; McAllister W.A.; Willis Jr. J.N.; Mercer E.E., *Spectrochim Acta* **22**, 1091 (1966).
- [33] Mojumdar S.C.; Melnik M.; Jona E., *Chem. Papers* **53**, 309 (1999).
- [34] Solloway Jr W.W.; Kestigion M., *Spectrchim Acta* **22**, 1381 (1966).
- [35] Wester D.; Edwards R. C.; Bush D. H., *Inorg. Chem.* **16**, 1055 (1977).
-

- [36] Lever A.B.P., *Inorganic Electronic Spectroscopy*, 2nd ed. Elsevier, Amsterdam (1984).
- [37] Allen G.C.; El-Fsharkawy G.A.M.; Warren K.D., *Inorg. Chem.* **12**, 2231 (1973).
- [38] Mesot J.; Staub Gullioume M.; Furrer A.; Yoos.I.; Kramer M.; Mc Callum R.; Maletta H.; Blank H.; Mutka H.; Osborn R.; Arai M.; Bowdin Z.; Taylor A. Z., *Phys. B* **95**, 301 (1994).

*CATECHOL -H₂O₂ REACTION - A COMPARATIVE STUDY OF
HOMOGENEOUS AND HETEROGENEOUS CATALYSIS BETWEEN
RUTHENIUM AND NEODYMIUM*

7.1 Introduction

Aromatic hydroxylation reactions are important bacterial metabolic processes, but are difficult to perform using traditional chemical synthesis. Use of biological catalyst to convert benzene into industrially relevant intermediates through oxidation reaction was investigated. It was discovered that toluene-4-mono-oxygenase, toluene-3-mono-oxygenase and toluene ortho mono-oxygenase convert benzene to phenol, catechol and 1,2,3-trihydroxybenzene by successive hydroxylations.¹

Attempts to explore substances that mimic the biological catalysts led recent chemists to the field of supported complexes. Recent reviews reveal that encapsulated complexes often act as biological models.² The catalytic properties of zeolite encapsulated transition metal complexes have been explored in various selective oxidation and hydrogenation reactions. Previous reports confirmed the encapsulation of copper salen complexes in super cages of faujasite type zeolite and are found to be effective catalyst for the oxidation of phenol and cyclohexane.³ Polymer supported complexes were also found to exhibit high efficiency in the catalytic oxidation reactions.

The present investigation aims at a study of homogeneous and heterogeneous catalysis of catechol oxidation reaction using simple and supported complexes of ruthenium and neodymium. The environment of the metal ion largely influences the

activity of the ion. The strain⁴ induced by the coordination of the ligand tunes the metal ion towards particular reaction. Hence the selectivity of the reaction products is characteristic of the ligand and the metal ion. In addition to the reactant and product selectivity due to size constraints, encapsulation in the cages of zeolite increases the lifetime of the catalyst to a certain extent.

In metalloenzymes and chemical catalysis the role of multimetallic species is well known. These complexes are reported to serve as models for biologically important species, which contain metal ions in macrocyclic environments. Bicopper centres are now well established in copper containing metalloproteins and function by binding and activating molecular oxygen as a key substrate. Coordination asymmetry in binuclear metalloproteins has been reported to be responsible for imparting unique reactivity to these centers.⁵⁻⁷ Non-porphyrinic ruthenium(III) complexes that exhibit selectivity toward oxofunctionalization of hydrocarbons of ruthenium were synthesized.⁸⁻¹¹ Their catalytic efficiency was tested towards hydroxylation reaction of catechol.

Catalysis of hydroxylation reaction of catechol by encapsulated and polymer supported complexes of ruthenium and neodymium has not yet been reported in the literature. Hence the present work is extended to study the catalytic performance of encapsulated and polymer supported complexes of ruthenium and neodymium towards hydroxylation reaction of catechol.

7.2 Experimental

7.2.1 Reagents

All the reagents used in the kinetic study were of highest purity available and were used as such without further purification. Simple and supported complexes of ruthenium and neodymium were synthesized according to the procedure described in previous chapters.

7.2.2 Preparation of substrate solution

A standard solution of catechol ($1 \times 10^{-2} \text{ mol dm}^{-3}$) was prepared by dissolving a definite weight ($2.75 \times 10^{-2} \text{ g}$) of catechol in methanol (25mL). The resultant solution was used as the stock solution. This solution was prepared afresh before each set of kinetic runs.

7.2.3 Preparation of stock solution of hydrogen peroxide

Hydrogen peroxide (30% w/v; 1mL) was diluted to 100mL in a standard flask and was used as such for the catalytic studies. The concentration of the stock solution was estimated permanganometrically.¹²

7.2.4 Preparation of solution of simple complexes

Solutions of the simple complexes of ruthenium and neodymium ($1 \times 10^{-4} \text{ M}$) were prepared in methanol.

7.2.5 Screening studies

A preliminary screening study of the catalytic activity was conducted towards catechol oxidation reaction using H_2O_2 . The products of the reaction were monitored spectrophotometrically.

7.2.6 Kinetic procedure

Catechol solution in methanol (9mL) was treated with H_2O_2 (1mL) and monitored spectrophotometrically. The maximas obtained were due to catechol. Hence it was understood that no reaction takes place in the absence of catalyst.

For following the reaction kinetically catechol solution (9mL) was mixed with the catalyst (2mL) and the reaction was initiated by adding H_2O_2 solution (1mL). The

reaction products were monitored spectrophotometrically at an interval of one minute by measuring the absorbance at 290nm¹ and at 390nm.¹³

A mixture of catechol solution (10 mL) and catalyst (2 mL) was used as blank. In the case of supported complexes catalyst was added as such (0.01 g) and reaction was monitored at stipulated wavelengths. The blank used was a mixture of catechol solution (9 mL) and water (1 mL). The reaction was monitored also at a third wavelength at which products of reaction do not absorb. The absorbance measured at this wavelength corresponds to the scattering due to the catalyst particles. To get the actual absorbance of the product at a particular wavelength, the absorbance due to scattering was deducted. The initial rate of the reaction was determined from the concentration-time plot. Initial rates were obtained by fitting the data into the polynomial of the form $[C] = a_0 + a_1t + a_2t^2 + \dots$ where C and t represent concentration and time respectively. a_0, a_1, a_2 etc. are constants. The coefficient of 't' gives the initial rate.¹⁴ The activity of the catalysts was compared with respect to the initial rate.

Screening of the catalysis by RuY and NdY was conducted towards catechol-H₂O₂ reaction. In both cases no product was formed.

7.3 Results and discussion

7.3.1 Comparison of catalytic activity of neat and encapsulated complexes of ruthenium

The initial rates obtained during the catalytic activity studies of the synthesized neat complexes of ruthenium are given in Table VII.1. The kinetic study conducted for catechol oxidation by hydrogen peroxide in the presence of neat complexes of ruthenium showed the formation of comparatively high percentage of the product. In the presence of neat complexes $[\text{Ru}_2(\text{qap})_2\text{Cl}_2(\text{H}_2\text{O})_2] \cdot \text{H}_2\text{O}$ and $[\text{Ru}_2(\text{qab})_2\text{Cl}_4(\text{H}_2\text{O})_2] \cdot 3\text{H}_2\text{O}$, reaction yielded o-benzoquinone and a very small

Table VII.1 Initial rates of catechol -H₂O₂ reaction using simple complexes of ruthenium as catalyst

$$[\text{catechol}] = 1 \times 10^{-2} \text{ mol dm}^{-3}$$

$$[\text{H}_2\text{O}_2] = 1 \times 10^{-2} \text{ mol dm}^{-3}$$

Product formed = o-benzoquinone

catalyst	Initial rate/unit weight of ruthenium $\times 10^4 \text{ mol dm}^{-3} \text{ s}^{-1}$
$[\text{Ru}_2(\text{qpd})\text{Cl}_4(\text{H}_2\text{O})_2] \cdot 2\text{H}_2\text{O}$	-
$[\text{Ru}_2(\text{qap})_2\text{Cl}_2(\text{H}_2\text{O})_2] \cdot \text{H}_2\text{O}$	34
$[\text{Ru}_2(\text{qab})_2\text{Cl}_4(\text{H}_2\text{O})_2] \cdot 3\text{H}_2\text{O}$	11
$[\text{Ru}_2(\text{salpd})_3\text{Cl}_2(\text{H}_2\text{O})_2]$	80
$[\text{Ru}_2(\text{salap})_4\text{Cl}_2] \cdot \text{H}_2\text{O}$	99
$[\text{Ru}(\text{salab})(\text{H}_2\text{O})_4]\text{Cl}_2 \cdot \text{H}_2\text{O}$	58

amount of 1,2,4-Trihydroxybenzene as the product. $[\text{Ru}_2(\text{qpd})\text{Cl}_4(\text{H}_2\text{O})_2] \cdot 2\text{H}_2\text{O}$ remained inactive while in the presence of $[\text{Ru}_2(\text{salpd})_3\text{Cl}_2(\text{H}_2\text{O})_2]$, $[\text{Ru}_2(\text{salap})_4\text{Cl}_2] \cdot \text{H}_2\text{O}$ and $[\text{Ru}(\text{salab})(\text{H}_2\text{O})_4]\text{Cl}_2 \cdot \text{H}_2\text{O}$ the product formed is o-benzoquinone. Also complexes formed from salicylaldehyde Schiff bases were more active than that formed from 3-hydroxyquinoxaline-2-carboxaldehyde Schiff bases. The oxidation of catechol by hydrogen peroxide in the presence of the ruthenium(III) complexes can proceed by oxidation of ruthenium(III) to ruthenium(V) state by H₂O₂ followed by reduction of ruthenium(V) by catechol. It is reported that the phenolate oxygen stabilizes the higher oxidation states of ruthenium¹⁵. Salicylaldehyde being more acidic than 3-hydroxyquinoxaline -2-carboxaldehyde formation of Ru(V) is easier. Also of the salicylaldehyde Schiff base complexes that formed from o-aminophenol was found to be more active. The catalytic activity of the complexes is in the order: $[\text{Ru}_2(\text{salap})_4\text{Cl}_2] \cdot \text{H}_2\text{O} > [\text{Ru}_2(\text{salpd})_3\text{Cl}_2(\text{H}_2\text{O})_2] > [\text{Ru}(\text{salab})(\text{H}_2\text{O})_4]\text{Cl}_2 \cdot \text{H}_2\text{O}$. The increase in activity of the salicylaldehyde Schiff base complexes is due to the coordination of the phenolato

oxygen atoms which makes the metal centre more electron rich,¹⁵ hence can be oxidized more easily to the +5 state than the complexes derived from the Schiff bases of 3-hydroxyquinoxaline-2-carboxaldehyde

The initial rates, percentage conversion and turn over frequency (TOF) obtained during the catalytic activity studies of the synthesized encapsulated complexes of ruthenium are given in Table VII.2. The reaction was found to be selective towards the formation of 1,2,4-trihydroxybenzene in the presence of encapsulated complexes of ruthenium. The product formed 1,2,4-trihydroxybenzene was identified by the UV/Visible spectrum. Two hydroxyl groups already present in the catechol directs the third hydroxyl group preferably to the para position, inhibiting the possibility of the formation of 1,2,3- trihydroxybenzene. The oxidation of Ru(III) by H₂O₂ is suggested to proceed in non complementary steps generating OH[•] leading to the formation of Ru(V). Ru(V) is then reduced by catechol to Ru(III). RuYqpd remained inactive as in the case of simple complex of qpd for some reason not clear. A Fenton type process might be operative in the case of hydrogen peroxide, resulting in the formation of hydroxyl radicals that attack coordinated Schiff base ligands causing oxidative decomposition of the complex yielding no product¹⁵. RuYqap complex was found to be more active compared to RuYqab, although initial rate of the reaction is high in the presence of RuYqab. In the presence of RuYqap 6.4% conversion was achieved in 30 minutes with a TOF (h⁻¹) of 3232. RuYqab complexes shows activity with lesser percent conversion and TOF. The catalytic activities of the salicylaldehyde complexes are in the order RuYsalap > RuYsalpd > RuYsalab.

The cyclic ability of the zeolite encapsulated complexes has been tested and found that no appreciable loss in the activity occurred after the first cycle. The cyclic ability and easy separation of the catalysts from the reaction mixture make the zeolite encapsulated complexes better catalysts than the neat ones.

Table VII.2 Initial rates and percent conversion of catechol -H₂O₂ reaction using encapsulated complexes of ruthenium as catalyst

$$[\text{catechol}] = 1 \times 10^{-2} \text{ mol dm}^{-3}$$

$$[\text{H}_2\text{O}_2] = 1 \times 10^{-2} \text{ mol dm}^{-3}$$

Product formed = 1,2,4-trihydroxybenzene

Catalyst	Initial rate/unit weight of ruthenium $\times 10^4$ (mol dm ⁻³ s ⁻¹)	Conversion % in 30 minutes	TOF (h ⁻¹)*
RuYqpd	-	-	-
RuYqap	18.6	6.4	3232
RuYqab	31.7	2.4	539
RuYsalpd	9.1	2.2	1481
RuYsalap	12.4	9.2	3097
RuYsalab	11.7	2.1	848

*TOF (h⁻¹) = no.of moles of substrate converted per mole of catalyst in 1h.

7.3.2 Comparison of catalytic activity of neat and encapsulated complexes of neodymium

Simple complexes of neodymium are less active as compared to ruthenium complexes as indicated by the initial rate (Table VII.3). In the presence of [Nd(qpd)₂(H₂O)Cl].2H₂O and [Nd(qab)₂(H₂O)₃Cl].2H₂O, the reaction does not yield either o-benzoquinone or 1,2,4-Benzenetriol as the product. However [Nd(qap)₂(H₂O)₃Cl].H₂O show slight activity towards the formation of o-benzoquinone. Zeolite encapsulated neodymium complexes of qpd, qap and qab show no activity towards the oxidation of catechol. But in the presence of encapsulated neodymium complexes of salpd, salap and salab, the reaction

Table VII.3 Initial rates of catechol -H₂O₂ reaction using simple & encapsulated complexes of neodymium as catalyst

$$[\text{catechol}] = 1 \times 10^{-2} \text{ mol dm}^{-3}$$

$$[\text{H}_2\text{O}_2] = 1 \times 10^{-2} \text{ mol dm}^{-3}$$

catalyst	$[\text{Nd}(\text{qpd})_2(\text{H}_2\text{O})\text{Cl}] \cdot 2\text{H}_2\text{O}$	$[\text{Nd}(\text{qap})_2(\text{H}_2\text{O})_3\text{Cl}] \cdot \text{H}_2\text{O}$	$[\text{Nd}(\text{qab})_2(\text{H}_2\text{O})_3\text{Cl}] \cdot 2\text{H}_2\text{O}$	NdYqpd	NdYqap	NdYqab	NdYsalpd	NdYsalap	NdYsalab
Product formed	o-benzoquinone			1,2,4-trihydroxybenzene					
Initial rate/unit weight of Nd $\times 10^4 \text{ mol dm}^{-3} \text{ s}^{-1}$	-	3.06	-	-	-	-	4.9	4.2	5.8

yielded 1,2,4-trihydroxybenzene, although the activity is less compared to the corresponding complexes of ruthenium. The catalytic activities of the complexes are in the order NdYsalab > NdYsalpd > NdYsalap. The decrease in activity compared to ruthenium complexes might be due to the influence of neodymium ion.

7.3.3 Catalytic activity study of polymer supported complexes of ruthenium

Catechol oxidation by H₂O₂ is known to give the product, o-benzoquinone.¹⁶ In the presence of the polymer supported complexes the reaction was found to be selective towards the formation of o-benzoquinone. The plots of absorbance versus time were shown in Fig. VII.1-VII.3. The obtained initial rates of the reaction are given in Table VII.4. These rates show that all the three ruthenium(III) complexes catalyze the oxidation. The percentage conversion of catechol to o-benzoquinone in 30 minutes

and TOF (h^{-1}) were also calculated and presented in Table VII.3. In the presence of $[\text{PS-abRuCl}_3(\text{H}_2\text{O})_2]$ 63% conversion was achieved in 30 minutes with a TOF (h^{-1}) of 5631. $[\text{PS-opdRuCl}_3(\text{H}_2\text{O})]$, $[\text{PS-apRuCl}_2(\text{H}_2\text{O})_2]$ complexes show activity with lesser percent conversion and TOF. The oxidation of catechol by hydrogen peroxide in the presence of the ruthenium(III) complexes can proceed either by oxidation of catechol by ruthenium(III) complex leading to the formation of ruthenium(II) state and the subsequent oxidation of ruthenium(II) by H_2O_2 ¹⁷ or by another mechanism, involving oxidation of ruthenium(III) to ruthenium(V) state by H_2O_2 followed by reduction of ruthenium(V) by catechol.

The catalytic activity of the complexes is in the order $[\text{PS-abRuCl}_3(\text{H}_2\text{O})_2] \gg [\text{PS-opdRuCl}_3(\text{H}_2\text{O})] > [\text{PS-apRuCl}_2(\text{H}_2\text{O})_2]$. It is reported that the phenolate oxygen stabilizes the higher oxidation states of ruthenium while imine nitrogen stabilizes the lower oxidation state of ruthenium¹⁸. As has been mentioned earlier, IR studies of these complexes showed that PS-ab binds to the metal atom through one imino nitrogen, PS-opd binds through two imino nitrogens and ps-ap binds through one phenolate oxygen and one imino nitrogen. As the rates of the reaction of $[\text{PS-abRuCl}_3(\text{H}_2\text{O})_2]$ and $[\text{PS-opdRuCl}_3(\text{H}_2\text{O})]$ are higher than that of the $[\text{PS-apRuCl}_2(\text{H}_2\text{O})_2]$, a lower oxidation state (Ru^{II}) is thought to be involved in this catalytic reaction. The lower value of $[\text{PS-opdRuCl}_3(\text{H}_2\text{O})]$ than $[\text{PS-abRuCl}_3(\text{H}_2\text{O})_2]$ may be due to the steric hindrance caused by the involvement of two polymer chains at the reaction centre. If the reaction proceeded through ruthenium(V) formation, a reverse trend in the activity of the complexes would have been observed.

Table VII.4 Initial rates and percent conversion obtained in the oxidation of catechol by H_2O_2 in the presence of polymer supported complexes of ruthenium as catalysts

$$[\text{Catechol}] = 1 \times 10^{-2} \text{ mol dm}^{-3}$$

$$[\text{H}_2\text{O}_2] = 1 \times 10^{-2} \text{ mol dm}^{-3}$$

catalyst	Initial rate / unit weight of ruthenium $\times 10^5$, $\text{mol dm}^{-3} \text{ s}^{-1} \text{ g}^{-1}$	Conversion(%) in 30 minutes	TOF (h^{-1}) [*]
[PS-opdRuCl ₃ (H ₂ O)]	12.2	43.1	2172
[PS-ap RuCl ₂ (H ₂ O) ₂]	2.9	7.8	1040
[PS-ab RuCl ₃ (H ₂ O) ₂]	473.1	63.0	5631

* TOF (h^{-1}) = no. of moles of substrate converted per mole of catalyst in 1h.

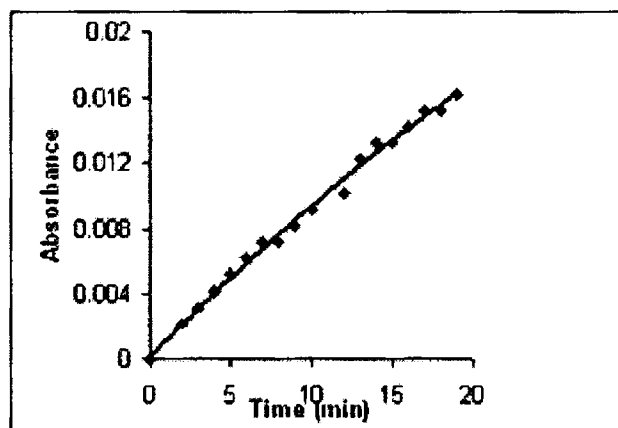


Figure VII.1 Kinetic plot of absorbance versus time for catechol- H_2O_2 reaction catalyzed by [PS-opdRuCl₃ H₂O]

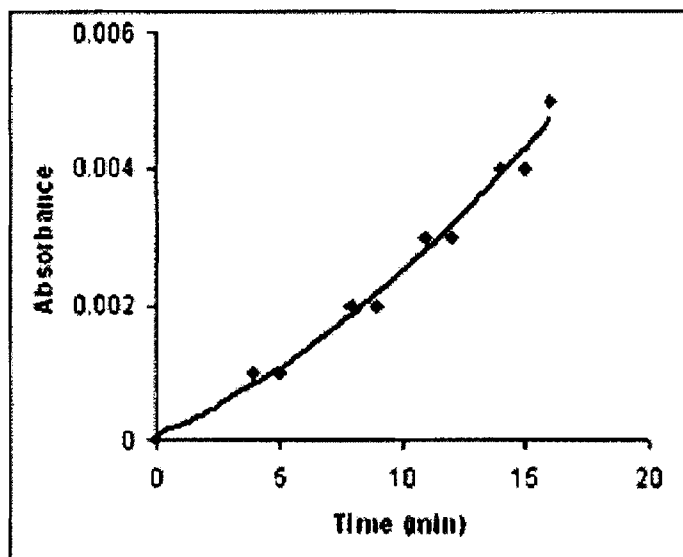


Figure VII.2 Kinetic plot of absorbance versus time for catechol-H₂O₂ reaction catalyzed by [PS-apRuCl₂(H₂O)₂].

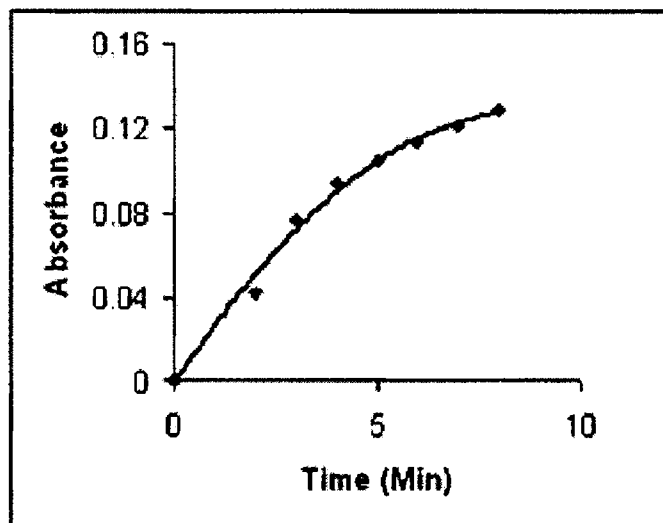


Figure VII.3 Kinetic plot of absorbance versus time for catechol-H₂O₂ reaction catalyzed by [PS-abRuCl₃(H₂O)₂].

7.3.4 Catalytic activity study of polymer supported complexes of neodymium

Table VII.5 Initial rates and percent conversion obtained in the oxidation of catechol by H₂O₂ in the presence of polymer supported complexes of neodymium as catalysts

$$[\text{Catechol}] = 1 \times 10^{-2} \text{ mol dm}^{-3}$$

$$[\text{H}_2\text{O}_2] = 1 \times 10^{-2} \text{ mol dm}^{-3}$$

catalyst	Initial rate / unit weight of neodymium $\times 10^5$, $\text{mol dm}^{-3} \text{s}^{-1} \text{g}^{-1}$	Conversion(%) in 30 minutes	TOF (h^{-1}) [*]
[PS-opdNdCl ₃ (H ₂ O) ₃]	3.0	8.5	546
[PS-ap NdCl ₂ (H ₂ O) ₄]	2.8	1.6	149
[PS-ab NdCl ₃ (H ₂ O) ₄]	10.9	5.1	454

* TOF (h^{-1}) = no. of moles of substrate converted per mole of catalyst in 1h.

Activities of neodymium complexes were very small as compared with ruthenium complexes. However the product formed in both cases is same. [PS-abNdCl₃(H₂O)₄] and [PS-apNdCl₂(H₂O)₄] yielded a negligible percentage of 1,2,4-trihydroxybenzene in addition to o-benzoquinone. The plots of absorbance versus time were shown in Fig. VII.4-VII.6. The obtained initial rates of the reaction, the percentage conversion of catechol to o-benzoquinone in 30 minutes and TOF (h^{-1}) are given in Table VII.5. Initial rate study show that [PS-abNdCl₃(H₂O)₄] is more active compared to other two complexes. However the percent conversion and turn over frequency of the complex is slightly less than [PS-opdNdCl₃(H₂O)₃].

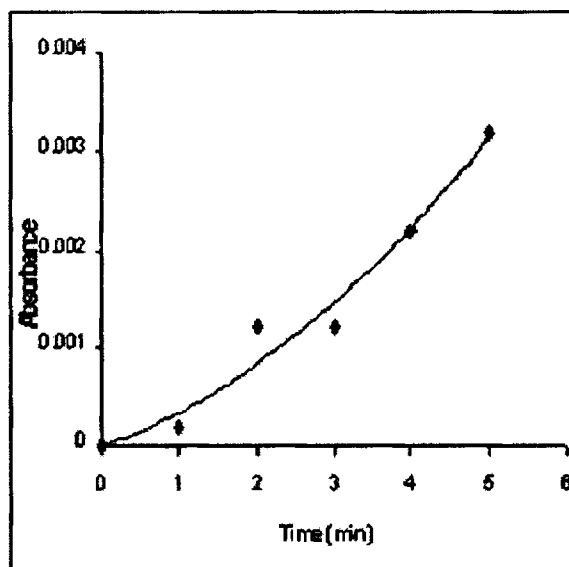


Figure VII.4 Kinetic plot of absorbance versus time for catechol-H₂O₂ reaction catalyzed by [PS-opdNdCl₃(H₂O)₃]

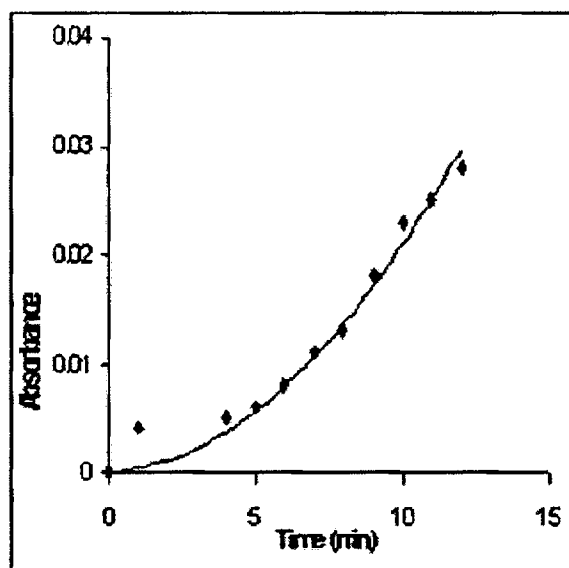


Figure VII.5 Kinetic plot of absorbance versus time for catechol-H₂O₂ reaction catalyzed by [PS-apNdCl₂(H₂O)₄]

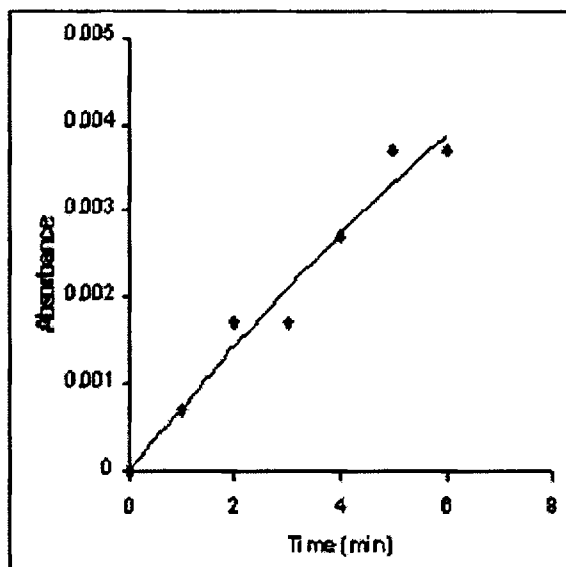


Figure VII.6 Kinetic plot of absorbance versus time for catechol-H₂O₂ reaction catalyzed by [PS-abNdCl₃(H₂O)₄]

Conclusion

The present study compares the catalytic activity of 4d transition metal ruthenium and 4f inner transition metal neodymium ion with respect to the ligands derived from quinoxaline aldehyde and salicylaldehyde. Results indicate that catalytic activity of these catalysts is very much dependent on the steric and electronic environment of the Schiff base complexes which influences the selectivity of the product. However the rate of the reaction is largely controlled by the nature of the metal ion. It is evident from these studies that the activity of the ruthenium complexes is higher than that of the neodymium complexes.

References

- [1] Ying Tao.; Ayelet Fishman.; William E Bentley.; Thomas K wood., Applied and Environmental Microbiology, (7) **70**, 3814 (2004).
- [2] Parton R.; De Vos D.; Jacobs P.A., zeolite microporous solids: Synthesis, structure and reactivity, edited by E G Deroune (kluwer, Netherlands) 555 (1992).
- [3] Jacob C. R.; Varkey S. P.; Ratnasamy P., J. Appl. Catal. (1997).
- [4] Sharma V. S.; Schubert J., Inorg. Chem. **10**, 251 (1971).
- [5] Mohan G.; Sharma R. C.; Parashar R. K., Polish J. Chem. **929**, (1992).
- [6] Satcher J.H.; Droege M. W.; Weakly T. J.R.; Taylor R.T., Inorg. Chem, **34**, 3317 (1995).
- [7] Yong G., Leone C.; Strothcamp K. G., Biochemistry **29**, 9684 (1990).
- [8] Nasir M.S.; Karlin K.D.; McGoety D.; Zubeita J., J.Am. Chem. Soc. **113**, 698 (1991).
- [9] Mahroff Tahir M.; Murth N. N.; Karlin K.D.; Blackburn N.J.; Shaikh S.N., Zubeita J. Inorg. Chem **31**, 3001 (1992).
- [10] Adams H.; Candeland G.; Crane J.D.; Fenton D.E.; Smith A.J., J. Chem. Soc. Chem. Commun. **93** (1990).
- [11] Crane J.D.; Fenton D.E.; Latour J. M.; Smith A. J., J. Chem. Soc. Dalton Trans. 2979 (1991).
- [12] Jeffery H.; Bassett J.; Mendham J.; Denney R.C., Vogel's Text book of Quantitative Inorganic Analysis-5th Edition-ELBS-Longman Singapore publishers (1991).
- [13] Latif Abuhijleh A.; Clifton woods; Ekaterini Bogas; Gaelle Le Guenniou, Inorganica Chimica Acta, **195**, 67 (1992).

- [14] Mayadevi S.; Sridevi N.; Yusuff K. K. M., *Indian J. Chem.* **37A**, 413 (1998).
- [15] Debabrata Chatterjee ; Anannya Mitra, *J. Coord. Chem.* **57 (3)**, 175 (2004).
- [16] Lloyd; Ingraham L., *Arch. Biochem. Biophys.* **81**, 309 (1959).
- [17] Alan S.Goldstein.; Robert H.Beer.; Russell S.Drago., *J. Am. Chem. Soc.* **116**, 2424 (1994).
- [18] Renata Drozdak.; Bart Allaert.; Nele Ledoux.; Ileana Dragutan.; Valerian Dragutan.; Francis Verpoort., *Coord. Chem. Rev.* **249**, 3055 (2005).

CHAPTER VIII

CATALYTIC HYDROXYLATION OF PHENOL

8.1 Introduction

Phenol is listed as a priority pollutant and is highly toxic. Poor degradability of phenol makes the situation worse. Drastic conditions such as temperature, pressure and solvent conditions needed for the conversion of phenol to harmless products are environmentally unsafe. Hydroxylation of phenol is a reaction of commercial importance as it yields catechol and hydroquinone. Catechol and hydroquinone are important intermediates for the synthesis of pharmaceuticals, agrochemicals, flavors, polymerization inhibitors and antioxidants.^{1,2} Hydroquinone is a powerful reducing agent which finds application as photographic developer and as an antiseptic. Homogeneous catalysts are effective towards oxidation reaction of phenol. However the recovery of the catalysts from the reaction site is difficult and expensive. Inorganic supports possess a rigid structure, which circumvents the deactivation process like intermolecular condensation and chelation by multiple anchored ligand coordination.³ Catalysis is dependent mainly on the stability of the metal complex. Thermal stability of the anchored complex enhances the possibility of administering such complexes in catalysis. Among the inorganic supports zeolites are superior as they themselves are active for certain reactions. Their relatively rigid inorganic matrices with cavities and channels of molecular dimensions of different sizes and shape provide selectivity for certain reactions. It has been reported that catalytic efficiency of compounds can be increased by combining a porous support like zeolite and an active site for the adsorption of organic compound. This causes activation of H_2O_2 and leads to complete oxidation.^{4,5}

Polymer supports possess flexibility to permit interaction of polymer bound anchoring groups with the metal complex. They are not susceptible to poisoning by impurities since the catalytic sites are protected by the polymer matrix. They can retain

catalytic activity over a wide range of concentration. The quest for an easier and cheaper method of conversion of phenol to useful products led to the synthesis of some polymer supported and encapsulated complexes. The efficiencies of these compounds as catalysts were tested towards hydroxylation reaction of phenol in presence of H_2O_2 . Reports show that activity coefficient of phenol in water is much higher than in any other solvent.⁶ Hence more activity is expected in water for the phenol- H_2O_2 reaction.

8.2 Materials

The details of the materials used in the catalytic study are given in Chapter II. The neat and supported complexes used, as catalysts in the reaction were prepared according to the procedure explained in previous chapters.

8.3 Procedure

Hydroxylation reaction of phenol was carried out in a thermostated reactor of 100mL volume fitted with a magnetic stirrer. The reaction was equipped with a reflux condenser. For high temperature reactions temperature controlled oil-bath was used. For the reaction phenol (1mL), H_2O_2 (5mL), and H_2O (5mL) were taken. Reaction was initiated by adding 40 mg Catalyst. Reactions were done at room temperature and 80 °C. Solution from the reaction vessel was withdrawn at definite intervals of time 1h, 2h, 3h,... The reaction mixture was cooled to room temperature and the products were analyzed.

8.3.1 Analysis of products

Products of hydroxylation reaction were analyzed in a gas chromatograph equipped with flame ionisation detector using SE 30 column. The identity of the products was further confirmed by GCMS.

Blank Run

Phenol hydroxylation was carried out in the absence of the catalyst. It was found that no product was formed even after 6 h.

8.4 Results and discussion

Neat and zeolite encapsulated complexes of ruthenium with the Schiff bases derived by condensing o-phenylenediamine with a) 3-hydroxyquinoxaline-2-carboxaldehyde b) salicylaldehyde and polymer supported complexes of o-phenylenediamine were screened for their catalytic activity towards phenol hydroxylation reaction. The reaction was monitored at different time intervals at room temperature and at 80°C. The percentage conversion obtained with various catalysts is given in Table VIII.1- VIII.5 and represented graphically (Figure VIII.1-VIII.5). The only product formed was hydroquinone.

In the presence of simple complex $[\text{Ru}_2(\text{qpd})\text{Cl}_4(\text{H}_2\text{O})_2]$, more than 50% conversion of phenol to hydroquinone takes place in one hour. However only 15% conversion of phenol takes place in the next four hours and in the sixth hour there is a reduction in the percentage of hydroquinone formed. This might be due to the oxidation of hydroquinone to benzoquinone.

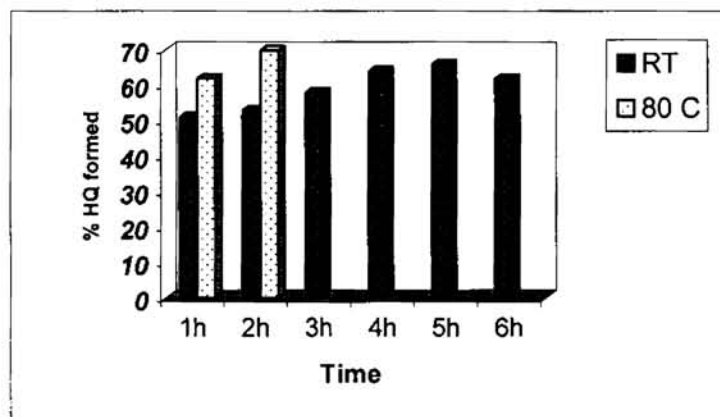


Fig. VIII.1 Percentage of hydroquinone formed in the presence of $[\text{Ru}_2(\text{qpd})\text{Cl}_4(\text{H}_2\text{O})_2]$ at different intervals

**TABLE VIII.1 Effect of Temperature & Time On Oxidation
of Phenol in the presence of $[\text{Ru}_2(\text{qpd})\text{Cl}_4(\text{H}_2\text{O})_2]$**

$[\text{Ru}_2(\text{qpd})\text{Cl}_4(\text{H}_2\text{O})_2]$	1 h	2h	3h	4h	5h	6h
	%HQ	%HQ	%HQ	%HQ	%HQ	%HQ
RT	51	53	58	64	66	62
80°C	62	70	Tar	-	-	-

At higher temperature higher percentage of hydroquinone was formed initially. But in the third hour a tarry product was formed. Hence it is not advisable to prolong the reaction if conducted at higher temperature.

In the presence of zeolite encapsulated complex RuYqpd, oxidation of phenol follows a similar trend as observed in the case of analogous simple complex. However higher percentage of hydroquinone was formed in each case. Increase in temperature in this case did not affect the percentage conversion much, although a slight increase in the

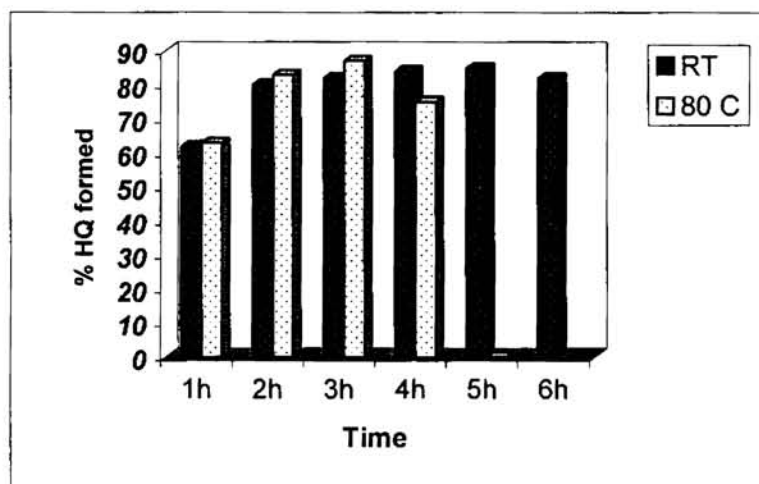


**Fig. VIII.2 Percentage of hydroquinone formed in the presence
of RuYqpd at different intervals**

yield of product was noted. However the stability of the catalyst was increased at higher temperature due to encapsulation. But with increase in time the reaction was found to be affected negatively. Hence at high temperature the reaction should be allowed to continue up to an optimum time.

TABLE VIII. 2 Effect of Temperature & Time On Oxidation of Phenol in the presence of RuYqpd

RuYqpd	1 h	2h	3h	4h	5h	6h
	%HQ	%HQ	%HQ	%HQ	%HQ	%HQ
RT	62	80	82	84	85	82
80°C	63	83	87	75	Tar	-

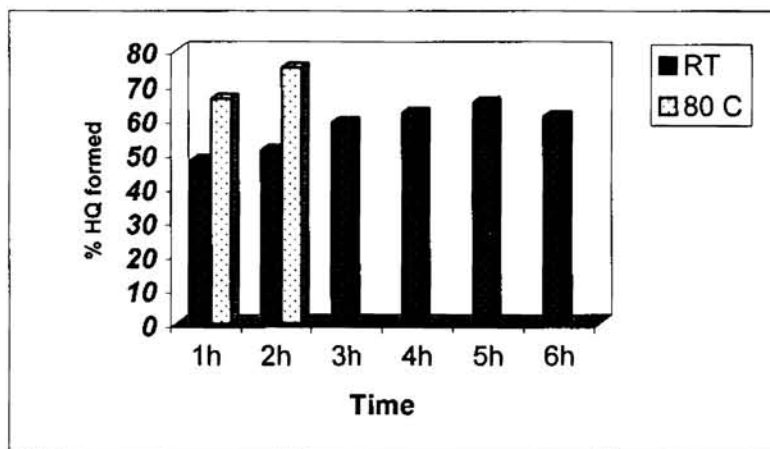


Fig. VIII.3 Percentage of hydroquinone formed in the presence of $[\text{Ru}_2(\text{salpd})_3\text{Cl}_2(\text{H}_2\text{O})_2]$ at different intervals

Simple complexes derived from salicylaldehyde and o-phenylenediamine show catalytic activity comparable to that of simple complexes derived from 3-hydroxy

quinoxaline-2-carboxaldehyde and o-phenylenediamine. In the presence of $[\text{Ru}_2(\text{salpd})_3\text{Cl}_2(\text{H}_2\text{O})_2]$ hydroxylation of phenol resulted in the formation of hydroquinone and amount of product formed followed a regular increase up to 5 h. There after a decrease in reaction product was noticed indicating further oxidation of hydroquinone. At high temperature there was a considerable increase in product initially but after two hours a tarry product was formed.

TABLE VIII.3 Effect of Temperature & Time On Oxidation of Phenol in the presence of $[\text{Ru}_2(\text{salpd})_3\text{Cl}_2(\text{H}_2\text{O})_2]$

$[\text{Ru}_2(\text{salpd})_3\text{Cl}_2(\text{H}_2\text{O})_2]$	1 h	2h	3h	4h	5h	6h
	%HQ	%HQ	%HQ	%HQ	%HQ	%HQ
RT	48	51	59	62	65	61
80°C	66	75	Tar	-	-	-

Zeolite encapsulated complex of salpd gave better result when compared with simple complex and tarry product was formed only after 4 h in contrary to the simple complexes. This shows the increase in stability of the complexes on encapsulating in cages.

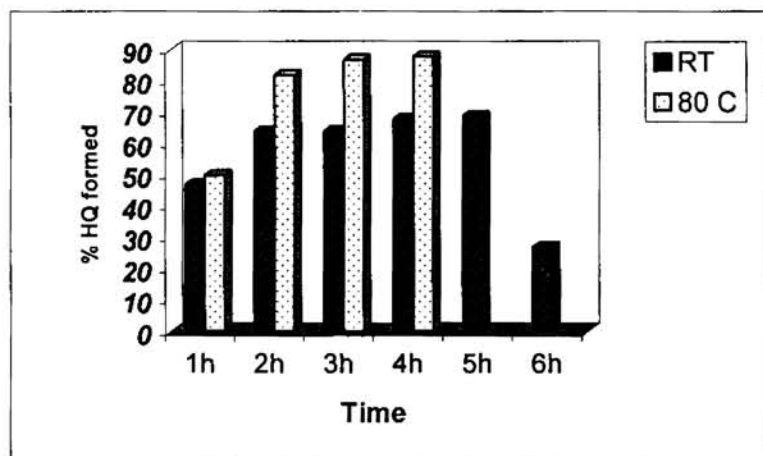


Fig. VIII.4 Percentage of hydroquinone formed in the presence of RuYsalpd at different intervals

TABLE VIII.4 Effect of Temperature & Time on Oxidation of Phenol in the presence of RuYsalpd

RuYsalpd	1 h	2h	3h	4h	5h	6h
	%HQ	%HQ	%HQ	%HQ	%HQ	%HQ
RT	47	64	64	68	69	27
80°C	50	82	87	88	-	-

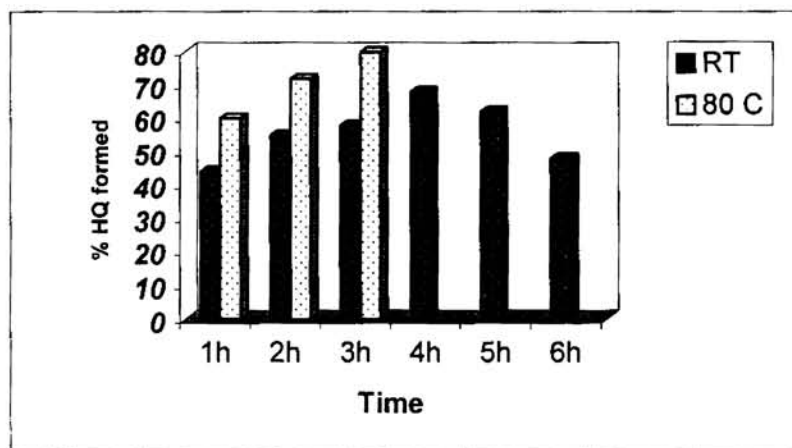


Fig. VIII.5 Percentage of hydroquinone formed in the presence of [PS-opdRuCl₃H₂O] at different intervals

TABLE VIII.5 Effect of Temperature & Time On Oxidation of Phenol in the presence of [PS-opdRuCl₃(H₂O)]

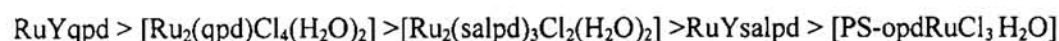
[PS-opdRuCl ₃ (H ₂ O)]	1 h	2h	3h	4h	5h	6h
	%HQ	%HQ	%HQ	%HQ	%HQ	%HQ
RT	44	55	58	68	62	48
80°C	60	72	80	Tar	-	-

Presence of polymer supported complex [PS-opdRuCl₃(H₂O)] resulted in the formation of hydroquinone and the rate of reaction was comparable to that of simple complex. The nature of behaviour with time and temperature were also similar.

8.4.1 Comparison of the catalytic activity of the complexes under study at regular intervals.

Catalytic activity at 1 hr

At room temperature the catalytic activity of the complexes towards hydroxylation reaction of phenol are in the order



Encapsulated qpd complex reacts much faster than all other complexes. The activities of other catalysts are approximately of the same order (figure VIII.6).

At high temperature the order of activity slightly changes and follows the order

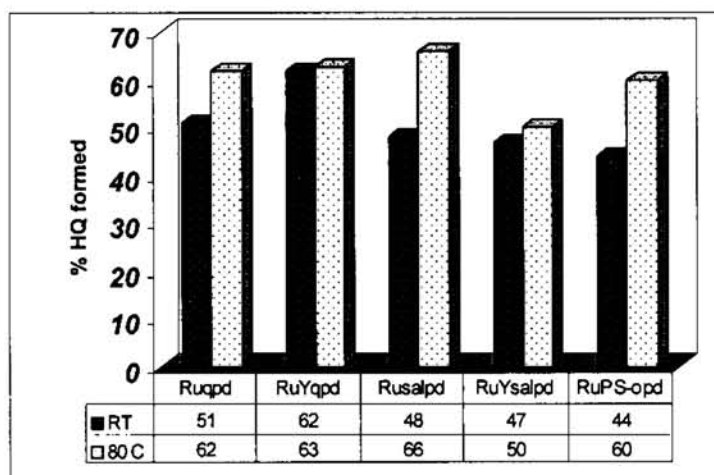
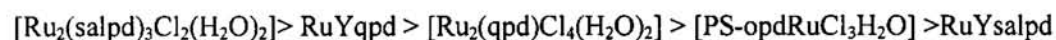
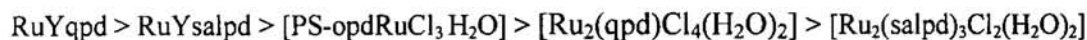


Fig. VIII.6 Percentage of hydroquinone formed in the presence of different complexes at 1 h

Catalytic activity at 2 hrs

The percentage of hydroquinone formed at 2h in the presence of the complexes follows the order



At high temperature the activity of all the complexes are reasonably high, equal to or greater than 70% and follows the order (Figure VIII.7).

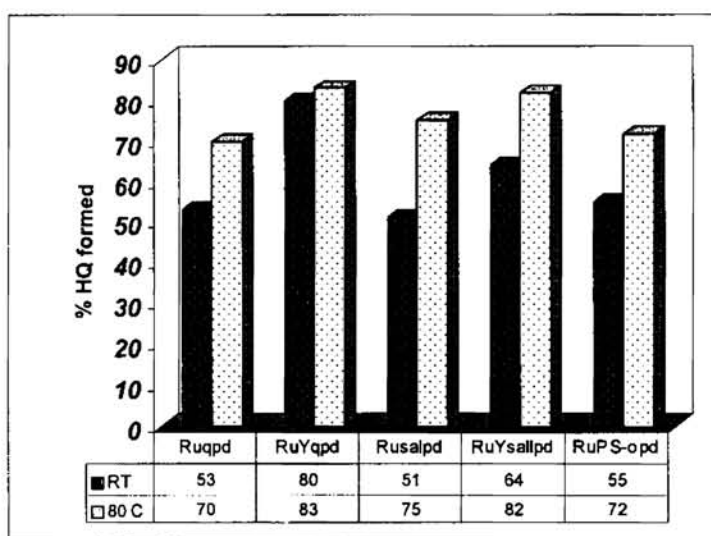
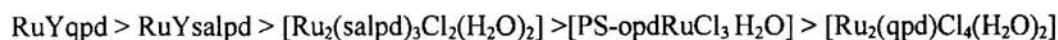
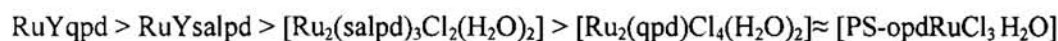


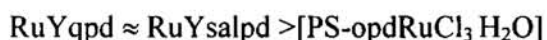
Fig. VIII.7 Percentage of hydroquinone formed in the presence of different complexes at 2 h.

Catalytic activity at 3 hrs

At room temperature RuYqpd was found to be more active compared to other complexes and the order of activity can be given as



At high temperature in the presence of simple complexes the reaction mixture was converted to tarry products. However encapsulated and polymer supported complexes gave reasonably high yield of products (Figure.VIII.8). The order of activity is given by



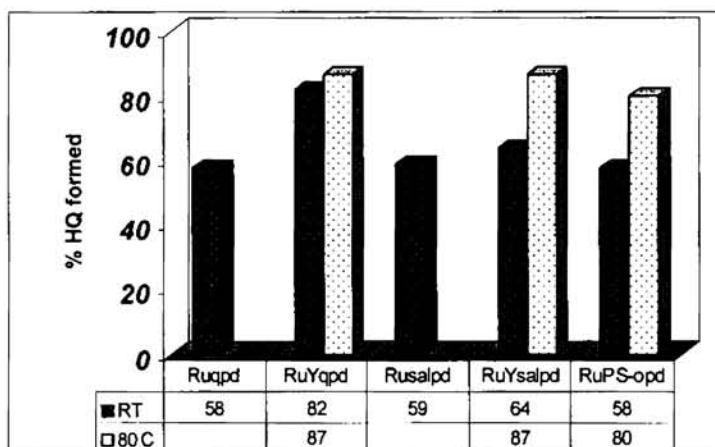


Fig. VIII.8 Percentage of hydroquinone formed in the presence of different complexes at 3h.

Catalytic activity at 4hrs

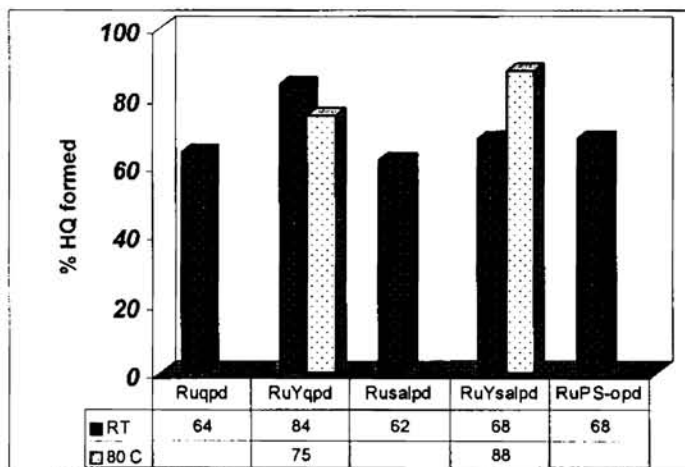
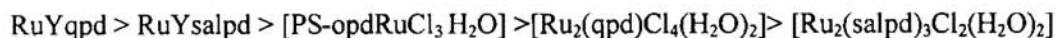


Fig. VIII.9 Percentage of hydroquinone formed in the presence of different complexes at 4 h

At room temperature the order of activity is given by



At 80°C the activity of RuYqpd decreased slightly as indicated by the percentage of hydroquinone formed (Figure VIII.9). This might be due to the conversion of hydroquinone to benzoquinone. The reaction mixture containing [PS-opdRuCl₃ H₂O] was converted to tar at this stage implying that polymer supported complex could not act as a suitable catalyst under this condition. However RuYsalpd showed reasonably high activity.

Catalytic activity at 5hrs

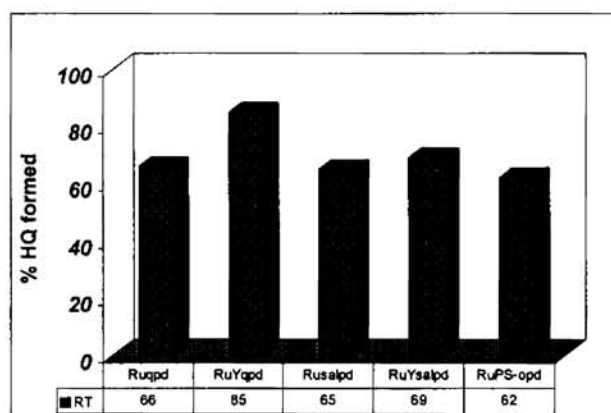
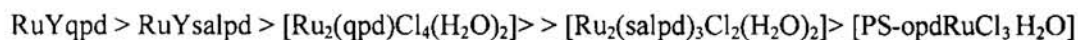


Fig. VIII.10 Percentage of hydroquinone formed in the Presence of different complexes at 5 h

The activity of the complexes at 5h are in the order



In all cases the reaction mixture was converted to tarry product at 80 °C (Figure VIII.10).

Catalytic activity at 6hrs

The activity of the catalysts decreased in all cases probably due to the oxidation of hydroquinone to benzoquinone (Figure VIII.11).

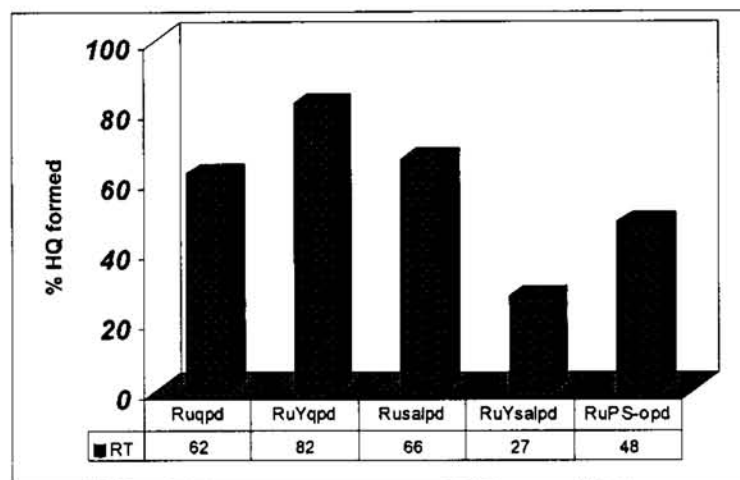


Fig. VIII.11 Percentage of hydroquinone formed in the presence of different complexes at 6 h

Conclusion

Of the three types of complexes simple, encapsulated and polymer supported, zeolite encapsulated complexes were found to be more active towards hydroxylation reaction of phenol. This might be due to the shape selectivity of the zeolite pore and vacant coordination sites of the metal ion inside the pore. Literature survey reveals that zeolite encapsulated complexes act as active catalysts for hydrogen peroxide mediated oxidation reactions such as hydroxylation of phenol to the corresponding hydroxylated aromatics.⁷ This could be the result of various factors like surface area, pore volume, redox properties of metal complexes and the electric field gradient inside the zeolite.

Optimum conditions for good yield of product could be selected as room temperature up to 4 h. At higher temperature the reaction products soon get converted to tarry product in all cases. Reasonably high yield of product was formed initially. However it was noted that encapsulated complexes withstand high temperature. Also on analyzing the facts it can be concluded that encapsulated complexes are more active as

compared to simple and polymer supported complexes towards hydroxylation reaction of phenol as the metal ion concentrations per unit mass of zeolite Y complexes in the reaction mixture are very low. Phenol hydroxylation reaction takes place at the external surface as well as in the internal pores. The reaction in the internal pores leads mainly to the formation of hydroquinone whereas the reaction on the external surface leads to the production of catechol as well as tarry products. On comparing the activities of the complexes, the encapsulated quinoxaline based complex RuYqpd was found to be most active catalyst on the basis of stability and reactivity.

References

- [1] Draths K. M.; Frost J. W., *J. Am. Chem. Soc.* **113**, 9361 (1991).
- [2] Draths K.M. ; Frost J.W., *J. Am. Chem. Soc.* **117**, 2395 (1995).
- [3] Murell L. L.; *Advanced materials in catalysis*, Academic Press, New York (1977).
- [4] Vangham D.E.W., *Catal.Today.* **2**, 187 (1988).
- [5] Figueras F., *Catal. Rev. Sci. Eng*, **30**, 457 (1988).
- [6] Ch. Subramanyan; Louis B.; Viswanathan B.; Renken A.; Varadarajan T.K., *Eurasian Chem. Tech. J.* **3**, 5963 (2001).
- [7] Chandra R Jacob; Saji P.Varkey; Paul Ratnasamy, *Appl. Catal. A.* **168**, 353 (1998).
- [8] Tuel A.; Moussa-khouzami S.; Ben Taarit Y.; Naccache C., *J. Mol.Catal.* **68**, 45 (1991).

CHAPTER IX

***IN VITRO EVALUATION OF ANTIBACTERIAL AND ANTIFUNGAL
ACTIVITY OF COMPLEXES OF RUTHENIUM AND NEODYMIUM***

9.1 Introduction

Inorganic chemists are interested in complexes with multidentate ligands having delocalized π orbital systems due to their vast application in biological field.^{1,2} Schiff base complexes are of great importance in this field.

Interaction of metal ions with nitrogen and oxygen containing organic moieties has attracted much attention in recent years.^{3,4} Such ligands and their complexes have become important due to their biological activity^{5,6} and also because they provide a better understanding of metal- protein binding.⁷ Thus Schiff bases containing these groups could act as a versatile model of metallic biosites.⁸

Some quinoxaline derivatives are known to possess antibacterial activities. The quinoxaline antibiotics were reported to have activity against gram positive bacteria and certain tumours. They inhibit RNA synthesis.⁹

Benzimidazoles are significant in determining the function of a number of biologically active metal complexes. A wide range of benzimidazole derivatives are known for their chemotherapeutic importance.¹⁰⁻¹⁵ Oxadiazole compounds have shown biological activity against parasites¹⁶ and bacteria.¹⁷ Some heterocyclic moieties such as triazole nucleus are known to possess antibacterial¹⁸ and fungicidal¹⁹ properties. Furthermore, Schiff bases possess anticancer^{20,21} activity in animal screening.

Schiff base complexes derived from salicylaldehyde are also expected to have good biological activity. Amines such as o-aminophenol and o-phenylenediamine are reported to have promising influence in the biological field.

Literature survey reveals the biological applications of coumarin derivatives of rare earth metals. These type of complexes have been found to exhibit anticoagulant and plant growth regulating properties.²² It has been shown that many interesting metal organic compounds of lanthanides displayed antitumour activity.²³⁻²⁷ These complexes possess cell proliferation inhibiting effects compared to the inorganic salts. Unfortunately little is known about the complexing abilities and biological activity of rare earth metal complexes.

The aim of the present work is to carry out the antibacterial and antifungal screening studies of the synthesized complexes of ruthenium and neodymium with the Schiff bases formed in the condensation of 3-hydroxyquinoxaline-2-aldehyde with o-phenylenediamine, o-aminophenol or aminobenzimidazole. Also ruthenium complexes of Schiff bases derived from salicylaldehyde with o-phenylenediamine, o-aminophenol or aminobenzimidazole were screened for their antibacterial and antifungal activity. The results of the antibacterial and antifungal studies done on these complexes are presented in this chapter.

9.2 Experimental

9.2.1 Antibacterial screening test

Antimicrobial activities of the synthesized complexes were performed according to the disk diffusion method²⁸ with slight modifications. The ligands and complexes were tested for *in vitro* growth inhibitory activity against one strain of gram positive bacteria *Klebsiella Pneumoniae*, gram negative bacteria *Escherichia Coli* and *Pseudomonas aeruginosa*.

Nutrient agar plates (NA) were surface inoculated uniformly from the broth culture of the tested microorganisms. The impregnated disks were placed on the medium suitably placed apart and kept for 5 minutes for the agar surface to dry. Wells were made on the agar medium at suitable distances. Solution (1 mg mL^{-1}) of the synthesized ligands and complexes was prepared in DMSO. Definite volumes of solution ($5 \mu\text{L}$, $10 \mu\text{L}$, $15 \mu\text{L}$ and $20 \mu\text{L}$) were added to different wells and the plates were incubated at 37°C for 24h. Discs without test solution was used as control. The diameter (in mm) of the observed inhibition zones was taken as a measure of inhibitory activity.

9.2.2. Antifungal screening test

The antifungal activity of all the synthesized ligands and complexes were evaluated towards plant pathogenic fungus *Aspergillus Niger*. Potato Dextrose Agar (PDA) was used as basal medium. PDA broth was prepared in a 250 mL conical flask. To the sterilized broth spore suspension of *Aspergillus Niger* was inoculated. The suspension was prepared by dispersing the spores of *Aspergillus Niger* into sterilized distilled water. The flasks were gently rotated for uniform mixing of the inoculum. Inoculated flasks were incubated for 7 days at room temperature. Gelatin agar medium poured into sterile Petri plates aseptically with the help of a micropipette. Spore suspension (0.1mL) was prepared by adding sterile distilled water (5 mL) to *Aspergillus Niger* culture, filtered and was placed into the well. The plates were incubated for 24-48 h at room temperature. Test solution was poured into the wells as before and inhibition zones were measured after 48 h.

9.3 Results and discussion

9.3.1 Antibacterial screening

The inhibition zones caused by the various compounds in the microorganisms were listed in Table IX.1. It is evident from Table IX.I that Schiff bases under investigation except salab are inactive against all the bacteria. The ligand salab is slightly active against *Pseudomonas aeruginosa* (gram –ve). Results indicate that the growth of

TABLE IX.I Antibacterial activities of Schiff bases and their ruthenium complexes

Compound	Diameter of inhibition zone (mm)											
	<i>Klebsiella Pneumoniae</i>				<i>Escherichia Coli</i>				<i>Pseudomonas aeruginosa</i>			
	Concentration in ppm											
	5	10	15	20	5	10	15	20	5	10	15	12
qpd	-	-	-	-	-	-	-	-	-	-	-	-
[Ru ₂ (qpd)Cl ₄ (H ₂ O) ₂].2H ₂ O	5	10	15	20	10	14	16	24	12	16	18	22
qap	-	-	-	-	-	-	-	-	-	-	-	-
[Ru ₂ (qap) ₂ Cl ₂ (H ₂ O) ₂].H ₂ O	10	12	15	20	6	7	9	11	10	14	18	24
qab	-	-	-	-	-	-	-	-	-	-	-	-
[Ru ₂ (qab) ₂ Cl ₄ (H ₂ O) ₂].3H ₂ O	6	8	10	15	18	19	20	22	14	17	20	22
salpd	-	-	-	-	-	-	-	-	-	-	-	-
[Ru ₂ (salpd) ₃ Cl ₂ (H ₂ O) ₂]	10	13	15	20	14	15	18	20	16	20	23	26
salap	-	-	-	-	-	-	-	-	-	-	-	-
[Ru ₂ (salap) ₄ Cl ₂].H ₂ O	5	8	10	12	12	15	18	20	14	17	20	22
salab	-	-	-	-	-	-	-	-	-	-	-	6
[Ru(salab)(H ₂ O) ₄]Cl ₂ .H ₂ O	5	10	12	20	12	20	22	28	16	17	20	22

the microbes are inhibited in the presence of the complexes. The diameter of the inhibition zone shows the extent to which inhibition occurs. On complexing with ruthenium ion, ligands that were inactive showed considerable inhibitory action on bacterial multiplication.²⁹ Also the activity of all the complexes are found to be increased considerably with increase in concentration. The increase in the antibacterial activity of ruthenium chelates with increase in concentration is due to the effect of metal ion on the normal cell process. Such increased activity of the metal chelates can be explained on the basis of chelation theory.³⁰ Furthermore, the mode of action of the compounds may

involve formation of hydrogen bond through azomethine group with the active centres of all constituents, resulting in interference with the normal cell process.³¹

Neodymium complexes formed from quinoxaline based Schiff bases except $[\text{Nd}(\text{qab})_2(\text{H}_2\text{O})_3\text{Cl}]\cdot 2\text{H}_2\text{O}$ were found to be active against the gram positive microbe *Klebsiella Pneumoniae*, but the activity was less compared to ruthenium complexes.

Ruthenium complexes derived from quinoxaline based Schiff bases were active against gram negative bacteria *Escherichia Coli* and *Pseudomonas aeruginosa*, but corresponding complexes of neodymium were inactive

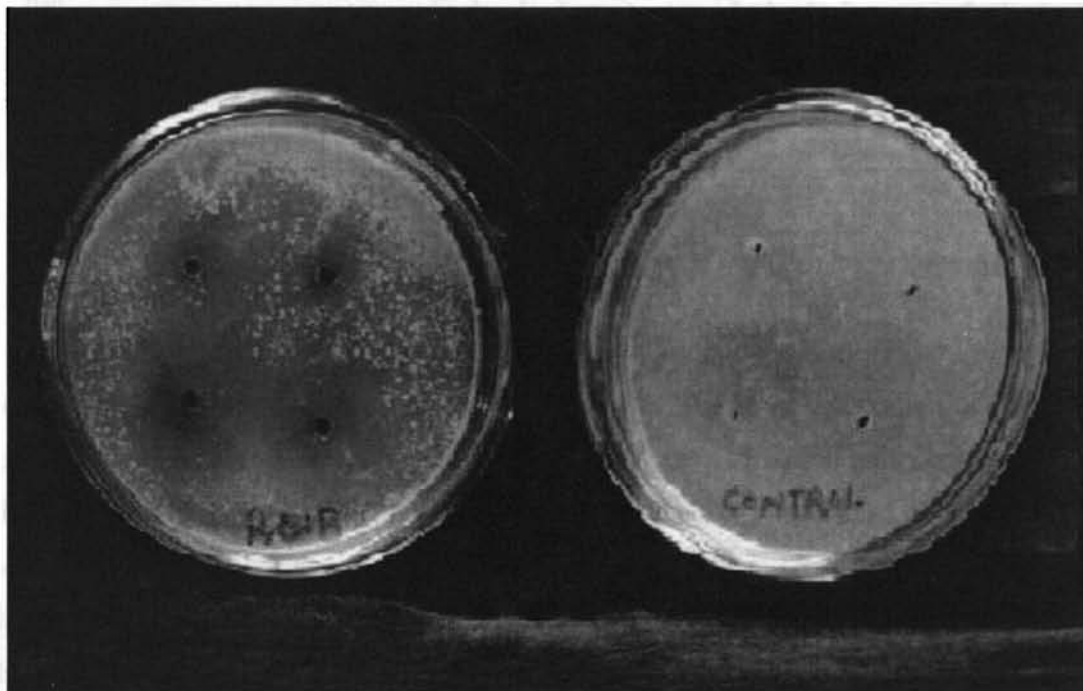


Figure IX.1 Zone of inhibition against *Escherichia Coli*

TABLE IX.2 Antibacterial activities of Schiff bases and their neodymium complexes
Diameter of inhibition zone (mm)

compound	Concentration in ppm											
	<i>Klebsiella Pneumoniae</i>				<i>Escherichia Coli</i>				<i>Pseudomonas aeruginosa</i>			
	5	10	15	20	5	10	15	20	5	10	15	20
qpd	-	-	-	-	-	-	-	-	-	-	-	-
[Nd(qpd) ₂ (H ₂ O)Cl].2H ₂ O	10	12	18	20	-	-	-	-	-	-	-	-
qap	-	-	-	-	-	-	-	-	-	-	-	-
[Nd(qap) ₂ (H ₂ O) ₃ Cl].H ₂ O	5	12	18	20	-	-	-	-	-	-	-	-
qab	-	-	-	-	-	-	-	-	-	-	-	-
[Nd(qab) ₂ (H ₂ O) ₃ Cl].2H ₂ O	-	-	-	-	-	-	-	-	-	-	-	-

9.3.2 Antifungal screening

All the ligands were found to be slightly active against *Aspergillus Niger*. The activity of qab against *Aspergillus Niger* is notable. But on complexation activity was greatly increased in the case of ruthenium complexes. Neodymium complexes also showed activity, but less than that of ruthenium complexes. However qpd complex of neodymium is inactive against *Aspergillus Niger*. The variation in the effectiveness of different compounds against different organisms depends either on the impermeability of the cells of the microbes or differences in ribosomes of microbial cells.³² In all cases it has been noted that the toxicity of the complexes increases with increase in the concentration of the solution.

TABLE 1X.3 Antifungal activities of Schiff bases and their ruthenium complexes

Diameter of inhibition zone (mm)

<i>Aspergillus Niger</i>				
compound	Concentration in ppm			
	5	10	15	20
qpd	-	-	-	5
[Ru ₂ (qpd)Cl ₄ (H ₂ O) ₂].2H ₂ O	13	16	17	26
qap	-	3	5	6
[Ru ₂ (qap) ₂ Cl ₂ (H ₂ O) ₂].H ₂ O	11	14	15	19
qab	7	10	12	14
[Ru ₂ (qab) ₂ Cl ₄ (H ₂ O) ₂].3H ₂ O	28	31	33	34
salpd	-	-	-	6
[Ru ₂ (salpd) ₃ Cl ₂ (H ₂ O) ₂]	27	28	30	32
salap	-	-	-	10
[Ru ₂ (salap) ₄ Cl ₂].H ₂ O	14	18	20	23
salab	4	5	6	8
[Ru(salab)(H ₂ O) ₄]Cl ₂ .H ₂ O	15	18	19	23

TABLE 1X.4 Antifungal activities of Schiff bases and their neodymium complexes

Diameter of inhibition zone (mm)

<i>Aspergillus Niger</i>				
compound	Concentration in ppm			
	5	10	15	20
qpd	-	-	-	5
[Nd(qpd) ₂ (H ₂ O)Cl].2H ₂ O	-	-	-	-
qap	-	3	5	6
[Nd(qap) ₂ (H ₂ O) ₃ Cl].H ₂ O	9	10	12	14
qab	7	10	12	14
[Nd(qab) ₂ (H ₂ O) ₃ Cl].2H ₂ O	7	8	8	9

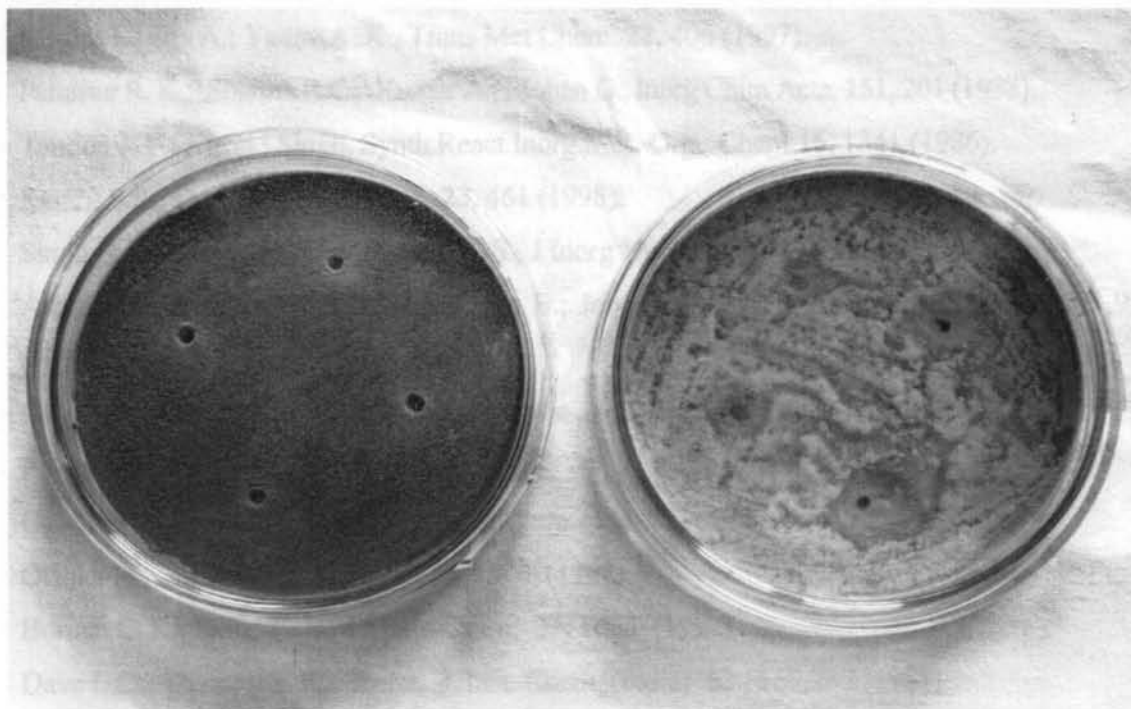


Figure IX.2 Zone of inhibition against *Aspergillus Niger*

Conclusion

From the results it can be concluded that Schiff base complexes derived from salicylaldehyde possess very good anti-microbiological activity compared to the Schiff base complexes derived from quinoxaline aldehyde. The decreased activity of quinoxaline-based complexes can be explained on the basis of the steric effect which hinders the interaction of the cells of the microbes with the azomethine group. Compared to neodymium complexes, ruthenium complexes showed greater activity. The conclusion arrived at from the present investigation is that Schiff base complexes of ruthenium derived from salicylaldehyde are biologically active to a great extent.

References

- [1] Mishra L.; Jha A.; Yadav A. K., *Trans Met Chem.* **22**, 406 (1997).
- [2] Parashar R. K.; Sharma R.C.; Kumar A.; Mohan G., *Inorg Chim Acta*, **151**, 201 (1988).
- [3] Tandon J. P.; Kiron ; Singh, *Synth.React.Inorg.Met.-Org. Chem.***16**, 1341 (1986).
- [4] Kandil S.S., *Transition Met.Chem.* **23**, 461 (1998).
- [5] Singh H.; Yadav L. D. S.; Mishra S. B. S., *J Inorg Nucl Chem.* **43**,1701 (1981).
- [6] Albanus L.; Bjorklund N. E.; Gustafssan B.; Johnson M., *Acta Pharm.Toxic Suppl.* **26** ,93 (1975).
- [7] Bermejo M. R.; Sousa A.; Garcia-Deibe A.; Maneiro M.; Sanmartin J.; Fondo F., *Polyhedron* **18**, 511 (1998).
- [8] Casella L.; Gullotti M.; Vigano P.,*Inorg.Chim.Acta* **121**, 124 (1986).
- [9] Otsuka H.; Shoji J., *Tetrahedron* **23**, 1536 (1967).
- [10] Boruah C. R.; Skibo E. B., *J.Med. Chem.* **37**, 1625 (1994).
- [11] Dave L.D.; Thampy S. K., *Shelat, J. Inst. Chem. (India)* **53** , 169,237 (1981).
- [12] Srivastava R. P.; Sharma S., *Die. Pharmazie* **45**, 34 (1990).
- [13] Kubo K.; Inoda Y.; Kohara Y.; Sugiura Y.; Ojima M.; Itoh K.; Furukawa Y.; Nishikawa K.; Naka T. J., *Med. Chem.* **36**, 1772 (1993).
- [14] Kubo K.; Kohara Y.; Imamiya E.; Sugiura Y.; Inada Y.; Furukawa Y.; Nishikawa K.; Naka T. J., *Med. Chem.* **36**, 2182 (1993).
- [15] Kubo K.; Kohara Y.; Yoshmora Y.; Inada Y.; Shibouta Y.; Furukawa Y.; Kato T.; Nishikawa K.; Naka T. J., *Med. Chem.* **36**, 2343 (1993).
- [16] Ito K.; Kagawa H.; Fududa T.; Yoshino K.; Nose T., *Arzneim- Forsch.* **31**, 49 (1982).
- [17] Rizk M., J., *Egypt Pharm. Sci.* **34**, 243 (1993).
- [18] Kassem; Emad M. M.; El-masry Afaf, *Proceedings of The First International Scientific Conference (Sciences & Development) Cairo* **119** (1995).
- [19] Chiyomara E.Y.; Dohke G., *Japan Pat.* **460**, 7339 (1973) *Chem. Abstr.* **81**, 73392 (1974).
- [20] Greenfield A.; Michael C.S.; Von Meyer W.C., (Rohm & Hass Co.) *Ger. Offen.*, **966**, 806 (1974) *Chem. Abstr.* **82**, 150485 (1975).

-
- [21] Popp D., J. Org. Chem . **26**, 1566 (1961).
- [22] Popp F. D., J. Med. Chem. **7**, 210 (1964).
- [23] Irena Kostova P.;I Ilia; Monolov ; Maritza K.; Radulova , Acta Pharm. **54**, 119 (2004).
- [24] Kostova I.; Manolov I.; Konstantinov S.; Karaivanova M., European J. Med. Chem. **34 (1)** 63 (1999).
- [25] Kostova I. P.; Manolov II.; Nicolova I.; Dancher N. D., Farmaco II., **56 (9)** 707 (2001).
- [26] Kostova I.; Manolov I.; Nicolova I.; Konstantinov S.; Karaivanova M., European J. Med. Chem. **36 (4)**, 339 (2001).
- [27] Manolov I.; Kostova I.; Netzova T.; Konstantinov S.; Karaivanova M., Archiv der Pharmazie., Pharmaceutical and Medicinal Chem. **333 (4)**, 93 (2000).
- [28] Abou-Zeid, Abou-Zeid A; Shehata; Youssef, Indian J. Pharm **31,3**, 72 (1969).
- [29] Chohann Z.H.; Praveen M.; Ghaffar A., Synth React inorg Met.Org.Chem, **28** 1673. (1998).
- [30] Mishra L.; Singh V.K., Indian J.Chem. 446 (1993)
- [31] Dharmaraj N.; Vishwanathamurthi P.; Natarajan K., *Trans Met Chem.* **26**,105 (2001).
- [32] Lawrence P.G.; Harold P.L.; Francis O.G., Antibiot. Che-mother 1597 (1980).

SUMMARY AND CONCLUSION

The present study is mainly confined to the synthesis, characterization and application studies of neat, zeolite encapsulated and polymer supported Schiff base complexes of ruthenium and neodymium. Schiff bases were derived from 3-hydroxy quinoxaline-2-carboxaldehyde and salicylaldehyde with amines o-phenylenediamine, o-aminophenol and 2-aminobenzimidazole. Simple and zeolite encapsulated complexes of these ligands were prepared with Ru(III) and Nd(III). Schiff bases formed from polymer bound aldehyde and o-phenylenediamine, o-aminophenol and 2-aminobenzimidazole were also complexed with Ru(III) and Nd(III). The synthesized complexes were characterized by chemical analysis (ICP-AES and CHN analyses), magnetic moment studies, electronic, FTIR and EPR spectroscopy. The molecular weight and the electrolytic nature of the neat complexes were obtained from FAB mass spectral and conductance data respectively. Thermal stability of the synthesized complexes were understood from the TG data. Reduction in Surface area and pore volume suggests encapsulation of complexes inside zeolite pores and anchoring of complexes on polymer supports. XRD pattern suggests the crystallinity of the zeolite structure were not affected by encapsulation. SEM ensures the removal of surface adsorbed species by Soxhlet extraction. The catalytic behaviour of the synthesized complexes against hydroxylation reaction of catechol and phenol by H_2O_2 were studied. The synthesized complexes were also screened for their antimicrobial activity.

The thesis is divided into nine chapters. Chapter 1 represents review on Schiff bases and metal complexes including their importance in catalytic and biological field. It also provides a brief account of advantages of heterogenization of complexes with organic or inorganic supports. The scope of the present investigation is given at the end of the Chapter.

Chapter 2 presents the details of the materials and synthesis of the ligands qpd, qap, qab, salpd, salap and salab employed in the present study. Preparation of polymer bound Schiff base and metal exchanged zeolite are given in this chapter. The details regarding analytical and spectroscopic methods employed for the analysis of the ligands and their complexes and the techniques employed for the catalytic studies are also given.

Chapter 3 deals with the synthesis and characterization of ruthenium complexes of qpd, qap, qab, salpd, salap and salab. Elemental analyses give the molecular formulae of the complexes as $\text{Ru}_2(\text{qpd})\text{Cl}_4(\text{H}_2\text{O})_4$, $\text{Ru}_2(\text{qap})_2\text{Cl}_2(\text{H}_2\text{O})_3$, $\text{Ru}_2(\text{qab})_2\text{Cl}_4(\text{H}_2\text{O})_5$, $\text{Ru}_2(\text{salpd})_3\text{Cl}_4(\text{H}_2\text{O})_2$, $\text{Ru}_2(\text{salap})_4\text{Cl}_2(\text{H}_2\text{O})$ and $\text{Ru}(\text{salab})\text{Cl}_2(\text{H}_2\text{O})_5$ which was further supported by FAB mass spectra. Molar conductance values in methanol show that all the complexes except salab complex of ruthenium are non-electrolytes. This fact indicates that the anion and the ligand are coordinated to the central ruthenium(III) ion in the complexes. Ruthenium – salab complex show 1:2 electrolytic nature indicating that the two chloride anions present in the complex are not coordinated to the ruthenium(III) ion. The magnetic moment values of all the complexes correspond to one unpaired electron showing that ruthenium atom exists in +3 oxidation state in the complexes. Information regarding the number of water molecules coordinated and that held in the lattice has been obtained from the TG data. IR spectral data suggest that the deprotonated ligand and azomethine nitrogen atoms of the ligand are coordinated to the Ru(III) ion. The electronic spectral data for simple complexes in methanolic solution suggest octahedral nature. EPR spectra of the qpd, qab and salap complexes exhibit three g values indicating rhombohedral distortion of octahedral geometry. Complexes of qap and salab exhibit axial spectra with two g values while salpd complex gives a reverse axial spectrum with two g values. The present studies indicate that qpd acts as tetradentate, qap acts as tridentate while qab, salpd, salap and salab act as bidentate ligands. In all cases, except salab complex, the analytical and physico- chemical data suggest binuclear octahedral structure with chlorine bridges. In the case of salab complex a mononuclear octahedral complex with ruthenium has been suggested.

Chapter 4 deals with the heterogenization of ruthenium complexes by encapsulating in the cages of zeolite. Characterization of the synthesized complexes were done by various analytical and physico-chemical techniques. Metal analyses reveal the unit cell formula of ruthenium exchanged zeolite to be $\text{Na}_{44.14}\text{Ru}_{3.29}(\text{AlO}_2)_{54}(\text{SiO}_2)_{138}.n\text{H}_2\text{O}$. Reduction in surface area and pore volume of the complexes compared to ruthenium exchanged zeolite suggests encapsulation in cages. Initial weight loss recorded in TG curve till 200°C corresponds to the loss of intrazeolite water molecules. DSC curve shows endothermic peak corresponding to the deaquation of the sample around 100°C which is followed by an exothermic maxima with centre at about 350°C corresponding to the decomposition of the encapsulated complex. Zeolite framework is destroyed only above 800°C . XRD follows similar pattern before and after encapsulation indicating that crystallinity is retained. SEM analyses show absence of surface species on the zeolite. IR spectral bands ascertain the coordination of nitrogen and oxygen to the central metal atom. Electronic absorptions of encapsulated complexes are of very low intensity. This might be due to the low concentration of the metal ion species in the zeolite. EPR spectra of RuYsalap gives three g values indicating rhombohedral distortion of the octahedral geometry. RuYqab and RuYsalab present an axial symmetry in the solid state with two g values.

Chapter 5 deals with the synthesis and characterization of neat complexes of neodymium with the Schiff bases qpd, qap and qab. Zeolite encapsulated complexes of neodymium with the Schiff bases qpd, qap, qab, salpd, salap and salab were also synthesized and characterized. Analytical, TG, IR, UV/vis and EPR spectral data of all the synthesized complexes and XRD of the encapsulated complexes have also been reported in this chapter. Neat complexes of neodymium are found to form eight coordinated structure. The complexes are proposed to have bicapped trigonal prismatic geometry.

Chapter 6 deals with the synthesis and characterization of ruthenium and neodymium polymer supported Schiff base complexes of 1,2-phenylenediamine, 2-

aminophenol and 2-aminobenzimidazole. Elemental analyses indicate the formation of complexes. The reduction in surface area and pore volume in nitrogen atmosphere suggests the anchoring of complexes on polymer support. The magnetic moment values calculated are as expected for Ru(III) and Nd(III) complexes. TG curves show a very small loss in weight at low temperatures, which might be due to the expulsion of physisorbed water. All the polymer supported complexes are stable up to $\sim 340^{\circ}\text{C}$ indicating increase in stability due to heterogenization. Comparison of spectral bands of the ligands and complexes confirms the coordination of azomethine nitrogen atom in all complexes. In psap complexes $\nu_{\text{C-O}}$ experiences a positive shift $\leq 10\text{cm}^{-1}$ confirming the coordination of phenolato oxygen atom to the central metal atom. The electronic spectra of the complexes show that ruthenium complexes possess octahedral geometry.

Chapter 7 deals with the catalytic activity studies of the simple, encapsulated and polymer supported complexes of ruthenium and neodymium towards catechol- H_2O_2 reaction. UV/vis spectrophotometric method is employed for the study. In the presence of simple complexes $[\text{Ru}_2(\text{qap})_2\text{Cl}_2(\text{H}_2\text{O})_2]\cdot\text{H}_2\text{O}$ and $[\text{Ru}_2(\text{qab})_2\text{Cl}_4(\text{H}_2\text{O})_2]\cdot 3\text{H}_2\text{O}$, reaction yielded 1,2,4-trihydroxybenzene and o-benzoquinone as the product. $[\text{Ru}_2(\text{qpd})\text{Cl}_4(\text{H}_2\text{O})_2]\cdot 2\text{H}_2\text{O}$ complex remained inactive while in the presence of $[\text{Ru}_2(\text{salpd})_3\text{Cl}_2(\text{H}_2\text{O})_2]$, $[\text{Ru}_2(\text{salap})_4\text{Cl}_2]\cdot\text{H}_2\text{O}$ and $[\text{Ru}(\text{salab})(\text{H}_2\text{O})_4]\text{Cl}_2\cdot\text{H}_2\text{O}$ complexes, the product formed is o-benzoquinone. The reaction was found to be selective towards the formation of 1,2,4-trihydroxybenzene in the presence of encapsulated complexes of ruthenium except in the case of RuYqpd. RuYqpd remained inactive. A comparative study of the initial rates of the reaction were done in all cases.

Catechol oxidation reactions catalyzed by polymer supported complexes were selective towards the formation of o-benzoquinone. Results show that ruthenium complexes act as better catalysts than the neodymium complexes. Of all the polymer supported complexes under investigation $[\text{PS-abRuCl}_3(\text{H}_2\text{O})_2]$ is the most active catalyst.

Chapter 8 contains a comparative study of simple, encapsulated and polymer supported ruthenium Schiff base complexes of 1,2-phenylenedimine towards the oxidation of phenol by H_2O_2 . The reaction products are monitored by gas chromatograph. The reactions were conducted at RT and at 80°C in a temperature controlled oil-bath. The only product formed in all cases was hydroquinone. Of the three types of complexes simple, encapsulated and polymer supported, zeolite encapsulated complexes were found to be the most active towards oxidation reaction of phenol. This might be due to the shape selectivity of the zeolite pore and the possibility of having vacant coordination sites in the complex.

Chapter 9 deals with the antibacterial and antifungal activities of the synthesized neat complexes of ruthenium and neodymium. The ligands and complexes were tested for *in Vitro* growth inhibitory activity against gram positive, *Klebsiella pneumonia*, gram negative *Escherichia Coli*, *Pseudomonas aeruginosa* bacteria. The complexes were also screened against plant pathogenic fungus, *Aspergillus Niger*. Results show that all the ligands are inactive except salab which shows very small activity in higher concentrations. All ruthenium complexes are highly active against both gram positive and gram negative bacteria. However neodymium complexes of quinoxaline complexes of Schiff bases are inactive against *Escherichia Coli* and *Pseudomonas aeruginosa* but qpd and qap complexes are active against *Klebsiella pneumonia*. The activities of salicylaldehyde Schiff base complexes of Nd are comparable to that of ruthenium complexes. Ligands showed very small antifungal activity against *Aspergillus Niger*. On complexation, activity is greatly increased for all ruthenium and neodymium complexes except for $[\text{Nd}(\text{qpd})_2(\text{H}_2\text{O})\text{Cl}]\cdot 2\text{H}_2\text{O}$. However activity of the ruthenium complexes are greater than that of neodymium complexes.